GEOMETRICALLY OPEN FILTERS IN BREAKWATERS

Master's Thesis

E.F. Uelman

12 May 2006

Faculty of Civil Engineering and Geosciences

Delft University of Technology

Geometrically Open Filters in Breakwaters

THESIS

Submitted in partial fulfillment of the
requirements for the degree of

MASTER OF SCIENCE

in

CIVIL ENGINEERING

with

SPECIALISATION IN HYDRAULIC ENGINEERING

by

E.F. UELMAN

Graduation Committee:
Prof. dr. ir. M. Stive
Dr. ir. H.L. Fontijn
Ir. H.J. Verhagen
Ir. G. Smith

Delft University of Technology
Faculty of Civil Engineering and Geosciences
Hydraulic Engineering

Preface

This is the final work for my Master's in Hydraulic Engineering at the faculty of Civil Engineering of Delft University of Technology.

This thesis is making a first step in creating design tools for geometrically open filter constructions in breakwaters with a sand core.

The goal of the Master's thesis is reached by studying the different aspects of the thesis's subject in Chapter 2, and by performing an experiment in the wave flume. The test set up of the experiment is described in Chapter 3. Observations of the wave flume experiment are presented in Chapter 4. A qualitatively analysis is presented in Chapter 5. The conclusions are drawn in chapter 6. The Master's thesis is closed with the recommendation for further research also in Chapter 6.

I would like to thank all co-workers of the Laboratory of fluid mechanics, the people of the multi media studio of civil engineering and Van Oord nv for their contribution on the realization of this thesis.
Finally I would like to thank the following members of the graduation commission for their support and dedication:

Prof. dr. ir. M. Stive
Dr. ir. H.L. Fontijn
Ir. H.J. Verhagen
Ir. G. Smith

Summary

A breakwater with a sand core and an unstable geometrically open filter can be a more economical solution than a 'conventional' breakwater with a rock core. Also more flexibility is obtained in designing a breakwater when it is possible to design a breakwater with an unstable geometrically open filter. For such a breakwater, insufficient knowledge is available to design geometrically open granular filter constructions, which allows an acceptable and a predictable loss of core material under certain conditions. At this moment no proper design tool is available to design a geometrically open filter for a breakwater with a sand core.

The Master thesis has two objectives. The first objective is to get an insight in the transportation of sandy material out the core into a very open granular filter under influence of wave load. The second objective is to obtain a relation ship between

- Transport rate of material
- Initiation of transport
- Grain diameter base material
- Grain diameter filter material
- Thickness of filter layer
- The hydraulic load

In order to reach the objective, more insight is necessary in the transport process inside the filter layer and at the interface of core and filter. To obtain that, some model tests have been conducted. These model tests have been executed in a wave flume.

Nine process based model tests have been performed with regular waves with a height of 10 cm and a period of 1.2 s. The first two experiments were used to tune the test setup. The other seven experiments had different thickness of the filter layer (d_f) and different grain size (D_{f50}) of the filter material. Due to limitations in time and availability of the facilities other parameters then the d_f and D_{f50} such as the wave height and the slope steepness have been kept constant at a value which is typical for breakwaters or wind waves.

During these seven tests, the profile of the core was measured and visual observations have been made. Based on the visual observations the erosion process was described. The transport of core material was governed by sheet flow transport and suspension transport. With a thick filter layer and a small grain size the core material was mainly transported by sheet flow transport. With a decreasing thickness of the filter layer and an increasing grain size of the filter layer, the transport of core

material was increasing and the transport was shifting from sheet flow transport to suspension transport. During the tests, a profile develops which resembles a bar profile of a sandy beach.

The profile of the core was measured by making every 300 waves a photo through the wall of the flume. These photos were interpreted with the computer in order to measure the profile of the core.

Point D (transition point of the erosion area to the sedimentation area) remained during an experiment at one place (see Figure 1).
The amount of erosion was dependent of the grain size and the filter thickness. An important parameter is the dimensionless parameter m (m = the filter thickness divided by the grain size of the filter material (d_f/D_{f50})). The total erosion, erosion depth, and the erosion length 2 after 2400 waves are dependent on d_f/D_{f50}. With an increasing d_f/D_{f50}, the total erosion, erosion depth (ds), and the erosion length 2 (Lr2) are decreasing.
From the measurements could be concluded that the erosion was decreasing in time but after 2400 waves no equilibrium was reached.

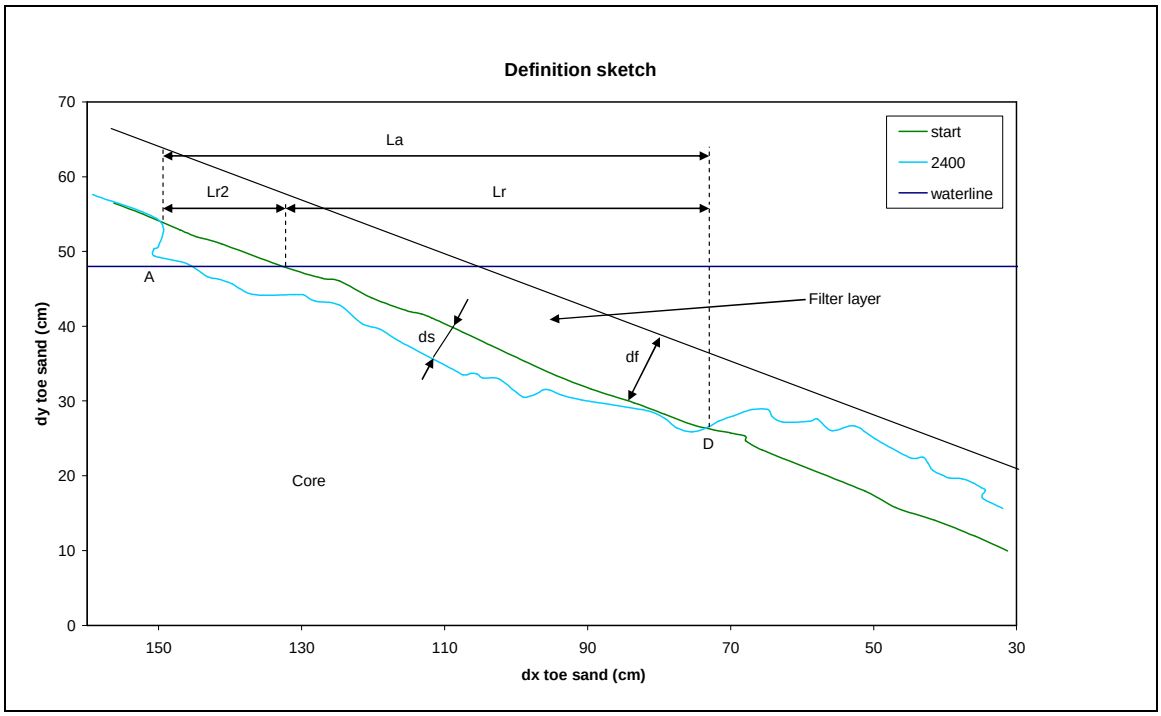

Figure 1 Definition Sketch

List of Symbols

D_{fx}	:	Grain size filter material where x % of the grain mass has a smaller diameter
D_{bx}	:	Grain size base material where x % of the grain mass has a smaller diameter
X_b	:	Parameter X, at, in or on the base material
X_f	:	Parameter X, at, in or on the filter material
n_x	:	Porosity of material x
n_f	:	Porosity of filter material
U	:	Mean velocity of the undisturbed flow
U_f	:	Filter velocity
U_{*cr}	:	Critical shear velocity according the Shields
I	:	Hydraulic gradient
I_{cr}	:	Critical hydraulic gradient
I_{fp}	:	Gradient inside the filter of the prototype
I_{fm}	:	Gradient inside the filter of the model
$I_{\perp}$	:	Gradient perpendicular to the interface
ψ	:	Shields parameter
a	:	Slope angle
Φ	:	Angle between interface and flow direction
g	:	Acceleration of gravity
d_f	:	Thickness of filter layer
d_s	:	Erosion depth
B	:	Diameter of circular pier
F_D	:	Drag force
F_l	:	Lift force
F_S	:	Shear force
F_w	:	Gravity force
F_F	:	Friction force
E_i	:	Incident energy
E_d	:	Energy dissipated on and within the structure
E_r	:	Reflected energy
E_t	:	Energy transmitted through the breakwater
f_l	:	Laminar resistance
f_i	:	Inertial resistance
f_t	:	Turbulence resistance

Re		:	Reynolds number
Fr		:	Froude number
KC		:	Keulegan-Carpenter number
ξ		:	Irribarren number
L		:	Characteristic length
ν		:	Kinematic fluid viscosity
η		:	Dynamic fluid viscosity
a,b,c	$\&$	:	Dimensional coefficients
α,β,γ			
C_t		:	Empirical constant
C_A		:	Added mass coefficient
K		:	Coefficient to take into account the difference of flow in open channels and in granular filters
x		:	Scaled parameter
n_x		:	Scale factor of the physical parameter or quantity x
n_t		:	Time scale
n_u		:	Velocity scale
n_l		:	Length scale
n_p		:	Pressure scale
H		:	Wave height
L_o		:	Deepwater wave length
T		:	Wave period
La		:	Absolute erosion lenght
Lr		:	Relative erosion length
Lr2		:	Relative erosion length 2
m		:	d_f/D_{f50}
p		:	Lr/D_{f50}

Table of contents

1 Problem Description

1.1 Problem Analysis

Breakwaters are used all over the world to protect the coastline from wave action and currents. The protection is mainly designed to protect vessels in port and for port facilities. However, breakwaters are also used for other purposes such as protection of channels against siltation, protection of beaches against erosion and providing facilities for loading cargo and passengers. Breakwater construction can be a complex and costly enterprise, in a difficult marine environment

Conventional Rubble Mound Breakwater

There are various types of breakwaters, but a widely applied concept is the rubble mound breakwater. Typical rubble mound breakwater designs are permeable and consist of different gradations of rubble mound material. Such a breakwater has four important features, as indicated in Figure 1-1;

- Core
- Armour layer
- Under layer or secondary armour layer
- Bedding layer

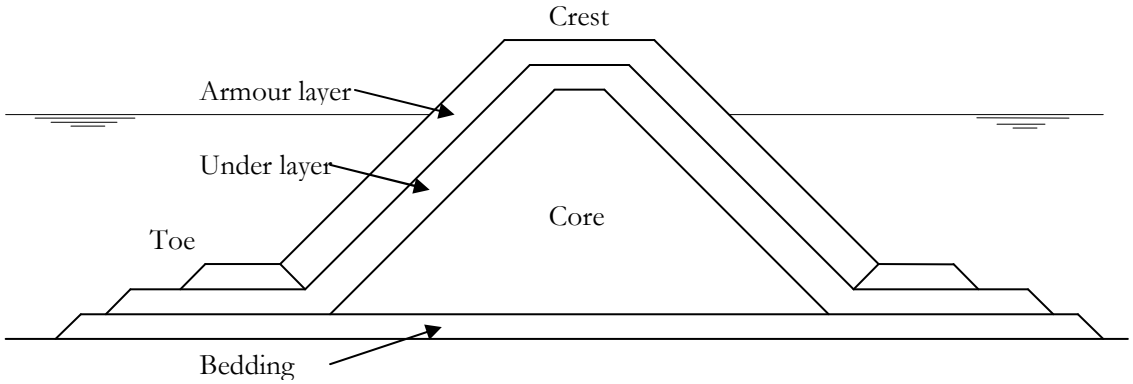

Figure 1-1 Composition of a typical rubble mound breakwater

The core of a rubble mound breakwater often consists of quarry run. The weight of stones in quarry run is commonly between 1 kg and 2000 kg. The core can have a very wide gradation, which means that the ratio

$\frac{D_{85}}{D_{15}}$ is quite large.

The armour layer is the layer that is directly attacked by waves and must be able to withstand these forces during design conditions. This layer has a narrow gradation and contains the largest elements of the breakwater. Instead of using quarry stones, armour units mostly made of concrete can also be used.

Filter layers are used between the breakwater and the sea bottom (bedding layer) and often also between core and armor layer (under layer or secondary armour layer). A filter layer must prevent erosion of the core and seabed beneath the breakwater. In practice, geometrically closed filter criteria are used to design the filter. This means that it is physically impossible for the base material (material which is directly under the filter layer, in this case core or bottom material) to pass through the filter.

Sand Core Breakwater

Instead of rock also sand can sometimes be a more economic way to construct the core. Several layers of filter material are required between the core and armor layer in order to prevent erosion of the sand. If these layers are designed by using geometrically closed filter criteria, a complex filter consisting of multiple layers can result. Instead of filter layers made of rock and gravel, a geotextile can be used, but a geotextile can be difficult to place in a marine environment, in waves and currents.

Alternative Composite Breakwater

As an alternative of using geometrically closed filter criteria to design a multilayered filter construction, geometrically open filter criteria might be possible in some situations. When designing according to geometrically open filter criteria, the hydraulic load on the base material has to be known. By taking the hydraulic load into account, it may be possible to design a stable structure under design constructions, meaning that no loss of material will occur during design conditions. Such a filter is called a 'hydraulic sand-tight filter' or a 'stable geometrically open filter'. By using hydraulic sand tight filters instead of geometrically sand tight filters, fewer filter layers might be necessary. By allowing an acceptable loss of material, the number of filter layers may decrease even more. This results in an easier to build structure. A filter, which is not hydraulically sand tight under design conditions, is called an unstable geometrically open filter.

A breakwater is designed for a given design condition. The design condition will statistically happen only once or twice or maybe not at all, during the lifetime of the breakwater. Some loss of material in this short period might not be a problem for the functioning of the breakwater. When a good estimation of the amount of loss of material is possible, this loss of material can be taken into account in the design.

Designing an unstable geometrically open filter requires knowledge about not only the load on the outside of the structure but also on the inside of the structure. After that the designer needs to know the behavior of the structure under that load. This can be split into two parts; the initiation of movement of core material and the transportation of core material through the filter layer. See Figure 1-2.

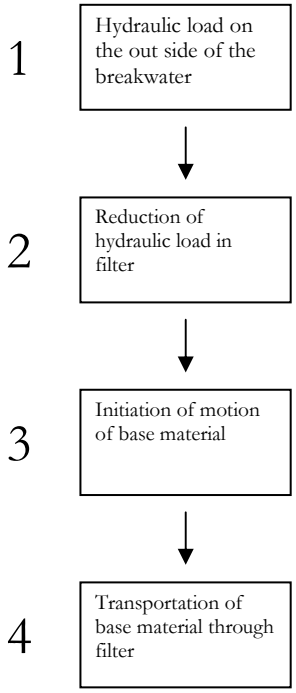

Figure 1-2 Design steps unstable geometrically open filter

1.2 Problem definition

A breakwater with a sand core and an unstable geometrically open filter is more economical to construct than a 'conventional' breakwater with a rock core. For such a breakwater, insufficient knowledge is available to design geometrically open granular filter constructions, which allow an acceptable and a predictable loss of core material under certain conditions. At this moment no proper design tool is available to design a geometrically open filter for a breakwater with a sand core.

1.3 Objective

The objective of this study is twofold;

- To get an insight in the transportation of sandy material out of the core into a very open granular filter under influence of wave load.
- To obtain the relationship between;
    - Transport rate of material
    - Initiation of transport
    - Grain diameter base material
    - Grain diameter filter material
    - Thickness of filter layer
    - The hydraulic load

This objective of the Master's thesis is reached through six chapters;

- Description of the Problem in Chapter 1
- Literature study in Chapter 2
- Experiment set-up in Chapter 3
- Observation wave flume experiment in Chapter0
- Analysis of measurements in chapter 5
- Conclusions and recommendations in Chapter 6

2 Literature Study of the Theory

In the first phase of the Master's thesis a literature study has been performed. In this chapter an overview of the most useful information will be given. The review of the literature study is focused on five subjects;

1. Geometrically closed filters
2. Geometrically open filters
3. Transportation of material through porous media
4. Wave attenuation in rubble mound material
5. Scaling of rubble mound structures under wave attack in a wave flume

In the following paragraphs, each subject will be discussed. All the formulae presented in the following paragraph are valid for loose non-cohesive soils.

2.1 Geometrically Closed Filters

Traditionally, filters are designed based on geometrically closed filter criteria. Geometrically closed filters do not allow particles from the base material to pass through the constrictions of the filter material. We speak of constrictions instead of pores because there are two types of pores; namely the pore channels -or constrictions- and the pore spaces. The pore spaces are the spaces between the grains and are the largest voids in a filter. These pore spaces are in contact with each other by relatively small channels, we call them pore channels or constrictions. These constrictions form the smallest voids in the filter and govern the working of the filter. If the constrictions are smaller than the characteristic grain size of the base material, the filter is called geometrically closed. According to Kenney[1] the characteristic constriction in the filter material is $D_{fc} \leq 0.2 D_{f15}$. The characteristic grain size of the base material is the D_{f85}.

This is similar to the stability criteria from the design rule first conducted by Terzaghi[2]. Besides the stability criteria Terzaghi set up two extra criteria, which a geometrically closed granular filter must fulfill;

[1] Kenny, 1985 according to Bakker, 1993 [4]

[2] Terzaghi, 1922 according to Schiereck, 2000 [31]

$$\frac{D_{f15}}{D_{b85}} < 5 \quad \textit{Stability criteria}$$

$$\frac{D_{b60}}{D_{b10}} < 10 \quad \textit{Internal stability criteria}$$

$$\frac{D_{f15}}{D_{b15}} > 15 \quad \textit{Permeability criteria}$$

The internal stability criteria has to make sure that the range of grain diameter in the base material is not too large, so the larger grains of the base material are able to block the smaller grains of the base material. The permeability criteria ensure that particles from the base material will not clog up the filter, in order to prevent water pressure from building up beneath the filter layer. When designing breakwaters a more strict stability criterion is used.

An advantage of using geometrically closed filter criteria is that the loading conditions on the filter and base material do not need to be specified. A result of this is that the design of the filter can be conservative.

2.2 Geometrically Open Filters

By taking hydraulic loading conditions into account, a more economical design is possible. The characteristic grain size of the base material is able to pass through the constrictions of the filter. This is called a geometrically open filter. The filter is now responsible for reducing the hydraulic load at the base material. If the hydraulic load is reduced enough so the base material is not moved, we speak of a stable geometrically open filter or a hydraulic sand tight filter.
Research has been performed to create criteria for hydraulic sand tight filters under stationary and cyclic flow. These studies were focused to give a relation between the flow or gradient in the filter material and the start of motion of the base material. The transport mechanism in the filter depends on the direction of flow in the filter structure.

Four main loading situations can be distinguished;

1. Steady flow parallel to the interface.
2. Cyclic flow parallel to the interface.
3. Steady flow perpendicular to the interface.
4. Cyclic flow perpendicular to the interface.

These are described briefly in the following sections. Of course, all combinations of these loading situations may occur.

Steady & Cyclic Flow Parallel to Interface

The gradient in the filter layer and the base layer are about the same. Because of a greater permeability of the filter layer the flow velocity in the filter layer is much higher than the flow velocity in the base layer. Because of this velocity difference, a shear stress on the upper grains of the base material will exist. This shear stress is responsible for the movement of grains of the base material and the principle can be compared to the incipient motion of bed material in an open channel. Because the velocity in the filter layer is responsible for erosion of the base layer, the gradient in the filter layer determines the stability of the base material.

For cyclic flow with a period > 2s the critical filter velocities are the same as with steady flow[3].

Steady & Cyclic Flow Perpendicular to Interface

The discharge in the base layer and the filter layer are the same, causing a higher gradient in the base layer then in the filter layer due to the difference in permeability. Erosion of the base layer will occur due to fluidization of the base material. This happens if the grains of the filter material are much larger then the grains of the base material ($n_f * D_{f15}/D_{b50} > 6$ à 7). In this case, the base acts as if there is no filter at all. The critical gradient in the base material is then equal to one.

For a ratio ($n_f * D_{f15}/D_{b50}$) < 2.5 the filter is geometrically closed**.**

For ratios in between, 2.5 < ($n_f * D_{f15}/D_{b50}$) < 6 à 7, two mechanisms play a role;

- Grains that flow from the base layer into the filter layer, arrive in much larger pores with a much smaller flow velocities, so the forces on the grains decreases and the grains will not move any further.
- Another mechanism is arching. A pressure arch is formed by fine base material in front of a pore channel so the underlying base material cannot pass. In cyclic flow perpendicular to the interface the critical gradient is lower than with steady flow. This can be explained by the destruction of the arches in cyclic flow. See also Figure 2-1.

[3] Bezuijen, 1987 [6]

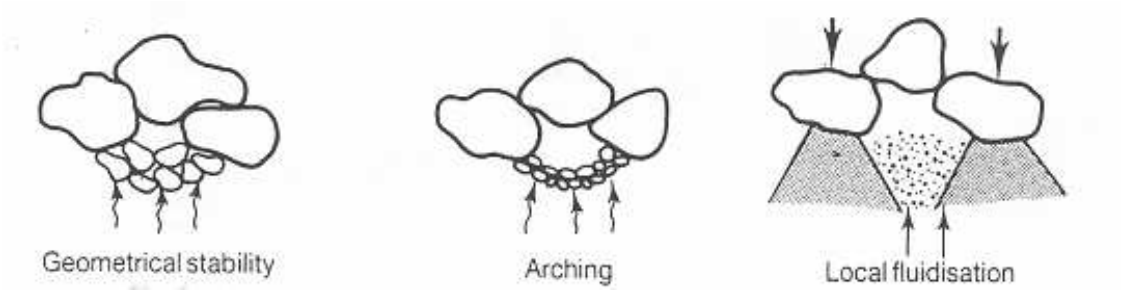

Figure 2-1 Stability principles under perpendicular flow

In general the critical hydraulic gradient is a function of;

1. The base material characteristics; grain shapes, grain sizes, grading density and grading packing.
2. The filter material characteristics; grain shapes, grain sizes, grading density and grading packing.
3. The flow type; function of filter velocity and the physical properties of water (density and viscosity).

By combining the most significant parameters from above a relation is found for the critical hydraulic gradient[4];

$$I_{cr} = f\left(D_b, \frac{D_f}{D_b}, n_f\right) \qquad [8]$$

Based on extensive research and assuming an analogy between pipe flow and flow inside porous media De Grauw conducted an empirical formula for flow parallel to the interface[5]. This to relate the critical gradient with the critical shear velocity according to Shields and a ratio between the grain size of the filter material with the grain size of the base material;

$$I_{cr} = \left(\frac{0.06}{n_f^3 D_{f15}^{4/3}} + \frac{n_f^{5/3} D_f^{1/3}}{1000 D_{b50}^{5/3}}\right) U_{*cr}^2 \qquad [8]$$

For a parallel cyclic load with a period > 2 sec De Grauw concluded that with a quasi-stationary approach, the use of the formula gives results on the safe side. However, the formula is derived from experiments with flow without a free water surface so it is not without question that the formula can be used with free surface flow.

[4] De Grauw, 1983 [8]

[5] De Grauw, 1983 [8]

If the size of the grains of the filter layer and related to that the size of the pore-holes of the filter layer is large with respect to the size of the grains of the base material, the hydraulic loading on the base material can be related with the hydraulic loading on the bottom of a open channel. It is assumed that the critical shear stress at the interface of the base material is equal to the critical shear at the bottom of an open channel with the same bed material as the base material. Based on this, M. Klein Breteler used the Shields criteria to give a formula in which a critical filter velocity is related with the D_{50} of the base material[6].

$$U_{fcr} = \frac{n_f}{\kappa}\sqrt{\underbrace{\psi_b \Delta_b g D_{b50}}_{1}\left(\underbrace{\left(\frac{\sin(\phi-\alpha)}{\sin\phi}\right)}_{2} - \underbrace{\frac{I_\perp}{\Delta_b(1-n_b)}}_{3}\right)} \qquad [22]$$

Where, K= coefficient to take into account the difference of flow in open channels and in granular filters

$K = 0.8\ Re_{cr}^{-0.2}$ for $0.1 < D_{b50} < 0.3$ mm

$K = 0.2$ for $0.5 < D_{b50} < 1.0$ mm

$K = 0.35$ for $D_{b50} > 2.0$ mm

The formula is composed of three parts; part 1 that is related with the hydraulic conditions, part 2 that brings the slope angle into account and part 3 which accounts for a perpendicular hydraulic gradient.

The filter velocity is directly related to the hydraulic gradient in the filter material. As the filter material is generally coarse, flow is assumed to be turbulent, for which the relationship reads[7];

$$I_f = \frac{C_7}{n_f^2 g D_{f15}} U_f^2 \qquad [4]$$

Where, C_7 = empirical constant

Combining this formula with the equation of M. Klein Breteler, a relation between the critical hydraulic gradient and the ratio D_{b50}/D_{f15} is found for flow parallel to the interface at a horizontal bed; $I_{fcr} = \frac{C_7 \psi_b \Delta_b D_{b50}}{\kappa^2 D_{f15}}$ [22]

[6] M. Klein Breteler, 1990 [22]

[7] Bakker, 1994 [4]

For design purposes M. Klein Breteler formulated a graph based on the formula for critical velocity;

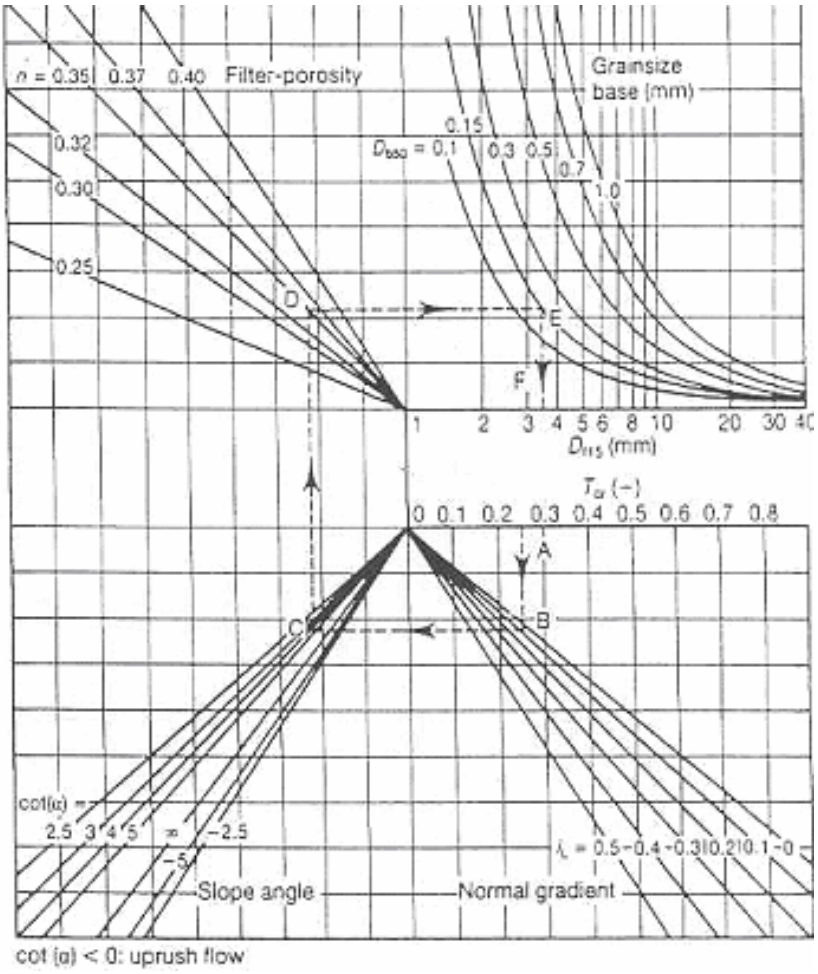

Figure 2-2 Design graph for stable granular open filters (M. K. Breteler 1990)

Wörman[8] performed - research to scour protection around bridge piers consisting out of one single layer of riprap material. Discovered was that the scour hole beneath the riprap protection had a similar shape as the scour hole in unprotected bed and that the relative erosion depth, d_s/B up to 0.3 has a linear relationship with $U^2/g*d_f$. Concluded was that the single-layer protection acted as a moderator of the erosion process due to the hydraulic filter effect. Erosion and transport of the base material through the filter is mainly governed by a ratio between the parameters

$$\frac{U^2}{g \cdot d_f} \text{ and } \frac{D_{b85}}{D_{f15}} \qquad [41]$$

U = Mean velocity of the undisturbed flow

g = Acceleration of gravity

[8] Wörman, 1989 [41]

d_f = Thickness of filter layer

On the upstream side of the pier Wörman found a linear relation for the initiation of motion of the base material;

$$\frac{U^2}{g \cdot d_f} \approx 6 \frac{D_{b85}}{D_{f15}} \qquad \text{if } \frac{D_{b85}}{D_{f15}} < 0.1 \ . \qquad [41]$$

If $\frac{D_{b85}}{D_{f15}} > 0.1$, $\frac{U^2}{g \cdot d_f}$ approaches asymptotically to infinity to a vertical line which corresponds to geometrically closed filter stability criteria.

2.3 Transport of Material

Third studied aspect of the Master's thesis is the transport of the material.

If the grains of the base material are smaller then the constrictions in the filter, a grain of the base material is able to move through the filter. Forces acting on a grain responsible for moving a grain through a constriction can be schematized in the following way;

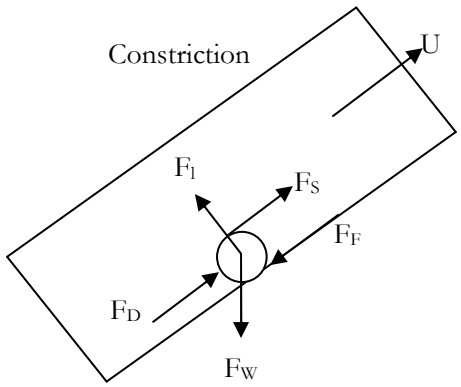

Figure 2-3 Schematization of the forces acting on a grain in a constriction

The drag force (F_D), the lift force (F_l) and the shear force (F_S) are proportional to the square of the velocity of the water near the grain and the grain surface. These forces are balanced by the submerged weight of the grain multiplied by the gravity (F_w) and the friction force (F_F). These forces are proportional to the weight of the grain. The water velocity is called critical when the frictional force and the gravity force are just large enough to balance the drag, lift and shear forces.

Extensive research has been done between 1987 and 1992 by Adel[9] and others in order to understand and to describe the transport of fine material through rubble mound relative coarse material. This has been done for two main flow types, namely the flow perpendicular to the interface of filter and base material and the flow parallel to the interface of the filter and base material. During tests, it was observed that the two flow types have different transport mechanism responsible for the transport of the material.

[9] Adel, 1992 [1,2,3]

The conclusions that can be drew after studying the subject, concerning flow perpendicular to the interface of base material and filter material are the following[10];

- Four different types of transport can be distinguished depending on the gradient in the base;
    - Low values of the gradient (1 to 2), grains of the base will only rotate and wiggle a bit inside the filter pore.
    - Slightly higher values of the gradient (2 to 3), sporadically sudden filling of pores will occur with a high density mixture of base material and water.
    - Flow with a gradient of 3 to 8, base material will be transported through a series of constrictions, which are more or less in a row; this is called the preferable channel. The transport stops suddenly if the transport on the upside of the preferable channel stops.
    - With a gradient in the order of 10, a thin mixture of base material and water flows up through the filter material.

- In all cases, the transport is collective. This arises from when a single grain moves from the base into the filter, the gradient will decrease and the grain will fall back into the base. When the gradient is just large enough, fluidization will occur and base material will be transported to the filter.

- A sharp boundary between the filter penetrated with base material and the filter not penetrated by material is observed.

The conclusions which can be drawn after studying the subject, concerning the measurements with flow parallel to the interface of base material and filter material, are the following[11];

- In contrast to flow perpendicular to the interface between base and filter, the transport of base material is governed by independent movement of grains of the base material.

- With low flow velocities (1 to 2 times the critical flow velocity) the grains of the base material will move along the interface between base and filter in a thin layer of one base-grain thick.

[10] Adel, 1992 [2]

[11] Adel, 1992 [3]

- With higher flow velocities, the distance of the transported grains to the interface becomes larger, thus the layer of transported material becomes thicker. But, still most of the grains move along the interface of base and filter.

- The speed of the individual grains is approximately half the flow velocity.

- If the ratio between the grain size of the filter and the base is smaller then approximately 15, the transported grains move also a little further from the interface. This because of the geometrically interference of the filter grains.

2.4 Wave Attenuation in Rubble Mound Layers

To estimate the sediment transport rate, accurate information on the local fluid velocity and turbulent intensity are crucial. In the following part, information about water motion inside porous structures is given.

2.4.1 Water motion

When a wave approaches a non-overtopped rubble mound breakwater, part of the incident energy (E_i) is dissipated on and within the structure (E_d), part is reflected (E_r), and the rest is transmitted through the breakwater (E_t);

$$E_i = E_d + E_r + E_t$$

The resistance of the porous material is responsible for the dissipation of the energy on and within the structure. The porous flow through sand material is dominated by laminar resistance (f_l). Inertial resistance (f_i) and turbulence resistance (f_t) are of minor importance. For porous flow through gravel and rubble mound structures, inertial resistance and turbulence resistance cannot be neglected.

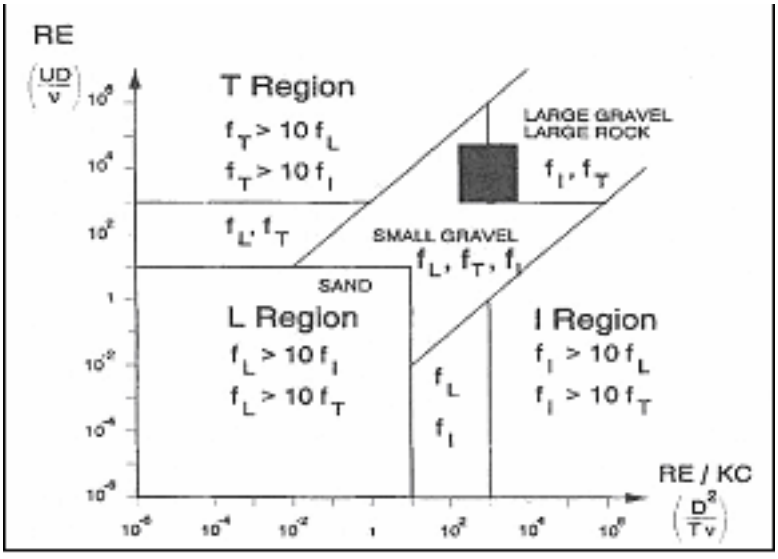

Figure 2-4 Dominating resistance types [37] (van Gent 1995)

An indication of which flow type is dominant is the dimensionless number of Reynolds;

$$\mathrm{Re} = \frac{U \cdot L}{\upsilon} \; or \; \mathrm{Re} = \frac{\rho \cdot U \cdot L}{\eta}$$

The Reynolds number is the ratio of inertial forces (U*ϱ) to viscous forces (η/L) and is used for determining whether a flow will be laminar or turbulent. Laminar flow occurs at low Reynolds numbers, where viscous forces are dominant, and is characterized by smooth, constant fluid motion, while turbulent flow occurs at high Reynolds numbers and is dominated by inertial forces, producing random eddies, vortices and other flow fluctuations.

Non-stationary porous flow can be described by the extended Forchheimer equation;

$$I = a \cdot U + b \cdot U \cdot |U| + c \frac{dU}{dt} \qquad [37]$$

The first term of the Forchheimer formula can be seen as the laminar friction term, the second term as the turbulence friction term, and the third term as a time dependent term (inertial resistance), which represents the resistance of the porous medium to accelerate the water.

$$a = \alpha \frac{(1-n)^2}{n^2} \frac{\nu}{g \cdot D_{n50}^2}$$

$$b = \beta \frac{1-n}{n^3} \frac{1}{g \cdot D_{n50}} \quad where \quad \beta = \beta_c \left(1 + \frac{7.5}{KC}\right) \quad with \quad KC = \frac{\hat{U} \cdot T}{n \cdot D_{n50}}$$

$$c = \left[1 + \gamma \frac{1-n}{n}\right] / (n \cdot g) \quad where \quad \gamma = \left(0.85 - \frac{0.015}{Ac}\right) \quad with \quad Ac = \frac{\hat{U}}{n \cdot g \cdot T}$$

In case of only laminar flow the Forchheimer equation reduces to the equation of Darcy[12]. Then the inverse of *a,* is the permeability of the porous material.

The coefficients (a,b,c)and (α,β,γ) are described by a lot of authors but the descriptions mentioned above have been derived by Van Gent who performed tests in a U tube water tunnel with oscillating and stationary flow[13]. The coefficient in the turbulence term, b, depends on the Keulegan-Carpenter (KC) number in case of non-stationary flow. Boundary layers will be destroyed if the flow direction changes. The destruction of the boundary layers requires an extra amount of momentum. The destruction of these boundary layers will be larger if the inertia term, relative to the turbulence term, is larger. This is inversely proportional to the KC-number since the KC-number can be seen as the ratio of influence of the turbulent term and the influence of inertia.

2.4.2 Phenomena

In this section two important phenomena will be discussed. First, the disconnection will be discussed, followed by the internal set-up. These phenomena will occur when a breakwater is attacked by a wave load and are important to describe the type of loading at the interface between core and filter layer.[14]

Disconnection

The internal water motion is influenced by wave height, wave steepness, slope angle and flow-induced friction of the granular material. Due to friction, the fluid velocity in the filter will be higher than the fluid velocity in the core. The velocity of the internal phreatic surface equals the fluid velocity near the phreatic surface. Because the filter velocity is higher than the water velocity in the

[12] van Gent,1995 [37]

[13] van Gent, 1995 [37]

[14] de Groot et al, 1988 [9]

core, the velocity of the internal phreatic surface in the filter is higher than the velocity of the internal phreatic surface in the core. Therefore, a discontinuity can exist at the boundary between core and filter material. This continuity is called a disconnection. This phenomenon also happens at every boundary between two interfaces with other permeability.

Internal set-up

Internal set-up means, that the water table inside the core of the breakwater is higher then the still water level outside the breakwater. Internal set-up can be explained by considering the length and cross section of a flow tube during in and out flow. During inflow the cross section is relatively large and the penetration distance is relatively short. Outflow mainly takes place in the lower part of the breakwater and there are long flow lines and a low phreatic surface (the higher the phreatic surface, the higher the hydraulic gradient, the more water will flow out). In order to obtain an outflow, which equals the inflow during each cycle, there must be a much higher outflow velocity. This requires a much higher-pressure gradient. Set-up leads to a decrease of the inflow, a greater cross section during outflow and a greater pressure gradient during outflow resulting in a higher outflow velocity. If the water is available to flow away at the backside of the structure, less or no set-up will occur.

2.4.3 Computer Models

Some models have been developed to describe the interaction between wave action and coastal structures. For an economic breakwater design, knowledge of the wave induced pore pressure is important. Within the framework of the European Mast-Coastal structures project research is done to develop a model that describes wave motion on and, within coastal structures. At Delft University of Technology a numerical program ODIFLOCS, *O*ne *Di*mensional *Flo*w on and in *C*oastal *S*tructures, has been developed[15]. In this model, a hydraulic model is coupled to a porous flow model. For the hydraulic model simulating the external flow, long wave equations has been used similar to the method of Kobayashi (basically long wave equation is a very simple form of the Navier-Stokes equation). This is a one-dimensional description of flow which includes hydrostatic pressure and the use of depth averaged velocities. For the porous flow model, use has been made of the extended Forchheimer equation as described in paragraph 2.4.1. However for α and β constant values have been used. For the coefficient c, a slightly different description has been used.

$$c = \left(1 + c_a\right) / \left(n \cdot g\right)$$

[15] van Gent, 1994 [37]

With ODIFLOCS wave run up, surface elevations and velocities can be calculated. But the program does not take turbulence generation-dissipation into account. Also, only an approximation of the velocity field can be given as only depth-averaged velocities are calculated.

Another program is VOFbreak², VOF-algorithm for breaking waves on breakwaters.[16] This is a two dimensional program to give a description of wave induced flows and pressures in porous structures. To describe the fluid motion in the vertical plane, Navier-Stokes equations, VOF method and continuity equation are used. To implement porous flow the extended Forchheimer equation replaces the viscosity term in the Navier-Stokes equation. As in ODIFLOCS, α and β are treated as constant and for c a slightly different description is used;

$$c = \frac{n + (1-n)C_m}{g} \quad with \quad C_m = 1 + C_A \qquad [38]$$

In which C_A (-) is the added mass coefficient. In comparison with ODIFLOCS, VOFbreak² gives a better wave induced velocity field, because of a two dimensional approach. But still no turbulence generation-dissipation is taken into account.

Liu developed a model based on the Volume-Averaged/Reynolds Averaged Navier-Stokes (VARANS) equations the Forchheimer equation and an improved k-ε model.[17] By doing so small-scale turbulence in porous media can be modeled.

All these models give an average velocity field inside the porous media. This is because it is not practical to resolve the flow field inside the pores, whose geometry is usually random. Because it is more manageable, the flow equations are averaged over a volume that is larger than the characteristic pore size and much smaller than the scale of spatial variation of the physical variables in the flow domain.

2.5 Scaling of the Filter and Core Material

2.5.1 Scaling Laws

To conduct physical model tests, a prototype must be scaled to a size, which can be handled by the test facility. When conclusions have to be drawn from model tests, the model must be a reliable representation of the prototype. When this model is a scaled representation of the prototype,

[16] Peter Troch, 1998 [35]

[17] Liu, 2002 [24]

similarity between model and prototype is necessary. The problem with scaling is that certain parameters cannot, or are difficult, to be scaled. Examples of these parameters are fluid characteristics and gravity. Scaling of the prototype will be done by dividing the physical parameters or quantities of the prototype by a scale factor;

$$n_x = \frac{x_p}{x_m}$$ where n_x is the scale factor of the physical parameter or quantity x

There are different types of similarity[18];

- Geometric similarity;
  The model is geometrically similar to the prototype if all geometrically dimensions of the prototype are scaled with the same scale factor.
- Kinematic similarity;
  The model is kinematically similar to the prototype if al the velocities in the prototype are scaled with the same scale factor.
- Dynamic similarity;
  The model is dynamically similar to the prototype if al the forces in the prototype are scaled with the same scale factor.

The different types of forces (inertia, gravity, viscous, etc), which are present in the prototype, are related to each other by independent dimensionless parameters. Complete similarity is reached when values of all these parameters are the same in the model and in the prototype. In other words, the scale factor of these dimensionless parameters is 1.
Two important dimensionless parameters are the Froude number and the Reynolds number.[19]

- The Froude number;

$$Fr = \frac{U}{\sqrt{gL}}$$

  The Froude number is the square root of the ratio between inertia and gravity forces. Physical models, in which wave action is the dominant force, are usually scaled by using the Froude scale rule. When maintaining the Froude number in model and prototype (n_{Fr}=1), the following expressions for time, velocity and pressure scales can be derived;

[18] van der Hoeven, 2002 [44]

[19]de Vries, 1976 [43]

$$n_t = n_u = n_l^{1/2} = n_p^{1/2}$$

- The Reynolds number;

$$\mathrm{Re} = \frac{UL}{\nu}$$

As mentioned above the Reynolds number is the ratio between inertia and viscous forces. When maintaining Reynolds number in model and prototype ($n_{Fr}=1$) the same, the following expressions for time, velocity and pressure scales can be derived;

$$n_t = n_l^2$$

$$n_u = n_l^{-1}$$

$$n_p = n_l^{-2}$$

When scaling a prototype, it is impossible to keep the Reynolds number and the Froude number the same in the model. If a prototype breakwater is scaled according to the Froude scale law, the viscous forces will be relatively large and the Reynolds number will be too low. Thus giving an under estimation of the amount of turbulence.

To give a better approximation of the flow field inside the breakwater Burcharth[20] developed a method in which the hydraulic gradient inside the breakwater core is kept the same in model and prototype. The hydraulic gradient can be calculated by using the extended Forchheimer equation. When scaling porous flow in breakwaters, the inertia term can be disregarded (according to Burcharth as sighted by Burcharth 1999). In this method, the flow velocities in the prototype will be scaled by using the Froude scale law. When maintaining the hydraulic gradient in model and prototype, a grain diameter of the core material can be calculated. The problem in this method is that the hydraulic gradient and the velocities are varying in space and time. So, it will be impossible to get a fully correct scaling of the prototype. In order to get a flow field in the model as similar as possible to the flow filed in the prototype, a characteristic hydraulic gradient with a corresponding flow velocity must be used. Burcharth proposed that the characteristic pore velocity can be chosen as the average velocity averaged over one wave period of six points inside the core.

[20] Burcharth, 1999 [7]

2.5.2 Extended method of Burcharth

In order to use the quantitative results of the model tests in the engineering problems, the model has to be scaled a real life situation. In order to do this, the method of Burcharth mentioned above can be used. The problem of this method is to determine a characteristic velocity inside the filter of the prototype. Burcharth proposed to use as a characteristic velocity, the average of the time-averaged velocities at six points in the core. In this case however, a characteristic velocity inside the filter layer is necessary. It is proposed to take the average of the critical velocity at the interface of core and filter material, because the main interest point of the model test is to determine the amount of washout of sand from the core into the filter that is governed by the flow velocity at the interface of filter and core. The calculated characteristic velocity in the prototype will be scaled using the Froude scale law to a characteristic velocity in the model. Both characteristic velocities will be filled in in the Forchheimer relation. Then, a grain size for the filter in the model can be computed. In short;

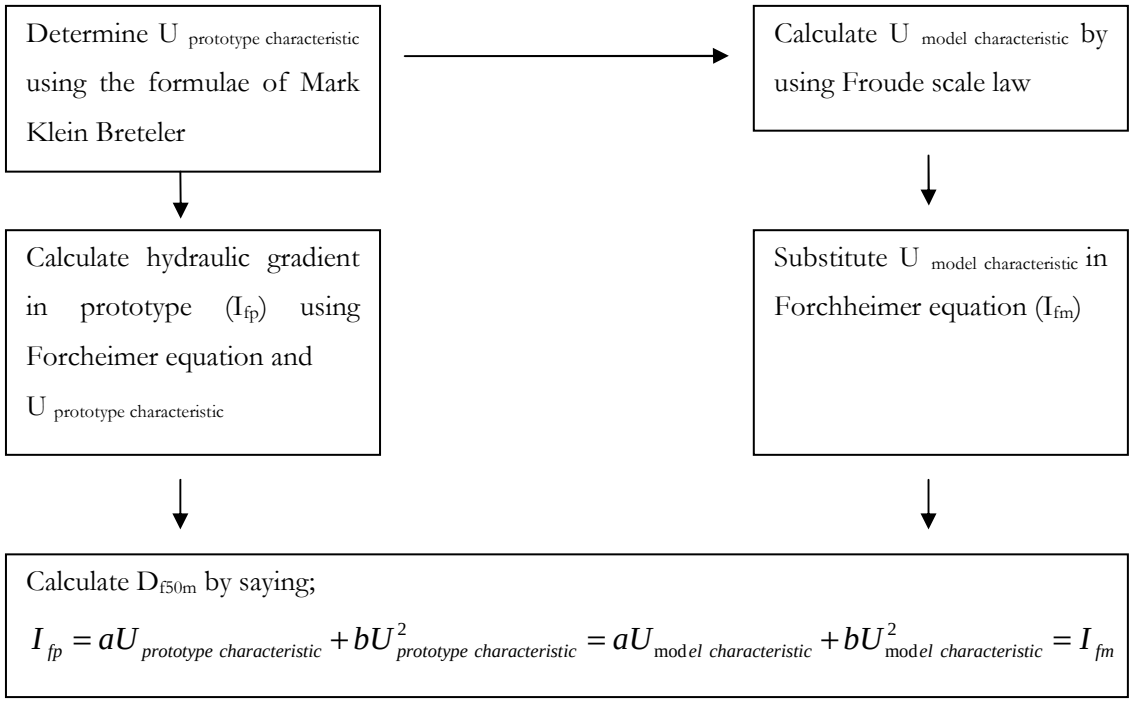

Table 2-1 Schematisation of steps in order to derive D_{f50m}

A problem when using this method is that during the test, the thickness of the filter will be changed in order to get erosion of the base material. As a result the velocities inside the filter of the model will not be the same as the characteristic velocity, so $I_p \neq I_m$ and thus no similarity between prototype and model. Suggestions to solve this problem are;

- Do not use the method of Burcharth and scale the prototype with the Froude scale law. This will result in high viscous forces and low Reynolds numbers and with the use of a bigger

grain size of the core material than it would be when scaled by use of Froude scale law, erosion and transport of the core material will be smaller then in reality.

- Do use the method of Burcharth, but instead of determining the characteristic velocity in the model by scaling the characteristic velocity in the prototype with Froude scale law, calculate the characteristic velocity in the model using the formula of M.KleinBreteler.

The last suggestion seems a good solution for the problem. The critical hydraulic gradients at the interface of core and filter are kept the same in model and prototype. This way, the transport or erosion process is as similar as possible. The problem of this method is that the ratio between core and filter material is not the same. In short this method looks like the following.

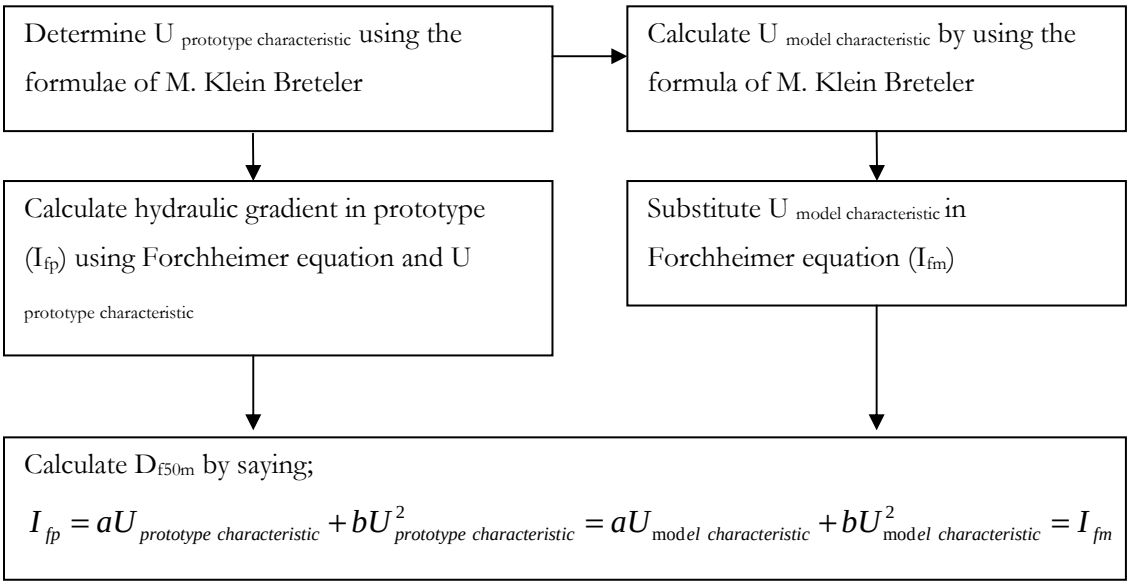

Table 2-2 Schematisation of the calculation of $D_{f50m,}$ by utilizing M. Klein Breteler

Because of the problems mentioned above, precaution must be taken in making conclusions based on the up-scaled results from the tests.

3 Experimental Set Up

3.1 Known & Unknown Factors

In this chapter, an approach to solve the problem mentioned in chapter 1 will be created. The objective was twofold:

- To get an insight in the transportation of sandy material out the core into a very open granular filter under influence of wave load

- To give a relation between;
    - Transport of material
    - Grain diameter base material
    - Grain diameter filter material
    - Thickness of filter layer
    - The hydraulic load

In the previous chapter the knowledge, which is available, is summarized. In short, this is;

- Knowledge is available about the start of motion of base material and the corresponding critical gradient or critical velocity at the interface of base and filter.

- Models have been developed to describe the water movement inside a rubble structure under wave attack.

- Limited knowledge is available about transport of material through a rubble mound structure. The models that have been created are only covering transport of material under influence of stationary flow perpendicular or parallel to the interface of base and filter.

- Limited knowledge is available about the amount of washout of sand particles from the core into the filter layer under a wave load.

- Limited knowledge is available about the behavior of the core material covered with an open filter layer under a wave load.

3.2 The Objective of the Experiments

To fulfill the objective of the Master's thesis as mention above, this research has to focus at three problems;

- The transport of sand under a non-stationary load through a filter layer of very coarse rubble mound material with a large ratio between the grains of the filter layer and the sand grains.

- The amount of sand washed out from the core and transported into the filter under a non-stationary load at the interface of core and filter.

- The transport rate of the sand through the filter layer.

Of course, these two problems are related to each other; the amount of transport might be affected by the amount of sand that is available to transport. Sand grains already washed out from the core can hinder the wash out of more sand grains. So, the faster the transport goes, the faster the sand grains will be moved away from the interface between core and filter, and the more sand grains can be washed out from the core.

When more insight is obtained in these problems and in combination with knowledge about the start of motion of sand material and the wave movement inside rubble mound structures, a model can be set up to describe the behavior of a rubble mount breakwater with a sandy core and a very open filter under wave load. First this will be a conceptual model with a physical foundation and then it might be possible to create a numerical model.

The main engineering question, which the model must be able to answer, is; what is the influence of the thickness of the filter layer with some grain size under a certain condition on the amount of transport of core material? When this question is answered an engineer will be able to create an economical design of a breakwater with a sandy core.

3.3 The Conceptual Model

It can be expected that the thickness of a filter layer will have influence on the amount of transport of core material in three ways;

- The filter layer will reduce the wave height exponentially when moving further inside the breakwater[21] (not because of breaking). So the thicker the filter layer, the smaller the wave load at the interface of core and filter, the smaller the amount of washed out material from the core, the smaller the amount of transport.

- When core material is transported through the filter layer it will make contact with the grains of the filter material. The sand grains from the core may bump or scratch along the grains of the filter reducing the velocity of the sand grains of the core material or may be even become zero. So the thicker a filter, the more a grain of the core will make contact with the filter material, the longer it will take for the core material to be washed out of the filter. When there is a high amount of core material present inside the filter layer there might be less wash out of material from the core so the process will be slowed down.

- The wave will break on the outside of the filter layer, causing a lot of turbulence. The turbulence will die out when moving further inside the filter layer. Turbulence is responsible for pressure fluctuations and for transporting sand grains away from the interface between the core and the filter layer. Pressure fluctuations direct above the interface between core and filter layer will lift sand grains out of the core.

It can be expected that the grain diameter of the base material and the filter material will have influence on the amount of transport of core material in three ways;

- The larger the grain size of the base material, the more difficult it is to wash the grain out of the core and to transport it. The amount of transport will then be smaller with increasing size of core material.

- The smaller the grain size of the filter material the larger the reduction of the wave load will be. The amount of transport will be smaller with decreasing size of filter material.

[21] Hólscher, 1988 [18]

- The smaller the ratio between the filter and base material is, the more the grains of the base material will collide with the filter material. The amount of transport will be smaller with decreasing ratio between filter and core material.

What are other properties of the breakwater that can influence the amount of transport, besides the parameters mentioned at the start of this chapter?

- The way of breaking, i.e. plunging or collapsing waves on the breakwater. Another type of breaking of the waves might be responsible for the generation of more or less turbulence. If the wave properties are the same the type of breaking is dependent of the slope of the breakwater. The Irribarren number represents a ratio of the slope steepness and the 'wave steepness' and gives an indication of the breaker type.

$$\xi = \frac{\tan\alpha}{\sqrt{H / L_0}} \quad with \quad L_0 = \frac{gT^2}{2\pi} \left(= deep - water - wavelenght\right)$$

  Surging ξ=5, collapsing ξ=3, plunging ξ=1.5, spilling ξ=0.2

- The uniformity of the filter material; the more uniform the filter material is, the more open the filter layer, so it is easier for a grain from the core to move trough the filter.

- The shape of the filter and core material, the roundness and the roughness will have influence on the transport and on the amount of washout from the core.

- The density of the core material. A high density of core material results in a low permeability that results in a higher internal set-up so the flow perpendicular to the interface between filter and core will increase. This means that the wash out of material from core into the filter will increase. On the other hand a higher density makes it more difficult for a grain from the core to move to the filter. This means that the wash out of material from core into the filter will decrease.

3.4 Model Test Set Up

In order to reach the objective, more insight is necessary in the whole process inside the filter layer and at the interface of core and filter. To obtain this, some model tests have been conducted. These model tests have been executed in a wave flume of the fluid mechanics laboratory of the Department of Hydraulic and Geotechnical Engineering of the faculty of Civil Engineering and Geosciences of Delft University of Technology.

The wave flume is a (sediment) transport flume with an effective length of 42.00m, a width of 0.80m and a maximum depth (h_{max}) of 1.00m. The bottom of the flume has a slope of 1:30 positioned at 8.8 m from the mid position of the wave board, and at one end of the flume an irregular, piston-type, electro-mechanically driven wave generator is placed with automatic reflection compensation and a stroke length of 2.00 meters.

3.4.1 Intended Learnings from the Test

After the test is performed, the following should be known;

- The erosion process can be described
- The amount of transport can be related to the influence of ratio between filter and core
- The amount of transport can be related to the influence of the thickness of the filter

3.4.2 Expected Observations during the Test

Because of the very low permeability of the base material and the much higher permeability of the filter the flow inside the filter at the interface of base and filter will be virtually parallel to the interface between base and filter. Den Adel concluded from tests with stationary flow parallel to the interface that the grains of the base were transported along the interface. But because we are dealing with a slope (which will force a grain under influence of the gravity to go down) and with cyclic flow with more turbulence because of the breaking of the waves it can be expected that the sand of the core will be transported further away from the interface and the sand will be moved in the direction of the toe of the breakwater when looking over a longer period then one wave cycle. At the toe smaller flow velocities will occur then at still water level, so sand might settle there. If not it will be washed out of the breakwater.

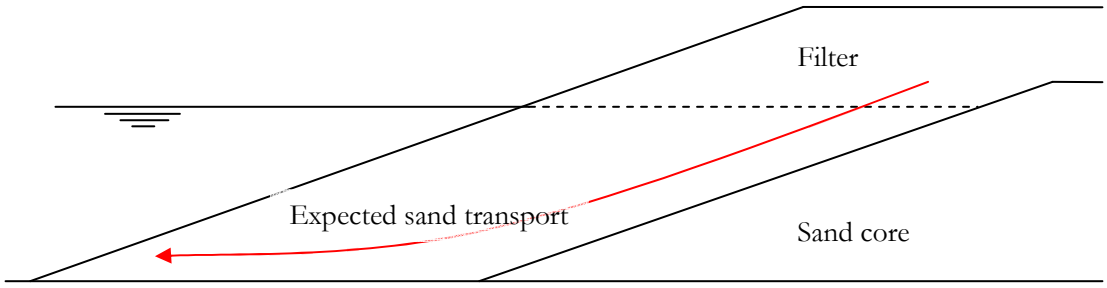

Figure 3-1 Schematisation of expected sand transport in breakwater

3.4.3 Process based Model Tests or Scaled Model Tests

When executing a model test, a choice has to be made between a process-based model test and a test based on a scaled prototype. In paragraph 2.5 a method based on the method of Burcharth has been developed to scale the filter material in case of a scaled prototype model test. The disadvantage of this method is that the velocities in the filter of the model as well as the velocities in the filter of the prototype must be estimated. Because of the limited knowledge of the processes inside the filter layer and the variable velocity in time, it is unknown which velocities must be used to have a good similarity between model and prototype.

A second problem when executing a scaled model test is that the core material (sand) cannot be scaled. When scaling sand, the grain size cannot be smaller than 100 μm, because when using sand with a grain size smaller than 100 μm it is not sand anymore but silt or clay. This means that the core material will get other properties such as cohesion, when the grain size of the core material is scaled to a value smaller than 100 μm. Cohesion will affect the transport of the core material, as cohesion makes it more difficult for a grain to move out of the core.

When scaling and then using the Froude scaling law (see paragraph 2.5), viscous forces are relatively too high and the amount of turbulence too low. Turbulence is believed to be important in the transportation process of the core material. Pressure fluctuations, due to turbulence, lift sand grains out of the core so, the water moving along the interface between the core and the filter, can take the sand grain along. As all dimensions are scaled with the same scale factor, the core material will be relatively large because sand cannot be scaled (see above). This results in less transport because a heavy grain is more difficult to move than a light and small grain. This, in combination with the relative small amount of turbulence and the limited knowledge of the processes inside the filter layer, will make it uncertain if model tests on a Froude scaled prototype will give reliable results.

When scaling using the Reynolds scaling law, other problems will rise. As the water velocity is reversibly proportional to the dimension, and the water velocity is dependent on the wave height, which is on her turn dependent on the flume dimensions, this results in a larger grain size of the filter in the model compared to the prototype. Using Reynolds scaling law is thus not feasible.

Lack of knowledge in the processes inside the filter of a breakwater makes it impossible to give a good estimate of the error in the results of a scaled model test when using one of the methods discussed above. Because of these problems, the choice has been made in executing process based model tests in order to increase the knowledge of the processes inside the filter layer of a breakwater.

3.4.4 Choice Test Parameters

In the model tests, several parameters can be varied. The most important are;

- The wave parameters:
  - Regular or irregular waves
  - Wave Height (H)
  - Wave period (T)
  - Total number of waves
- The filter layer parameters:
  - Grain size filter (D_f)
  - Grain distribution filter material
  - Thickness filter (d_f)
  - Shape filter material
  - Total number of filter layers
- The core material parameters:
  - Grain size core material (D_b)
  - Shape core material
  - Grain distribution core material
- Breakwater dimensions:
  - Steepness slope (α)

Due to limitations in time and availability of the facilities, a choice has to be made which of the above-mentioned parameters will be varied and which will be kept constant. For the parameters that were kept constant, values have been used which are typical for breakwaters and wind waves. The following parameters have been chosen to vary:

- The filter grain size. The filter grain size is chosen such that the ratio between filter material and core material is large.
- The filter thickness. The filter thickness is chosen such that erosion will occur. A first estimate for a filter thickness in the first experiment has been made based on the formulae of Mark Klein Breteler (see page 19) and that the wave height reduces exponentially when moving further into the filter. With the formulae of Mark Klein Breteler the critical velocity, belonging to the initiation of motion of the core material, is calculated. The water velocity at the interface is estimated by $U = \omega H/2$. Now a minimal filter thickness can be calculated in order to just have no erosion. Because erosion is wanted half of this thickness is taken.

For the other parameters the following values have been used:

- Regular waves instead of irregular because in a limited number of tests it is easier to compare the results of the different test with regular waves because in every test, the exact same wave conditions will occur.
- The wave period and wave height are chosen such that the steepness of the wave is typical for a wind wave. The wave height was 10 cm, the wave period was 1.2 s
- The total number of waves is chosen such that it is typical for a storm with a duration of 8 hours and with waves with an average period of 12 s.
- For the grain shape and grain distribution of the filter and core material, materials were used which were available. The grain size of the core material is taken rather small in order to make sure that erosion would take place.
- The total number of layers is chosen to be one. When using multiple layers with different grain sizes it makes it difficult to interpret the results. This one layer is a representation of the armour layers plus the under layers.

During the tests, hard measurements have been done as well as visual observations. The point of interest is the way the transport and erosion of the core material will occur. A very basic breakwater has been used as a starting point in these tests. The breakwater had the following features;

- Slope of 1:3
- Core of sand with a D_{b50} of 160 μm
- One thick geometrically open filter layer with different D_{f50} and different thickness:
  - D_{f50} = 1.8 cm, 3.25 cm, 4.4 cm (see Appendix 1)
  - d_f = 10 cm, 15 cm, 20 cm
- Wave parameters:
  - Regular waves
  - H = 10 cm

- T = 1.2 s
- In total, 9 experiments have been performed

3.4.5 Test Procedure

The tests were performed according to the following procedure:

- A board was placed vertically over the entire width and height of the flume, this was the rear side of the model. The board was placed 9 m from the toe of the 1:30 slope and 17.80 m from the mid position of the wave board (x_{wb}) (see Figure 3-4).

- Against this board, sand was installed. This was done by dropping the sand into the dry flume from a height of 1 m above the bottom of the flume (see Figure 3-2). The toe of the sand slope was 15.80 m from the mid position of the wave board and 7 m from the toe of the 1:30 slope ($x_{toe\ 1:30}$) (see Figure 3-4).

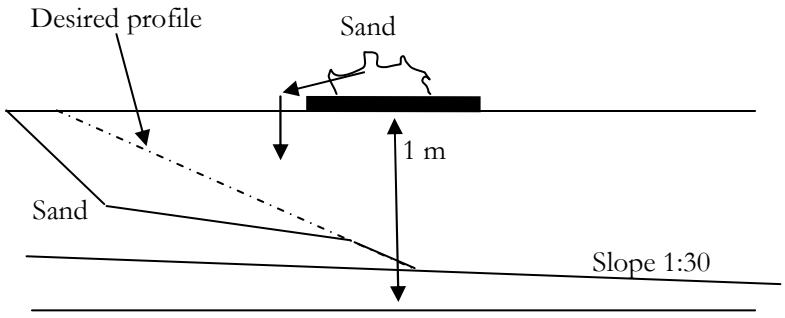

Figure 3-2 Cross-section of the model breakwater

- The flume was filled with water

- The slope was leveled and given a gradient of 1:3 by using a level device. This level device consisted out of a board which was guided by two rails put under the right gradient (see Figure 3-3)

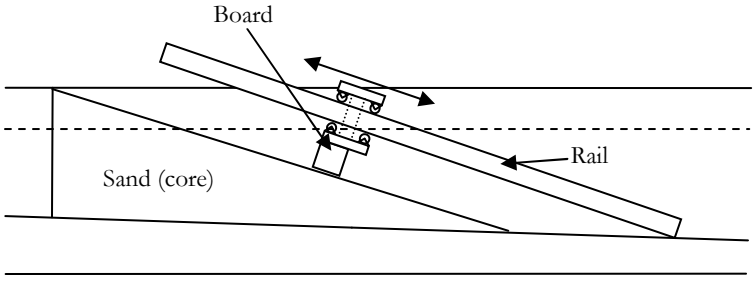

Figure 3-3 Level device

- On top of this sand slope the filter material was installed by dropping it from height of 10 cm above the sand into the right place. The last layer of stones was placed by hand. To ensure that the filter had the right thickness (d_f) the level device was placed with the required distance to the sand slope. Any holes under the board were filled with stones and at places which were to high stones were removed

- The water level (h) of the flume was checked with a normal tape roller and was set at 48 cm

- The wave gauge was placed at the toe of the breakwater and after that the wave gauge was validated

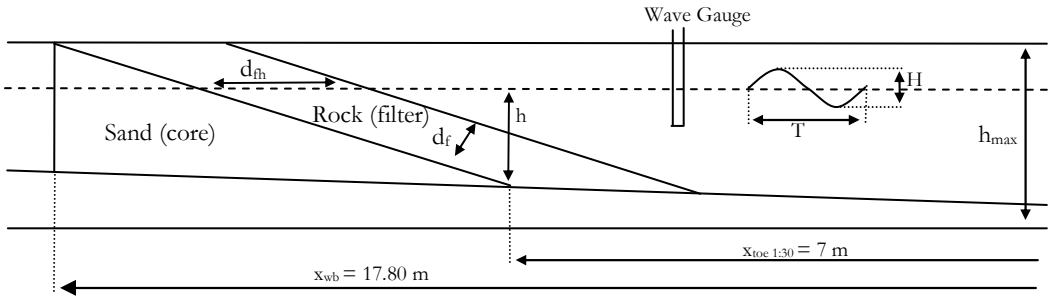

Figure 3-4 Test model in flume

- During these test the following factors have been measured;
  - The change of the profile of the sand slope in time
  - The wave properties at the toe of the breakwater
  - All have been monitored on video

- These parameters have been measured in the following way;
  - The change of the profile has been measured by taking every wave series a picture of the profile through the transparent wall of the flume (see Figure 3-5 and appendix 2). A wave series consisted out of 300 waves. These photos have been uploaded in a computer program, which is able to give the profile in series of x and y coordinates. Because this is done for every photo taken every 300 waves, the change of the profile in time can be plotted

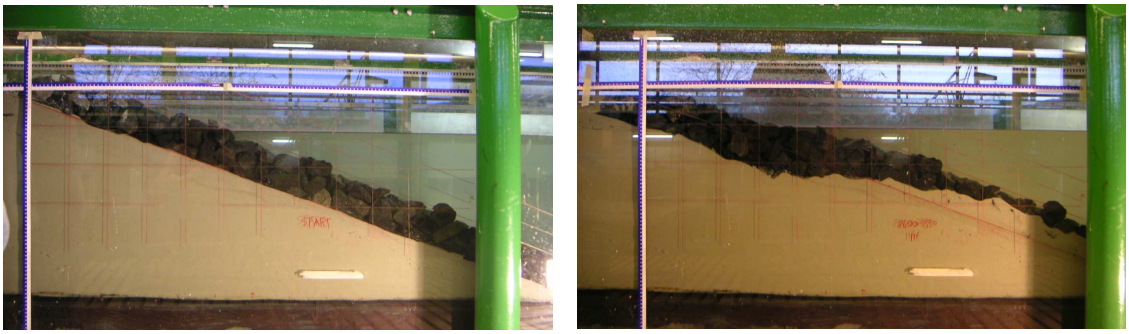

Figure 3-5 Profile of the test model observed through the transparent wall

- The wave properties have been measured by using standard wave gauges. This means that graphs with the surface elevation against time have been obtained. See Appendix 6

The parameters of the different experiments are listed in the following table, Table 3-1. The grading curves of the used filter materials and of the sand used for the core can be found in the appendix 1.

	filter thickness: df (cm)	grain size: Df50 (cm)	wave height: H (cm)	wave period: T (s)
Experiment 1	15	1.8	15	2
Experiment 2	15	1.8	varies	varies
Experiment 3	15	1.8	10	1.2
Experiment 4	20	1.8	10	1.2
Experiment 5	10	1.8	10	1.2
Experiment 6	15	3.3	10	1.2
Experiment 7	10	3.3	10	1.2
Experiment 8	15	4.2	10	1.2
Experiment 9	10	4.2	10	1.2

Table 3-1Overview of experiments

After the first experiment, the test procedure was changed into the test procedure as mentioned above. The original test procedure differed from the used test procedure in how the profile was measured. In the original test procedure, the change of the profile was measured by; carefully removing the filter layer after every 500 waves and measure the profile with a water level gauge. This proved to be not feasible, as the filter could not be removed without changing the profile. Also, this was a time-consuming operation.

In the first test, it was observed that the erosion process went too fast in order to receive a good description of the erosion process.
In the second test, other wave parameters have been tried to determine which wave parameters had to be used. The wave parameters that have been tried are:

- H = 15 cm, T = 2 s (Original wave)
- H = 5 cm, T = 0.8 s
- H = 7.5 cm, T = 1 s
- H = 10 cm, T = 1.2 s (used for test 3 to 9)
- H = 10 cm, T = 2 s

For the tests 3 till 9 the chosen wave parameters were: H = 10 cm and T = 1.2 s. These wave parameters were chosen based on visual observations through the wall (glass) of the flume. The erosion process was hardly visible with a wave with H = 5 cm, T = 0.8 s because there was hardly any transport of sand. Using waves with the parameters H = 15 cm, T = 2 s and H = 10 cm, T = 2 s resulted in a fast erosion process with much suspension transport. This makes it difficult to describe the erosion process. -This is subject of Chapter 4-

.

3.5 Validity Experiments

When executing model tests, faults will rise in the results. These faults can rise because of unwanted effects due to the test set up and because of inaccuracy in the measurements.

3.5.1 Measurements Inaccuracy

During the tests the following parameters were measured:

- Wave height
- Dimensions breakwater
- Sand profile core
- Thickness filter layer

The wave height was measured with a standard wave gauge this wave gauge has an accuracy of 0.5%. The waves were 100 mm thus the maximum fault in the wave height is 0.5 mm. The wave height was only measured to control if the wave generator was giving the desired wave. With the wave height no calculations were made. For all the tests the same wave input for the wave generator was used and because the tests were done with regular waves so the wave height can be averaged.

The dimensions of the breakwater and the water level were measured with a tape roller which has an accuracy of 1 mm. The smallest dimension which had to be measured was the filter thickness which was 100 mm. The maximum fault is then 1 %.

The sand profile was measured by making pictures of the profile and then by analyzing them with the software program GetData. The program converts the profile to a series of x and y coordinates. To obtain this series, the profile had to be traced by computer-mouse. In order to do this, the computer program was able to zoom in at the photo until only a few pixels of the photo were visible. The photos were taken with a 2 mega pixel camera; this means that multiple pixels per mm are available and so fault is smaller than 0.5 mm. But, as above the water level the profile was on some photos not clearly visible due to reflection, a larger fault has been made.

When installing the filter layer, use had been made of the level device. A tape roller was used to place this level device resulting in a fault in the thickness of 1 mm. The actual placement of the filter grains resulted in 5 mm fault in the filter thickness.

3.5.2 Faults due to Model Effects

Several model effects can be distinguished. The two most important in this research were:

- Wall effects
- Wave reflections

Wall effects have influence on the erosion of the core material. As it was not feasible to measure the profile in the center of the flume, it had to be measured by making photos through the wall of the flume. The wall of the flume probably had effects on the water movement and thus on the sediment transport. In order to estimate the fault, control measurements have been carried out. This has been done by carefully removing the filter layer and measuring the profile at several places along the width of the flume with a level gauge. The height along the width of the profile is chaotic so to give a reliable estimate of the fault, lots of measurements should have been made. Due to limitations in time, this has not been done. Only several control measurements have been made. It can be concluded that sometimes there was more erosion at the wall then in the center of the flume and sometimes it was the other way around. The profile along the width of the flume was not horizontal but showed small bumps and small holes influencing the measured results. Based on visual observations, wall effects seem to have an influence not larger then a few mm. No conclusions can be drawn that along the wall of the flume there is consistently more or less erosion than in the center

of the flume. Except at the top end of the erosion profile (point A in Figure 4-3) more erosion at the wall was observed than at the center.
In the experiments 7, 8 and 9 it was observed that the erosion on the right side of the flume was more than at the left side of the flume. This cannot be explained.

A piston type wave board equipped with automatic reflection compensation generated the waves. This reflection compensation makes sure that no reflected waves are returning from the wave board. In the wave records (see appendix 6), reflections can be observed. These reflections result in variations of wave height of approximately 3 mm.

4 Observations Wave Flume Experiments

In this section, the observations that have been made during the experiments will be presented. First, the observations concerning the sediment transport will be discussed, and then observations concerning the water movement will be discussed.

4.1 Sediment Transport Observations

The first observation made during the experiments is that a profile develops which resembles a bar profile on a sandy beach (see dotted line in Figure 4-2). During the experiments seven different areas can be distinguished. In these different areas different ways of sediment movement were observed. Each experiment that has been conducted resulted in the same basic shape of the sand profile. In the next two figures, Figure 4-1 and Figure 4-2, the seven different areas are indicated (A till G) and also the direction of the sediment flow is shown. The direction of sediment flow is divided in the direction of sediment flow when the wave is running down (red arrow) and in the direction of sediment flow during wave run-up (blue arrow). The sizes of the arrows give an indication of the amount of transport, the larger the arrow the larger the amount of transport. When no transport was observed a dot is placed. The amount of transport is estimated out of visual observations. The first figure, Figure 4-1, is at the start of the experiments and the second figure, Figure 4-2 is when a considerable amount of erosion and sedimentation has taken place.

Figure 4-3 is a photograph of the experiment taken at the ending stage, when a large amount of erosion has taken place.

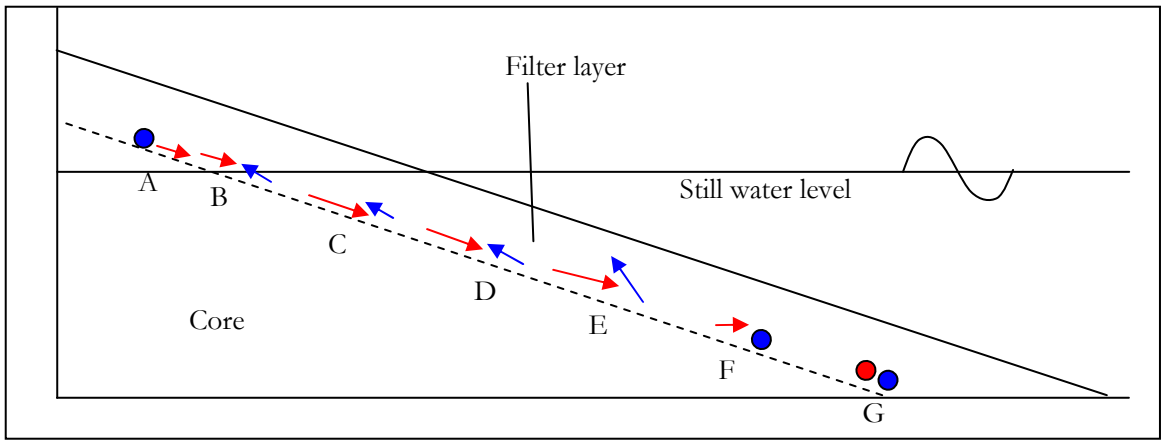

Figure 4-1 Schematisation of sediment transport observations, begin phase

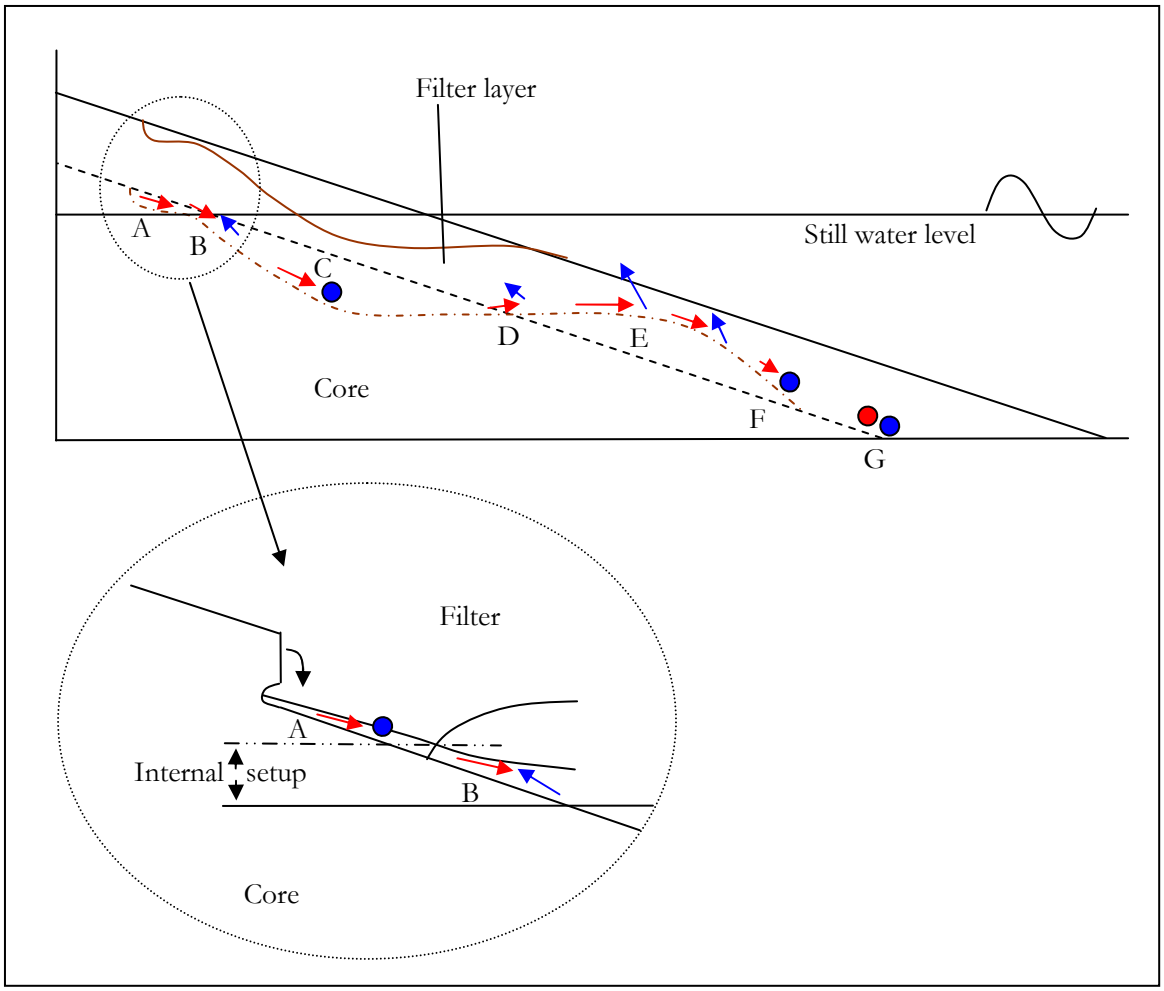

Figure 4-2 Schematisation of sediment transport with considerable amount of erosion

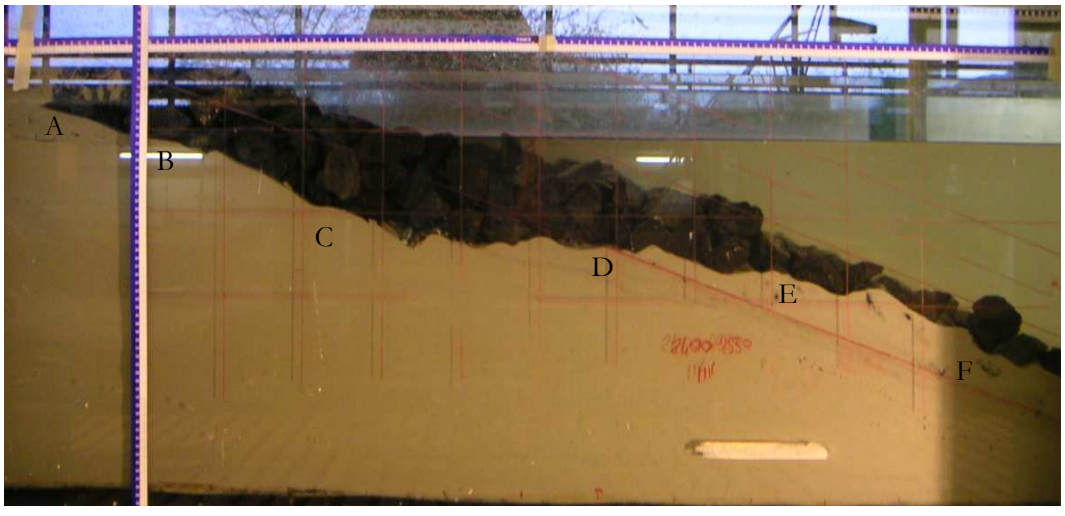

Figure 4-3 Photograph of sediment transport with amount of erosion

Bottom & Suspension Transport

Two different types of erosion have been observed during the experiments. These are the bottom transport and the suspension transport;

- Bottom transport can be visualized as a blanket of sand grains of some number of grains thick sliding over the sand slope, in other words the moving sand grains follow the sand slope as indicated in Figure 4-4. This type of bottom transport can be called sheet-flow transport. The thickness of the 'blanket' of sand grains could not exactly be determined but it is approximately in the range of one to 10 sand grains thick.

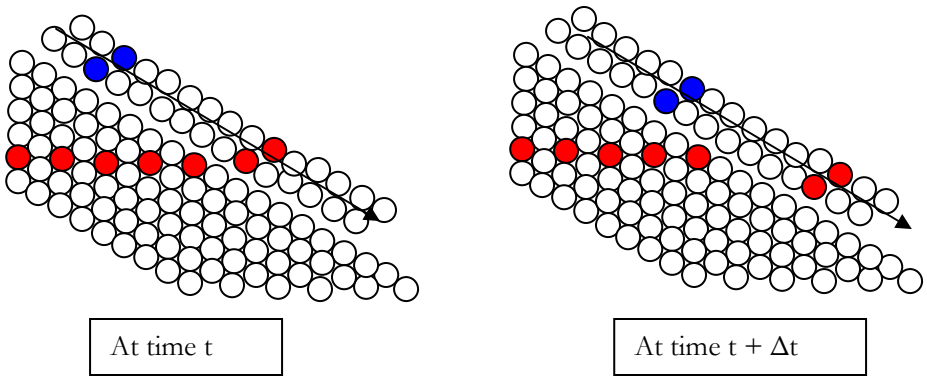

Figure 4-4 Bottom transport

- Suspension transport; individual sand grains are transported along the sand slope without making contact to it, as indicated in Figure 4-5

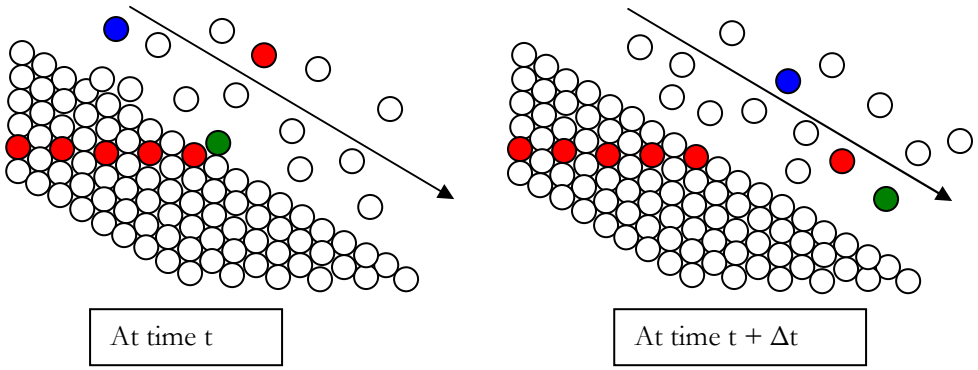

Figure 4-5Suspension transport

A combination of these two types of transport or only one of the two types can be responsible for the transport of the sand.

Description Sediment Transport Step-by-Step

This paragraph describes the sediment transport as observed during the experiments. For each point of the breakwater-interface between filter and core, A to G of Figure 4-1 and Figure 4-2, the sediment movement is described.

Point A

Point A lies a few centimeters above the still water level. At point A, erosion will take place. A steep, almost vertical sloop in the sand will develop, as indicated in the close-up in Figure 4-2. This steep slope is undermined by the reduced up-running wave. When enough sand is removed at the bottom of the steep slope, a part of the sand above the undermining will collapse and will be gradually moved in the direction of the toe of the breakwater.

Point B

This point lies around the intersection of the sand slope with the still water level. The sand is moving up and down along the sand slope under influence of the reduced wave inside the filter layer. The reduced wave and thus the up and down movement of the sand is not in phase with the up and down movement of the wave on the outside of the filter layer. Part of this transport of sand takes place as bottom transport and part of it as suspension transport. If the filter layer gets thicker, a larger part of the total transport is bottom transport. The same counts for the grain size; if the grain size of the filter material gets smaller, a larger part of the total transport is bottom transport. The width of the filter measured over the horizontal at still water level increases during a test, causing the amount of transport to decrease.

Point C

Point C lies in an area where net erosion takes place. During wave run-down the sand is mainly transported by bottom transport. Only with a large grain size of the filter material or a thin filter layer a small part of the transport is suspension transport. The amount of suspension transport during wave run-down will decrease during the test.

During wave run-up there is less transport of sand then during wave run-down, also a larger part of the transport is suspension transport. During the test the amount of transport during wave run-up will decrease, until there is no transport at all.

Point D

Point D lies at a point where the net erosion and net sedimentation is zero. During wave run-down the sand is mainly transported by bottom transport. Only with a large grain size of the filter material or a thin filter layer a small part of the transport is suspension transport.
During wave run-up a large part of the sand is transported by suspension transport. During the test, the amount of transported sand will decrease but will not become zero.

Point E
Point E lies at a point where net sedimentation takes place. During the tests this area becomes horizontal. With a large grain size of filter material and a thin filter layer this point can reach the outside of the filter layer after 2400 waves. A lot of suspension transport can be observed. The sand moves out of the filter layer with a thin filter layer and a large grain size of the filter material.

Point F
At start of the test the transport of the sand during wave run-down is bottom and suspension transport. At the end of the tests there is only bottom transport observed. During wave run-up there is no transport of the sand

Point G
Point G lies at the toe of the sand slope. As well as during wave run-up and during wave run down no transport of sand has been visualized.

For points C until G, the transport during wave run-up and during wave run-down it counts that with a thicker filter and a smaller grain size of the filter material the transport of sand will shift from suspension transport to bottom transport and the total transport is smaller.

4.2 Observations Water Movement

During the experiments internal setup has been observed in the filter layer. Because of the internal setup the average water level, at the interface of the filter layer and the core (long dash, double dot, line in Figure 4-2), is a few centimeters higher than the still water level.
This internal setup depends on the grain size and the thickness of the filter. In experiment 4 (d_f = 20 cm and D_{f50} = 1.8 cm), the internal setup is approximately 3 cm, while in experiment 9 (d_f = 10 cm and D_{f50} = 4.4 cm) the internal setup is almost 0 cm at the start of the experiment. At the end of experiment 9, the internal setup increases to approximately 1 cm. It has been tried to measure the internal setup by making screenshots out of the movie made of the experiments. These screenshots

have been made in "windows movie maker" and "adobe premiere pro" and interpret with Get Data to measure the internal setup. The waterline inside the filter layer was not always visible on the screenshots so this method did not work.

Concerning the water movement two different areas can be distinguished. The first area is between points A and B in Figure 4-2, the second area is between points C and F in Figure 4-2.

- Between point A and B, a small wave inside the filter layer develops after breaking of the wave on the outside of the filter layer. This reduced wave has an amplitude of approximately 1 to 2 cm and a period of 1.2 s. This reduced wave is running up and down the sand slope without breaking.
- Between points C and F. When the wave is running up the slope of the breakwater, the thickness of the water layer on the outside of the filter layer (d_{wu}) is much thicker then the thickness of the water layer on the outside of the filter layer (d_{wd}) when the wave is running down. (Figure 4-6) The amount of water running up and running down the breakwater during one wave cycle must be the same. So this in combination with the difference in thickness of the water layers it can be concluded that during wave one wave cycle the amount of water moving up the slope trough the filter layer is smaller then the amount of water moving down the slope through the filter layer. Resulting in a higher water velocity inside the filter layer when the wave is running down then when the wave is running up. Notice in the first picture of Figure 4-6 that the lowest point the wave is reaching on the slope is directly above point D. This is also the case for all the other experiments.

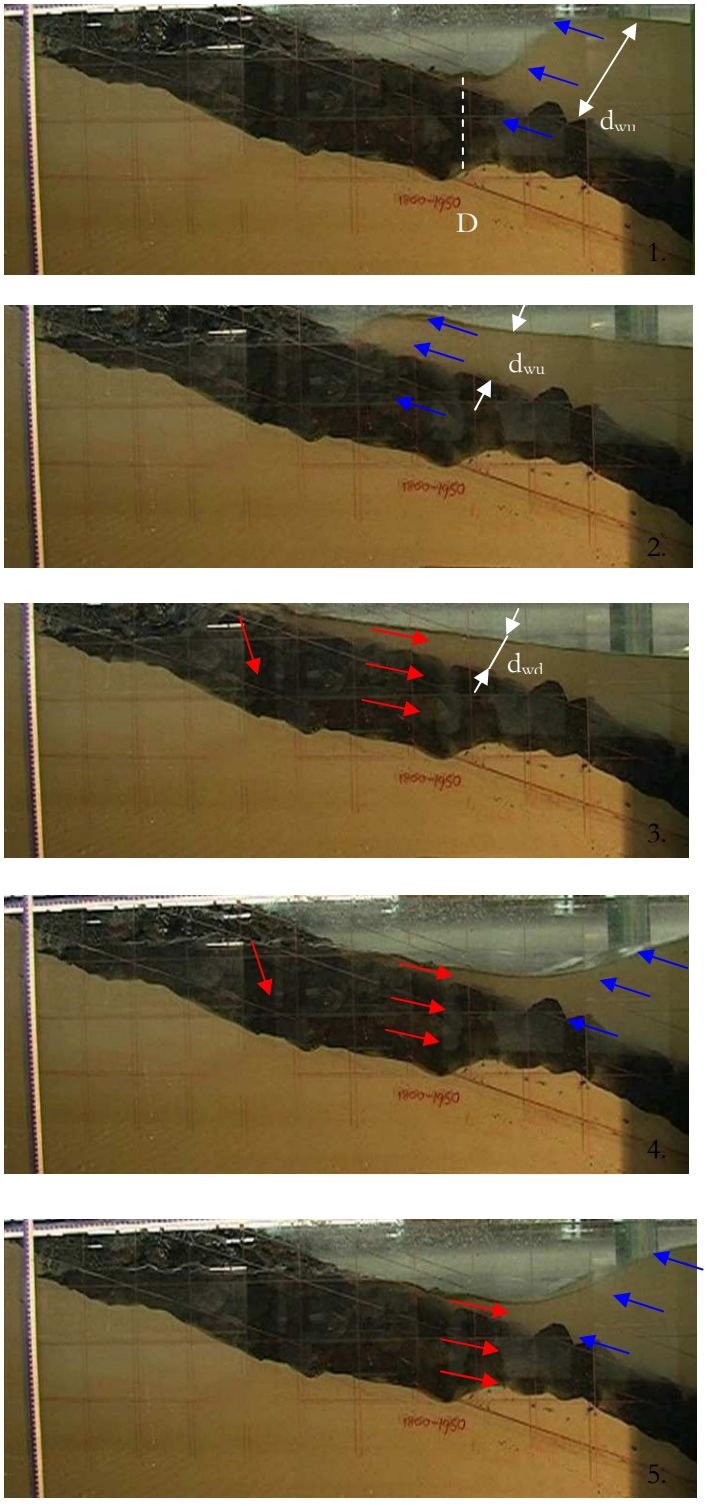

Figure 4-6 Observation of water movement

5 Quantitative Analysis

In this section, the measurements made during the experiments will be presented.

As mentioned in paragraph 3.4, the change of the sand profile has been monitored by taking every 300 waves a photo of the profile. To obtain the sand profile in series of x and y coordinates, these photos have been analyzed using the computer program 'Get Data' which is a program to digitalize scanned graphs. These series of x and y coordinates have been plotted, resulting in a graph in which the profile of the sand slope, after a number of waves, can be seen. When the profiles of one experiment after every 600 waves are plotted in one graph, the change of the profile in time is visualized (See Figure 5-1, Figure 5-2 and the graphs in appendix 3). When these graphs are examined, it can be seen that at points A, B and C erosion has been taken place and that at points E and F sedimentation is occurring. This is consisted with the observations made in chapter 4. The distance between two succeeding lines is the amount of sedimentation or erosion. It can be seen that at points C and B the amount of erosion is decreasing in time (i.e. the lines of the profiles after 1800 waves and 2400 waves are closer together than the lines of the profiles of the start and after 600 waves).

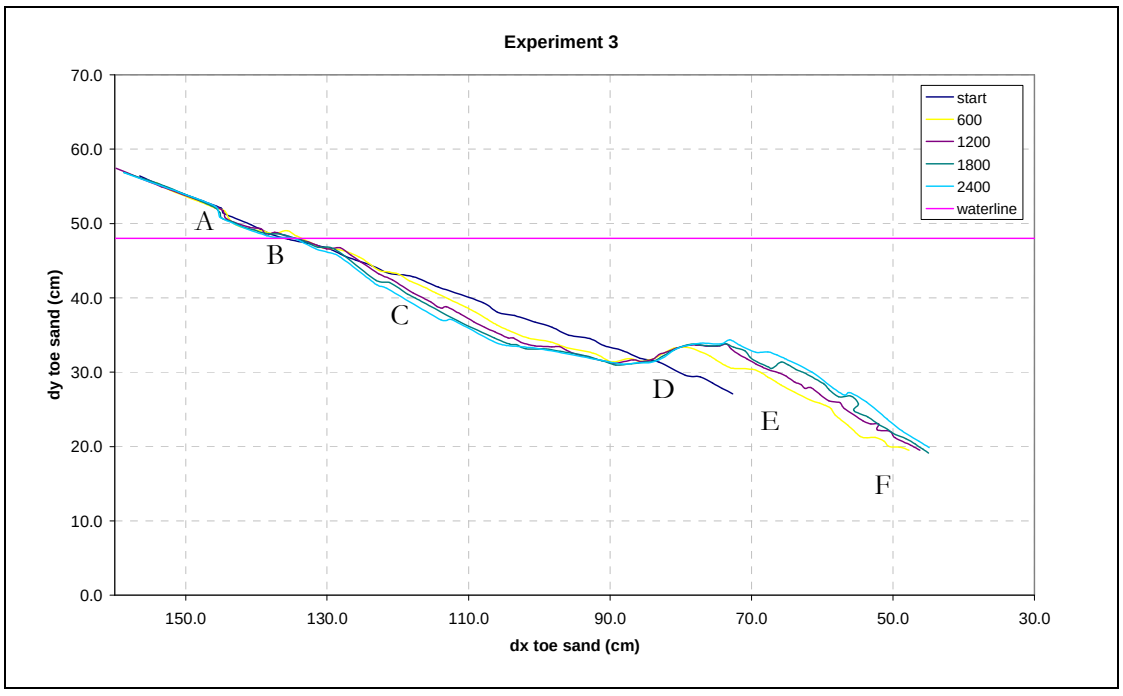

Figure 5-1 Profiles experiment 3 after every 600 waves

At point A, the change of the profile is not continuous like at points B and C. The erosion process at point A is discontinuous (see paragraph 4.1). This makes it difficult to see if the erosion is decreasing in time or not.

At Point D the profile is not changing in time.

At point E the change of the profile is decreasing in time meaning that the sedimentation at point E is decreasing in time. For experiments with thicker filter layers (i.e. experiments 3, 4, 6 and 8) the erosion at point B is smaller than the erosion at A and C, resulting in a 'bar' in the profile. The experiments with the thin filter layers (experiments 5, 7 and 9) this 'bar' is not there.

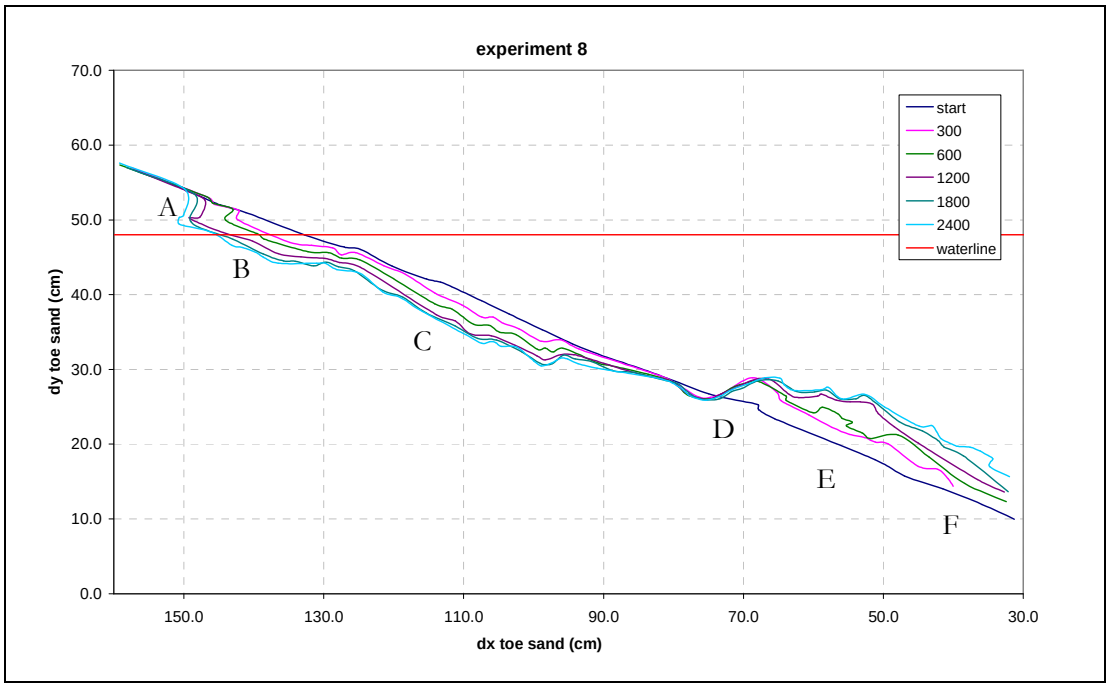

Figure 5-2: Profiles experiment 8 after every 600 waves

5.1 Erosion and Erosion Rate

To determine the total erosion after a certain number of waves X, the area between the start profile and the profile after X waves must be determined. Because the total erosion is calculated, the area is bounded at point D and A with the intersection of the start profile and the profile after X waves. This is done for the experiments 3 to 9. The total erosion is calculated after the first 300 waves and then after every 600 waves. This is plotted in Figure 5-3. In these figures it can be seen that:

- For all experiments the erosion rate (steepness graph) is decreasing in time. But after 2400 waves, the erosion has not become zero
- The thinner the filter layer, the more erosion is taken place
- The larger the grain size of the filter, the more erosion is taken place
- The erosion rate (steepness graph) after 2400 waves is smaller with a thick filter layer and a small grain size then with a thin filter layer and a large grain size.

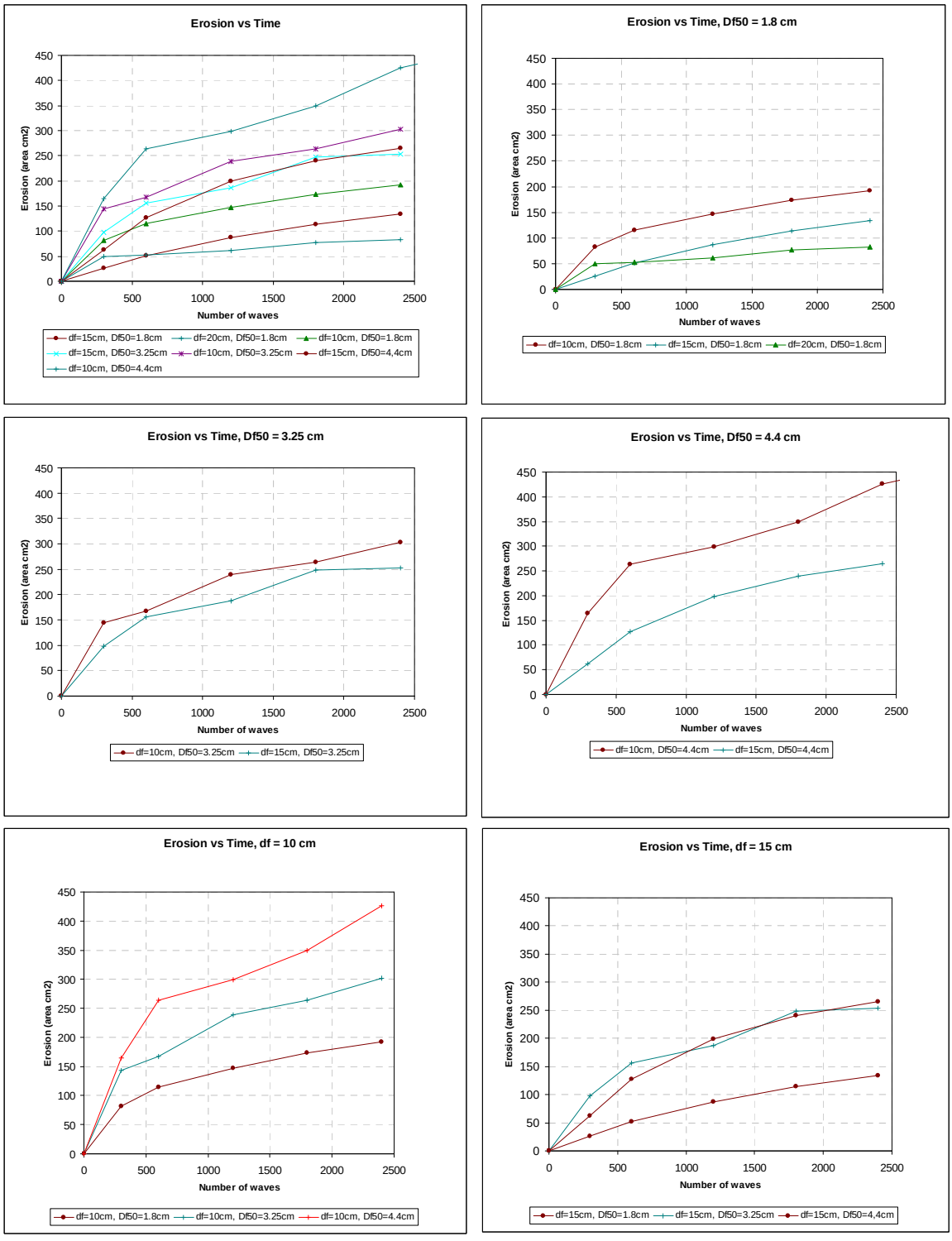

Figure 5-3: Erosion in time

There are three things that are not following the above-mentioned conclusions;

- At the start of the experiments the erosion goes faster at experiment 4 (df = 20 cm) then at experiment 3 (df = 15cm). This can be a result of inaccuracy in the measurements.
- Experiments 6 (D_{f50} = 3.25cm, d_f = 15 cm) and 8 (D_{f50} = 4.4 cm, d_f = 15 cm) are having almost the same erosion curve. This is strange as the grain size is different and the thickness the same
- For experiment 9; the figure is showing an increase of the erosion between 600 and 2400 waves, while al the other experiments are showing a decrease in the erosion. Experiment 9 was extended to 4600 waves the erosion is after 2400 waves decreasing in time (see Figure 5-4).

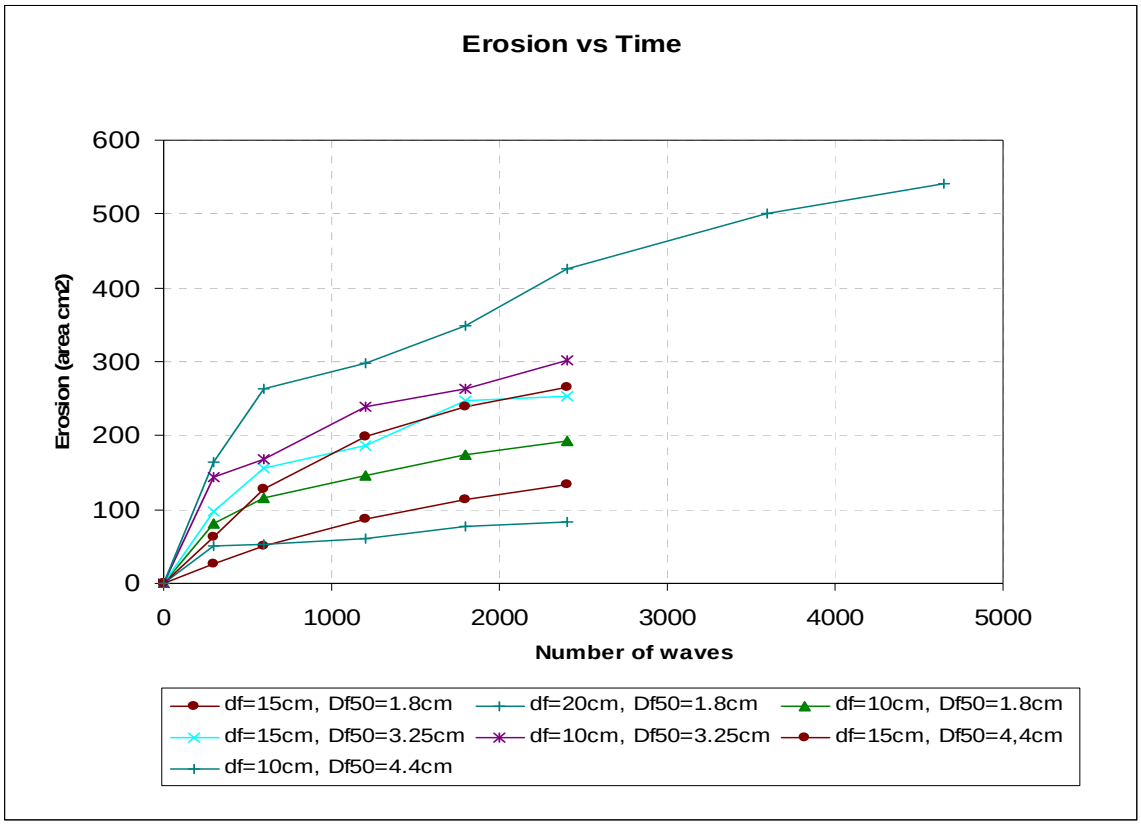

Figure 5-4 Erosion in time experiment 9 extended

Figure 5-3 shows that the erosion is dependent on the thickness of the filter and on the grain size of the filter. An increasing thickness and a decreasing grain size of the filter results in less erosion. This makes it reasonable to expect the erosion to be dependent on the filter thickness divided by the grain size of the filter material.

$$m = \frac{d_f}{D_{f50}}$$

m can be seen as an indication of the number of filter grains (*m*) on top of the core material. In other words; the erosion with a thick filter with large filter grains can be the same as the erosion with a thin filter and small filter grains.

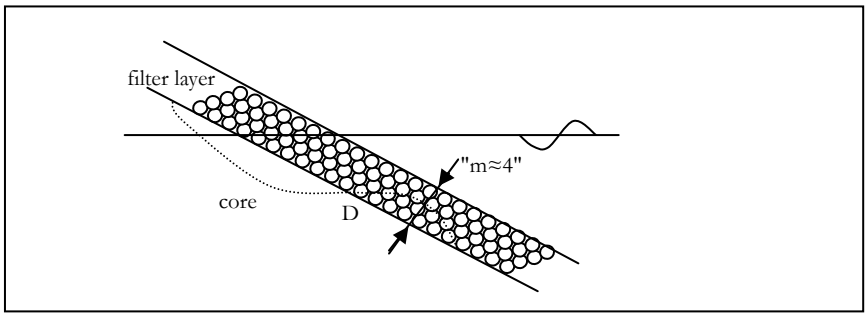

Figure 5-5 Definition sketch *m*

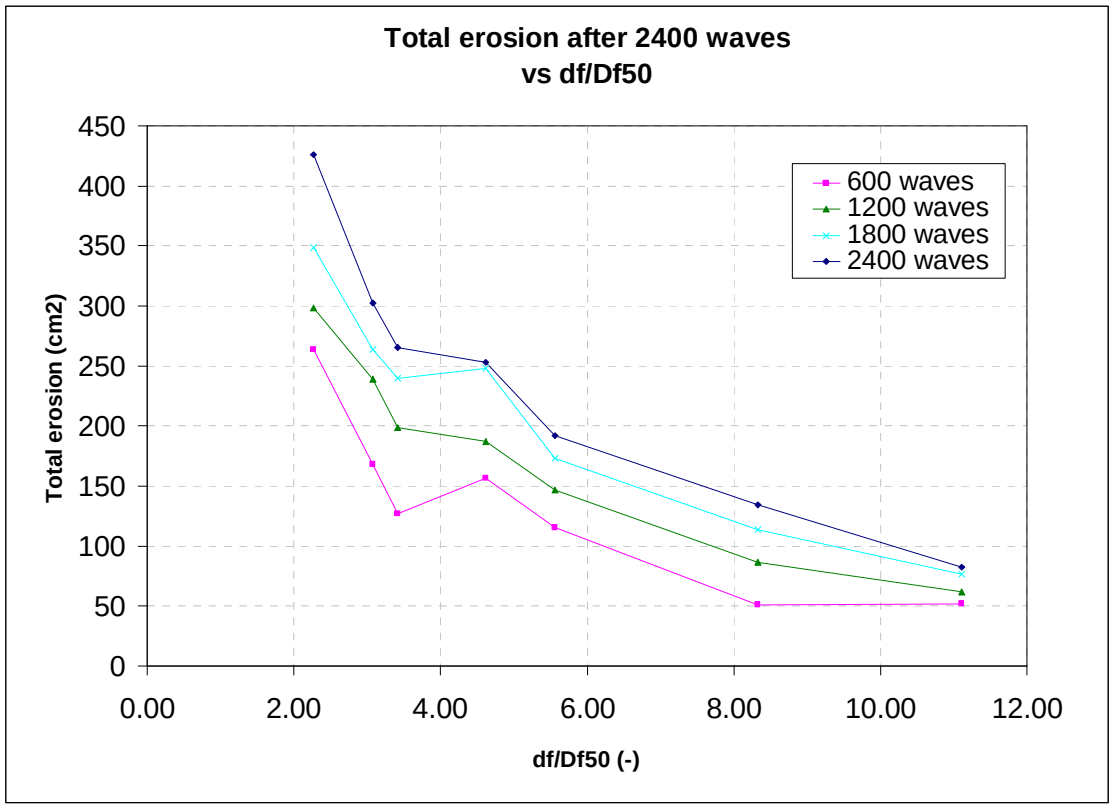

Figure 5-6 Erosion vs df/Df50

The erosion after a certain number of waves has been plotted against d_f/D_{f50} (see Figure 5-6). In this figure it can be seen that the erosion decreases with an increasing d_f/D_{f50}. It also can be seen that with an increasing d_f/D_{f50} the erosion is decreasing faster with a d_f/D_{f50} between 2 and 4 then when d_f/D_{f50} is larger then 5. In other words when there are less then 3.5 grains on top of the core material the erosion will increase enormously.

The erosion could also have been plotted against a d_f or D_{f50} which have been made dimensionless by the wave parameters. This has not been done because it would have only scaled the graphs, as the wave parameters were kept constant in all experiments.

In the next few paragraphs several other parameters have been plotted against the d_f/D_{f50}. This has been done for the same reason as mentioned above.

5.2 Relative Erosion Length

In Figure 5-7 and in appendix 5 can be seen that point D moves under influence of the filter thickness. It was expected that with an increasing filter thickness, point D would move up the slope. But, against expectations, point D moves down when increasing the filter thickness. The distance between D and the intersection of the start profile and the waterline (I), or in other words, the relative erosion length Lr (see Figure 5-8) is plotted against the filter thickness in Figure 5-9.

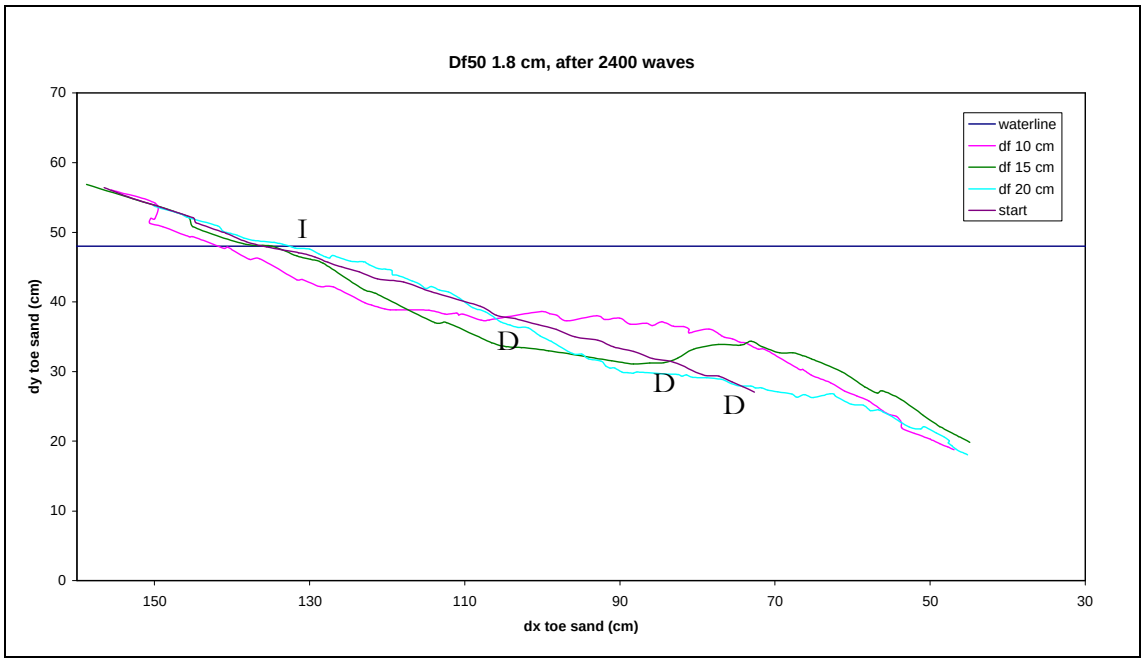

Figure 5-7 Profiles with different thickness and the same grain size

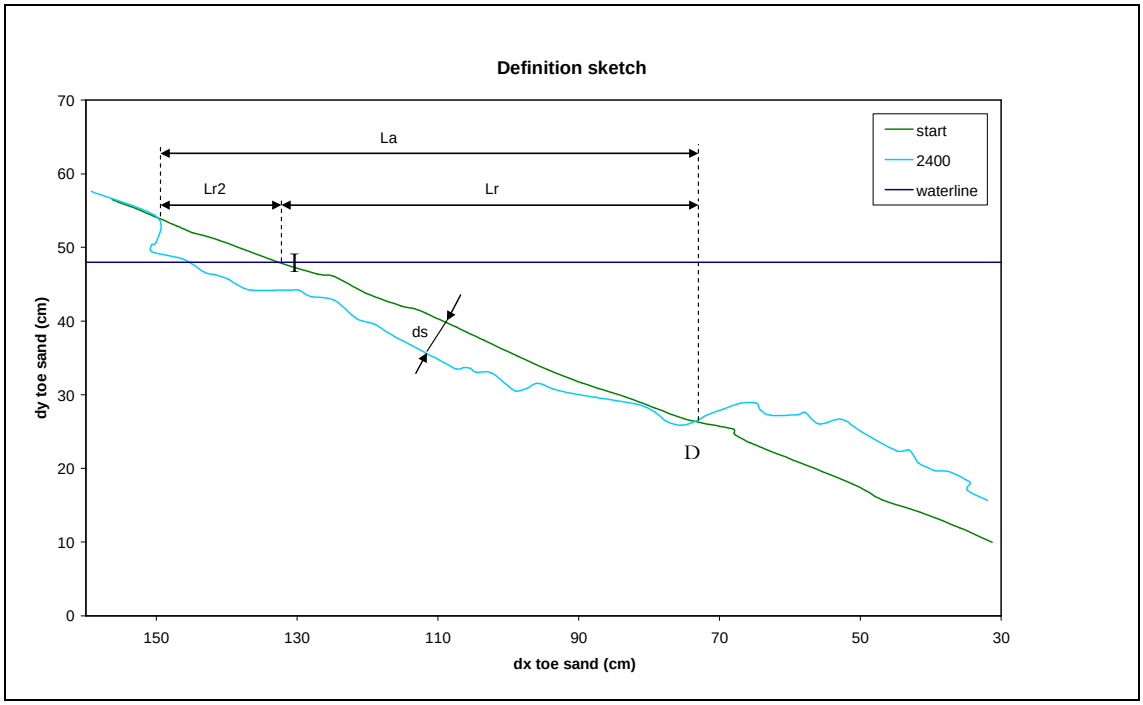

Figure 5-8 Definition sketch

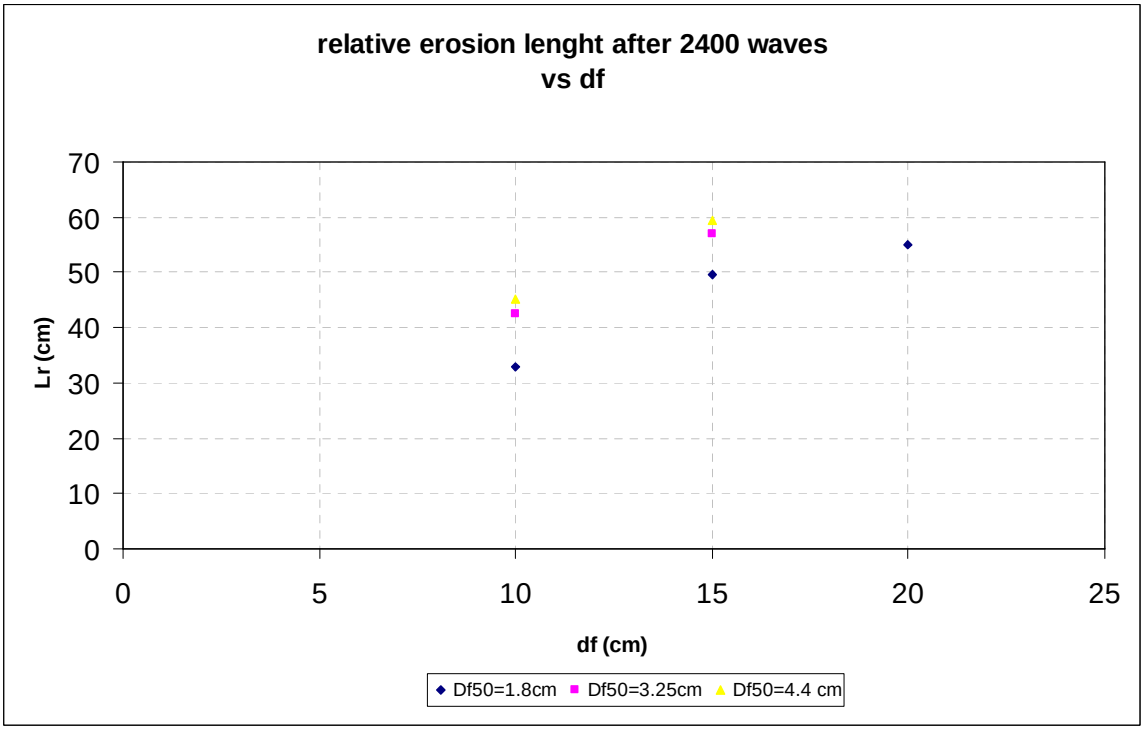

Figure 5-9 Relative erosion length against filter thickness

In Figure 5-9 can be seen that the relative erosion length is depended on the grain size and the filter thickness. The larger the grain size of the filter material, the longer the relative erosion length. This can be explained; with a larger grain size, the wave can penetrate more easily into the filter layer and

thus causing at deeper places erosion than the same wave at a filter layer with a smaller grain size, resulting in a longer Lr. This difference in relative erosion length is clearly visible between the Lr with a D_{f50} of 1.8 cm and the Lr with a D_{f50} of 3.25 cm, however this difference is not so clear between the Lr with a D_{f50} of 3.25 cm and the Lr with a D_{f50} of 4.4 cm.

In Figure 5-9 it can also be seen that the relative erosion length increases with an increasing filter thickness. This is strange because it is easier for a wave to penetrate through a thin filter layer then through a thick filter layer. Maybe, it can be explained with the observation made in paragraph 4.2 that point D is approximately directly under the run down point of the wave on the filter layer (run down point of the wave on the filter layer = lowest point the wave reach on the outside of the filter layer) see Figure 5-10.

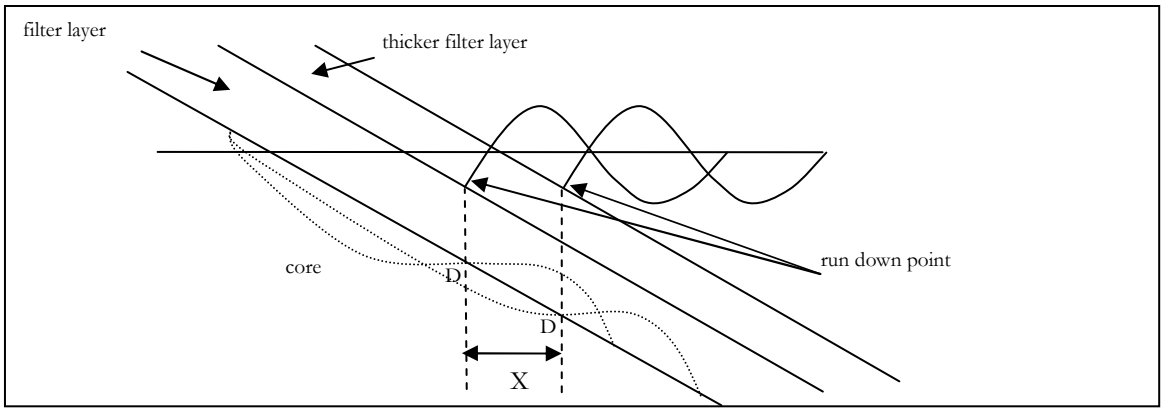

Figure 5-10 Sketch run down point versus point D

In Figure 5-11 the relative erosion length divided by the grain size of the filter material is plotted against the filter thickness divided by the grain size of the filter material.

The relative erosion length divided by the grain size of the filter material can be seen as an indication of the number of grains along the slope between the intersection of the interface with the still water level and point D.

$$p = \frac{Lr}{D_{f50}}$$

By drawing a trend line through the measurements points it can be shown that there is a linear relation between *m* and *p*.

$$p = 2.5 \times m + 4.5$$

$$\downarrow$$

$$\frac{Lr}{D_{f50}} = 2.5 \times \frac{d_f}{D_{f50}} + 4.5$$

$$\downarrow$$

$$Lr = \underbrace{2.5 \times d_f}_{1} + \underbrace{4.5 \times D_{f50}}_{2}$$

Part two of this equation is consistent with the explanation above; the larger the grain size of the filter material the longer the relative erosion length.

Part one of the equation seems strange because it says that with an increasing filter thickness the erosion length will increase. As mentioned above, this can be explained by the run down point of the wave on the outside of the filter layer (see Figure 5-10). If point D was only dependent on the run down point and not on the influence of d_f on the water movement, then d_f should have been multiplied with 3.2 and not with 2.5, because $x = 3.2 \times d_f$ (see Figure 5-10). The difference can be explained by the fact that the thicker the filter layer is, the more difficult it is for a wave to penetrate through the filter layer. This then results in a higher position of point D and thus a shorter relative erosion length. Care has to be taken when using this formula because it is based on a limited data set.

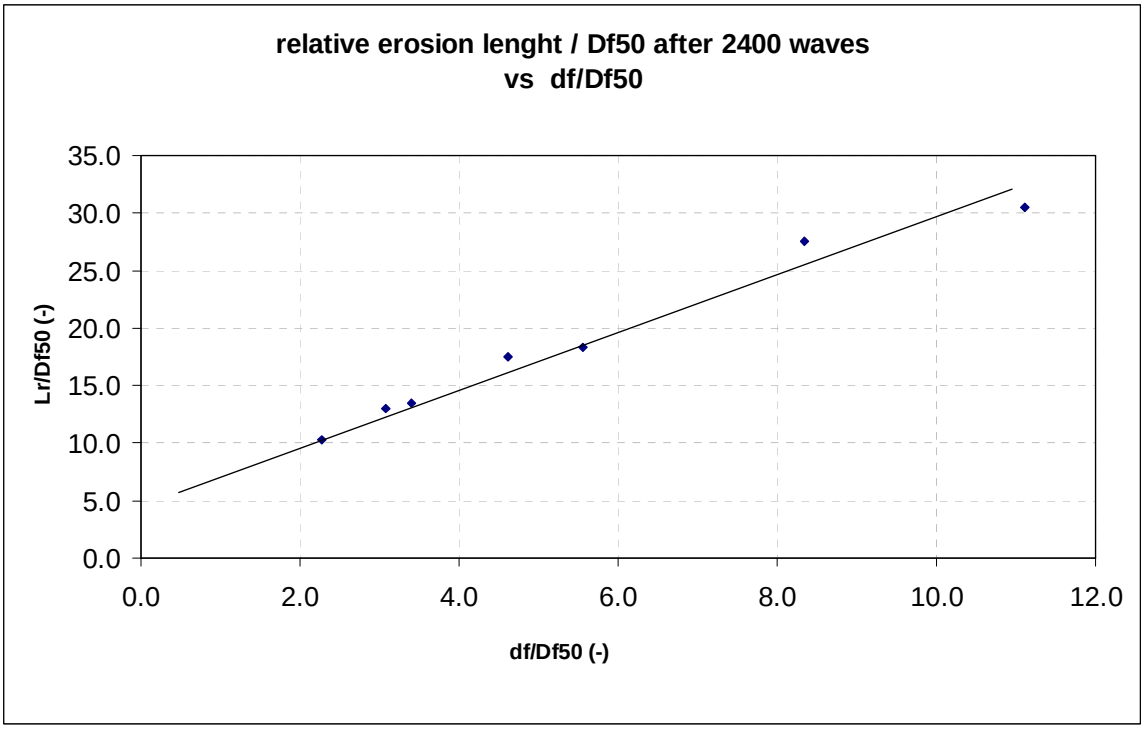

Figure 5-11 Relative erosion length/D_{f50} against filter thickness/D_{f50}

5.3 Relative Erosion Length 2, Lr2

The distance between point A and the intersection of the water line with the start profile (relative erosion length 2 (Lr2) (see Figure 5-8) is plotted in Figure 5-12. In this figure it can be seen that the relative erosion length 2 decreases with a thicker filter layer and with a smaller grain size of the filter layer. This makes sense as the erosion at point A governs the relative erosion length and the erosion

at point A is governed by the reduced wave. This reduced wave is reduced more when moving further into a filter layer and when the grain size of the filter layer is smaller.

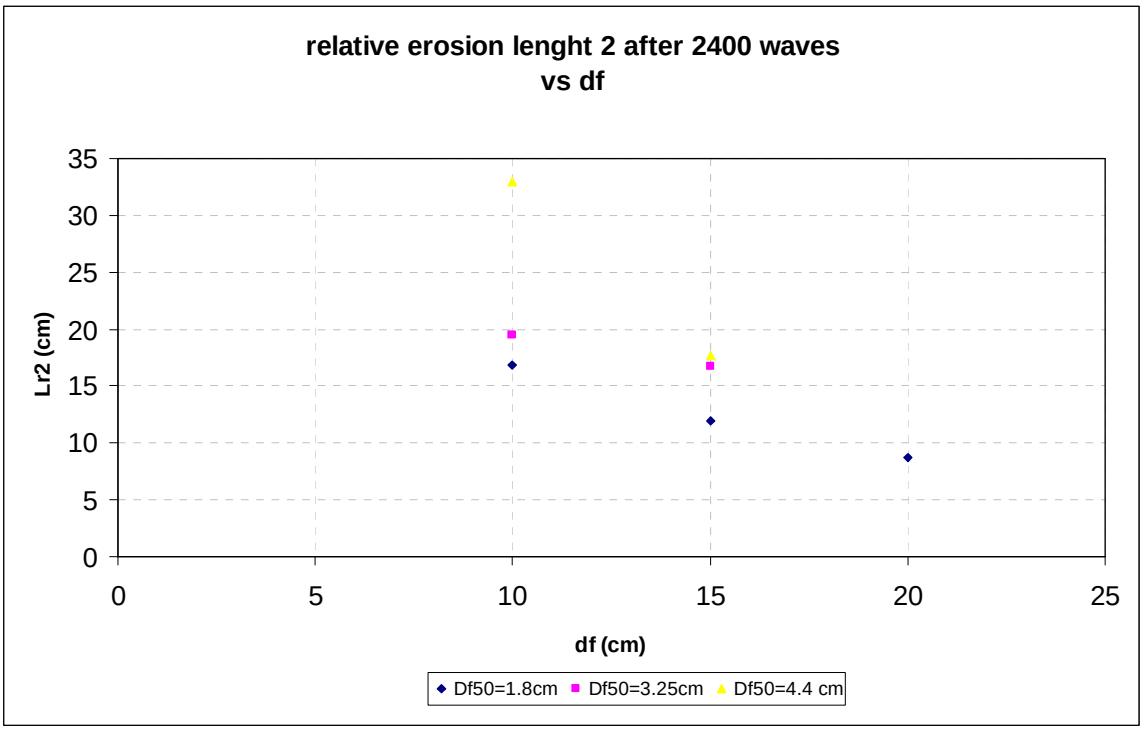

Figure 5-12 relative erosion length 2 against filter thickness

When the relative erosion length 2 is plotted against m (the filter thickness divided by the grain size of the filter material), it can be seen that the erosion length decreases with an increasing number of grains in the filter layer. Whether the trend line through the measurements points is a straight line (see Figure 5-13) or a curved line (see Figure 5-14), cannot be determined because too few measurements are available.

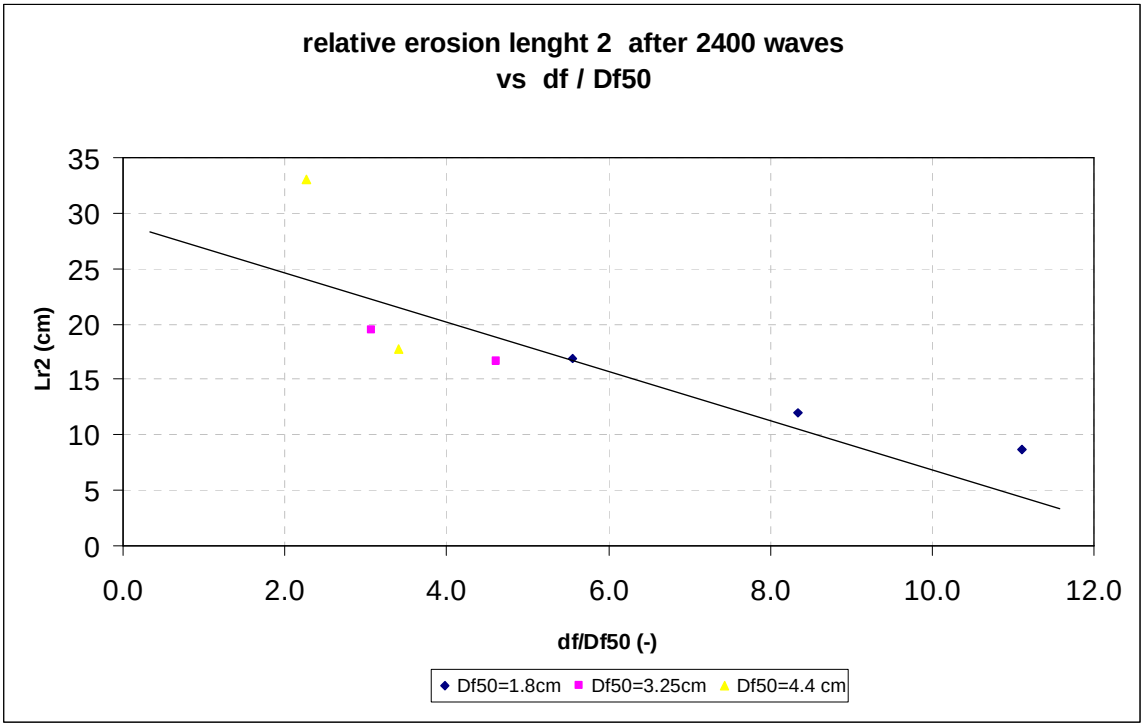

Figure 5-13 Relative erosion length 2 against filter thickness/filter grain size

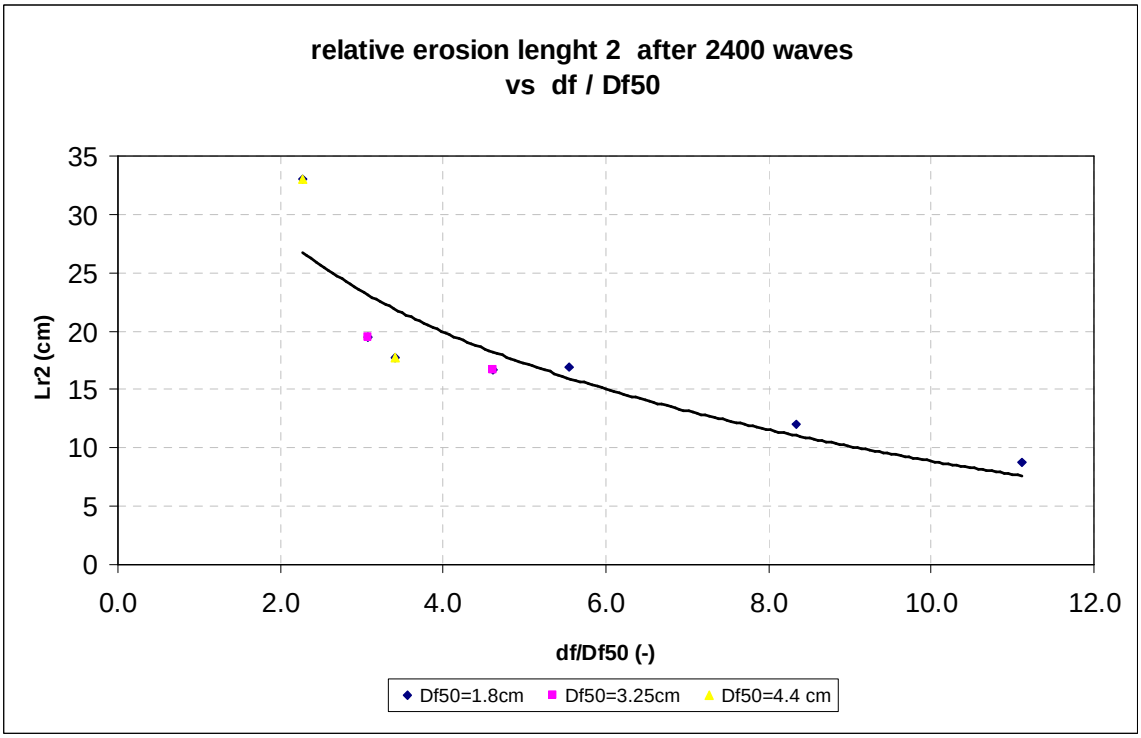

Figure 5-14 Relative erosion length 2 against filter thickness/filter grain size

5.4 Erosion Depth

Another important parameter is the erosion depth (d_s) (see Figure 5-8). The d_s is defined as the erosion at 2400 waves divided with the absolute erosion length (La). Much erosion with a small La results in a large d_s, while the same amount of erosion with a large La results in a small d_s which might be acceptable while the large d_s is not acceptable.

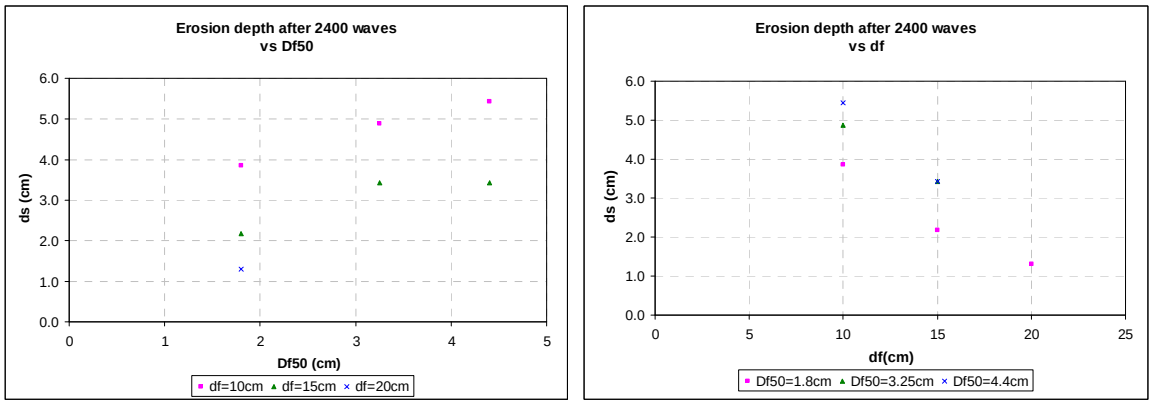

Figure 5-15 Erosion depth against grain size and erosion depth against filter thickness

In Figure 5-15 can be seen that with an increasing filter grain size (D_{f50}) the erosion depth is increasing. This seems reasonable because with a larger grain size of the filter material is easier for a wave to penetrate through the filter material and thus resulting in a larger amount of erosion.

In Figure 5-15 can also be seen that a thicker filter layer results in a smaller d_s. This can be explained with the reduction of the total erosion by a thicker filter layer.

By plotting the erosion depth (d_s) against m (m is the filter thickness divided by filter grain size) (see Figure 5-16) a linear relation between the erosion depth and the number of grains on top of the core material is obtained. With an increasing m, the erosion depth will decrease. This makes sense because the more grains on top of the core material will reduce the wave load on the interface between filter and core material and thus it will reduce the amount of erosion and thus the erosion depth will decrease. The relation between the erosion depth and m is:

$$d_s \approx 0.058 - 0.4 \times m \qquad \text{(m)}$$

$$d_s \approx 0.058 - 0.4 \times \frac{d_f}{D_{f50}} \qquad \text{(m)}$$

Care has to be taken when using this formula because it is based on a limited data set.

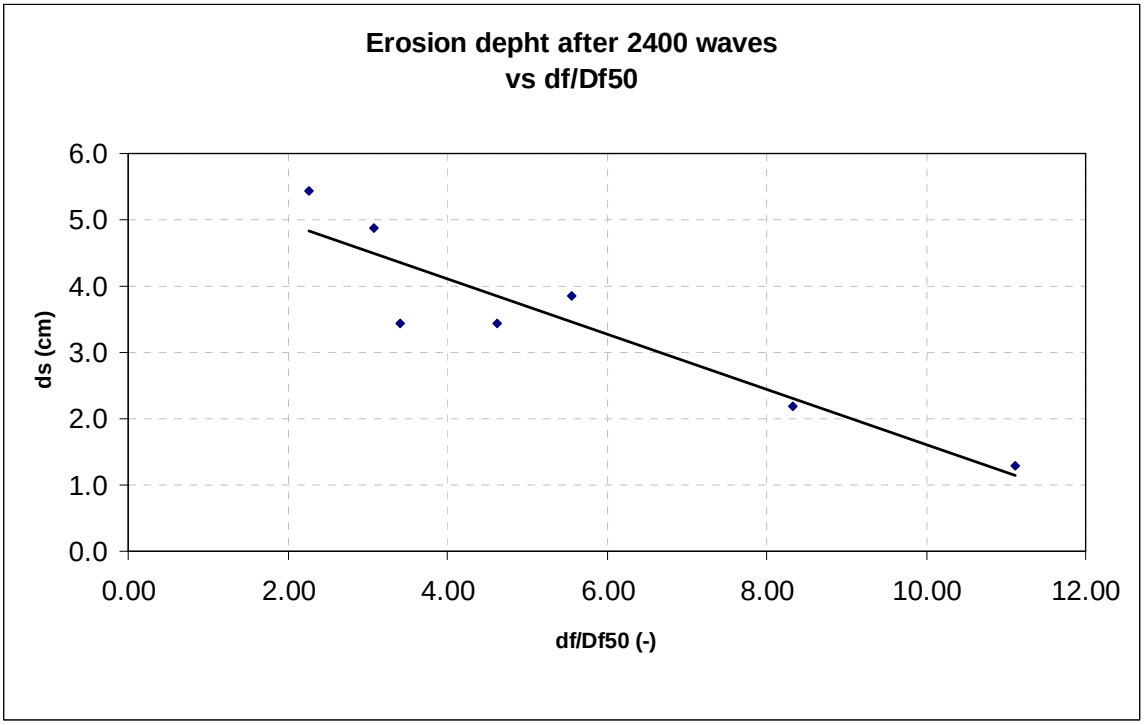

Figure 5-16 Erosion depth against filter thickness divided by filter grain size

6 Recommendations and conclusions

In this chapter the conclusions will be presented and a plan will be developed how to carry on with this research. The main questions of this plan are what parameters should be examined and how should that be done.

The objective of this thesis is

- To get an insight in the transportation of sandy material out of the core into a very open granular filter under influence of wave load.
- To obtain the relationship between;
    - Transport rate of material
    - Initiation of transport
    - Grain diameter base material
    - Grain diameter filter material
    - Thickness of filter layer
    - The hydraulic load

In order to reach these objectives, model test have been executed in a wave flume. In the model tests, several parameters could have been varied. The most important were;

- The wave parameters:
    - Regular or irregular waves
    - Wave Height (H)
    - Wave period (T)
- The filter layer parameters:
    - Grain size filter (D_f)
    - Grain distribution filter material
    - Thickness filter (d_f)
    - Shape filter material
- The core material parameters:
    - Grain size core material (D_b)
    - Shape core material
    - Grain distribution core material
- Breakwater dimensions:
    - Steepness slope (α)

From this list the grain size of the filter layer and the filter thickness were chosen to vary in the performed model tests. The other parameters might be just as important, but due to limitations in

time and availability of the facilities a choice had to be made. For the parameters that have been kept constant, values have been used based on wind waves and widely applied breakwaters.

For the parameters that have been kept constant, the following values have been used:

- Regular waves instead of irregular because in a limited number of tests it is easier to compare the results of the different test with regular waves because in every test, the exact same wave conditions will occur.
- The wave period and wave height are chosen such that the steepness of the wave is typical for a wind wave. The wave height was 10 cm, the wave period was 1.2 s
- The total number of waves is chosen such that it is typical for a storm with a duration of 8 hours. (Assuming waves with an average period of 12 s).
- For the grain shape and grain distribution of the filter and core material, materials were used which were available. The grain size of the core material is taken rather small in order to make sure that erosion would take place.
- The total number of layers is chosen to be one. When using multiple layers with different grain sizes it makes it difficult to interpret the results. This one layer is a representation of the amour layers plus the under layers.
- The slope of the breakwater in the model is chosen such that is typical for widely build breakwaters around the world.

In summary, the breakwater had the following features;

- Slope of 1:3
- Core of sand with a D_{b50} of 160 μm
- One thick geometrically open filter layer with different D_{f50} and different thickness:
  - D_{f50} = 1.8 cm, 3.25 cm, 4.4 cm (see Appendix 1)
  - d_f = 10 cm, 15 cm, 20 cm
- Wave parameters:
  - regular waves
  - H = 10 cm
  - T = 1.2 s
  - duration model tests: 2400 waves
- In total, 9 experiments have been performed

After the experiments the erosion, the erosion length (Lr and Lr2) and the erosion depth (ds) (see Figure 6-1) have been plotted against d_f and D_{f50}, a relation between these parameters was observed.

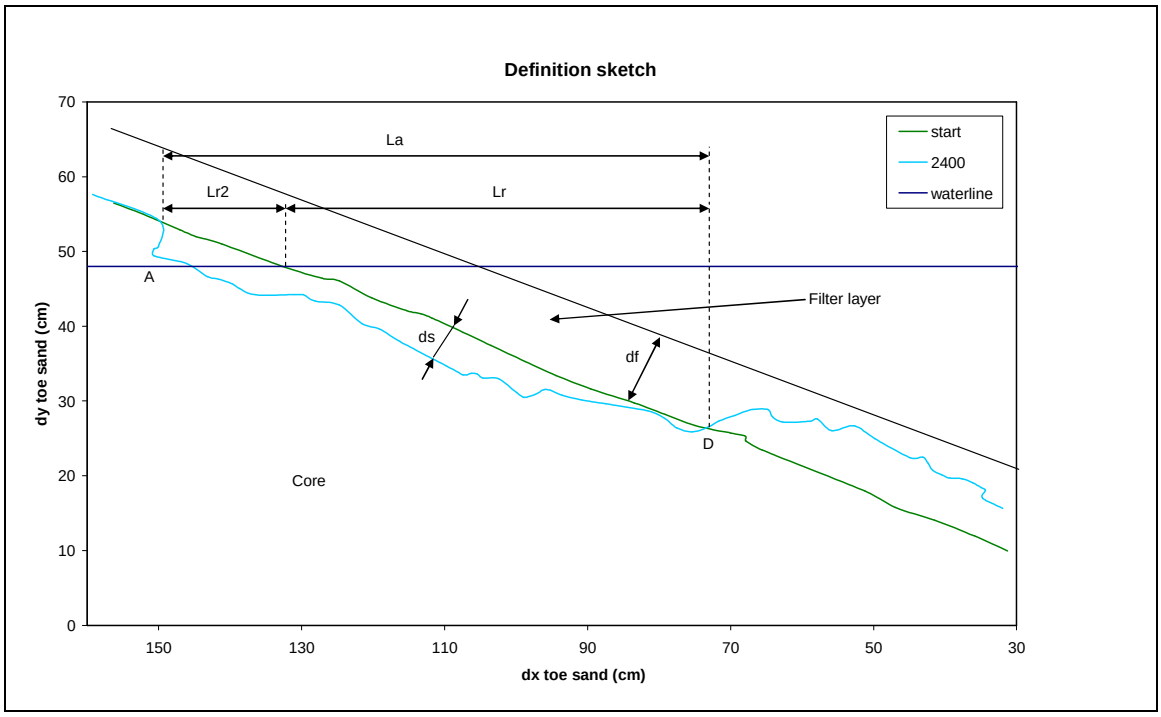

Figure 6-1 definition sketch

Because of these relations the erosion, Lr, Lr2 and ds have been plotted against the dimensionless parameter $m=d_f/D_{f50}$. This parameter can be seen as the thickness of the filter measured in number of stones. The parameters could also be made dimensionless with using the wave parameters, but this has not been done because it would only have scaled the graphs there the same wave parameters have been used in all experiments.

6.1 Conclusions

- The total erosion, erosion depth, and the erosion length 2 after 2400 waves are dependent on d_f/D_{f50}. With an increasing d_f/D_{f50}, the total erosion, erosion depth (ds), and the erosion length 2 (Lr2) are decreasing.

- A curved profile develops in the sand which looks like a bar profile of a sandy beach. (see Figure 4-2)

- Point D is fixed during the whole experiment.
- With an increasing d_f/D_{f50} the erosion is decreasing faster, with a d_f/D_{f50} between 2 and 4, then when d_f/D_{f50} is larger then 5.

- The erosion length is dependent on; d_f, D_{f50} and the run down point of the wave on the outside of the filter layer.

- The transport of the core material is governed by sheet flow transport and suspension transport.

- Two main water movements can be distinguished:
  - The main wave moving up and down the breakwater
  - A small wave which is moving inside the filter layer with a height of approximately 1cm

- Water is mainly moving up the slope on the outside of the filter layer and the water is mainly moving down the slope through the filter layer.

- For all experiments the erosion rate is decreasing in time. But after 2400 waves the erosion has not become zero.

- The erosion rate after 2400 waves is smaller with a thick filter layer and a small grain size compared to a thin filter and a large grain size.

6.2 Recommendations for further Research

To obtain a fully understanding of the process in order to develop a design tool or to perform scaled model test, 5 steps have to be taken:

1. In this step the conclusion based on the research performed in this thesis should be extended with more data. The conclusions are now based on a very limited number of experiments. Preferably by using another method to measure the profile of the sand core. A better result can then be expected because the influence of the wall is less in the center of the flume.
2. The insight in the transportation of sand trough an open filter layer under influence of a wave load has to be extended with respect to the other parameters as mentioned above. Based on observations made in experiment 2 it is suggested to start with improving the insight in the transportation of sand with respect to the wave conditions. Because still not enough knowledge is available to perform scaled model tests, a process based model test should be performed. In this model tests, regular waves should be used with different wave height and period and a different slope steepness of the breakwater. The slope steepness in

combination with the wave parameters forms the Irribarren parameter. The Irribarren parameter says something of the breaker type. The type of breaking might have influence on the water movement inside the filter layer and thus on the transport of core material.

3. The process based model test performed in this thesis and in step 1 should be repeated with irregular waves.
4. Insight in the water movement inside the filter layer must be obtained. May be a numerical calculation of the water movement insight the filter layer could be performed. A program developed by Troch (vofbreak[2]) or Liu (varans) can be used for this. The outcome of the simulation should be compared with the physical model tests in order to study the relation between the water movement and the erosion process.

   A model test in which the water movement is measured could also be performed but it must be noted that it is difficult to say if both methods will result to a good result
5. When step 1 to 4 has been completed, enough knowledge should be available to develop a theoretical description of the transport of sand inside a filter layer under influence of a wave load. When doing this research done about sheet flow transport in the surf zone (for example, the paper of Watanabe[22]. Research concerning dune erosion and research done concerning open filters should be used (for example; Den Adel[23], and Msc thesis of Halter[24], Jansens[25] and van Os[26]).

In summary; the recommendation for further research in order to be able to develop a design tool;

1. The data set obtained in this thesis should be extended
2. The erosion should be related to the wave parameters and the slope steepness of the breakwater. Suggested is to perform process-based experiments.
3. Model tests should be executed with irregular waves
4. Insight in the water movement inside the filter layer must be obtained.
5. A theoretical description of the transport of sand inside a filter layer under influence of a wave load should be developed.

---

[22] Watanabe, 2004 [44]

[23] Den Adel, 1992 [1,2,3]

[24] Halter, 1999 [11]

[25] Jansens, 2000 [12]

[26] Van Os, 1998 [28]

7 Literature

[1] den Adel H. *'Transportmodel voor filters dl 1 Samenvatting'*. 1992

[2] den Adel H. *'Transportmodel voor filters dl 2 loodrechte stroming'*. 1992

[3] den Adel H. *'Transportmodel voor filters dl 3 paralelle stroming'*. 1992

[4] Bakker K.J., Verheij H.J. & de Groot M.B. *'Design of Geometrical open Filters in Hydraulic Structures'*. Filters in Geotechnical and Hydraulic Engineering, Balkema, the Netherlands, 1993

[5] Bakker K.J., Verheij H.J. & de Groot M.B. *'Design Relationship for Filters in Bed Protection'*. Journal of Hydraulic Engineering Vol 120, No 9, 1994

[6] Bezuijen A., Klein Breteler M. & Bakker K.J. '*Design Criteria for Places Block Revetments and Granular Filters'*. 2de copedec, Beijing, China, 1987

[7] Burcharth H.F., Liu Z. & Troch P. *'Scaling of Core Material in Rubble Mound Breakwater Model Test'*. Coastal and Port Structures, South Africa, April, 1999

[8] de Grauw A., van der Meulen T. & van der Does de Bye M. *'Granular Filters: Design Criteria'*. Journal of Waterways, Port, Coastal and Ocean Engineering, 1984

[9] de Groot M.B., Bezuijen A., Burger A.m. & Konter J.L.M. *'The Interaction between Soil, Water and Bed or Slope Protection'*. Modeling Soil-Water-Structre Interactions, the Netherlands, Balkema, 1988

[10] de Groot M.B., Yamazaki H., van Gent M.R.A. & Kheyruri Z. '*Pore Pressure in Rubble Mound Breakwaters'*. Coastal Engineering 124, 1994

[11] Halter W., '*The behavior of erosion filters under the influence of wave loads'*, MSc thesis, Delft University of Technology, 1999

[12] Jansens R., '*Turbulent velocity fluctuations in filterlayer due to wave action'*, MSc thesis, Delft University of Technology, 2000

[13] de Jong W., Verhagen H.J. & Olthof J. *'Experimental Research on the Stability of Armour and Secondary Layer in a Single Layered Tetrapod Breakwater'*. International Conference on Coastal Engineering, Lisbon, 2004

[14] de Rouck J. & van Damme L. '*Overall Slope Stability Analysis of Rubble Mound Breakwaters*'. International Conference on Coastal Engineering, Orlando Florida, 1996

[15] Foster M. & Fell R. *'Assessing Embankment Dam Filters that do Satisfy Design Criteria'*. Journal of Geotechnical and Geo environmental Engineering, May, 2001

[16] Hagerty D.J. & Parola A.C. *'Seepage Effects in some Riprap Revetments'*. Journal of Hydraulic Engineering, July, 2001

[17] Helgason E., Burcharth H.F. & Grúne F. *'Pore Pressure Measurements inside Rubble Mound Breakwaters'*. International Conference on Coastal Engineering, Lisbon, 2004

[18] Hólscher P., de Groot M.B. & van der Meer J.W. '*Simulation of Internal Water Movement in Breakwaters'*. Modeling Soil-Water-Structures Interactions, Balkema, The Netherlands, 1988

[19] Hsu T.-J., Sakakiyama T. & Liu P.L.F. '*A Numerical Model for Wave Motions and Turbulence Flows in Front of a Composite Breakwater*'. Elsevier, Coastal Engineering 46 25-50, 2002

[20] Indrarantna B. & Radampola S. *'Analysis of Critical Hydraulic Gradient for Particle Movement in Filtration'*. Journal of Geotechnical and Geo environmental Engineering, April 2002

[21] Indraratna B. & Vafal F. *'Analytical Model for Particle Migration within Base Soil-Filter System'*. Journal of Geotechnical and Geo environmental Engineering, February, 1997

[22] Klein Breteler M., Bakker K.J. & den Del H. *'New Criteria for Granular Filters and Geotextile under Revetments'*. Coastal Engineering, 1990

[23] Lara J.L. '*A Numerical Wave Flume to Study the Functionality and Stability of Coastal Structures*'. PIANC Magazine AIPCN, no 121, October 2005

[24] Liu P.L.F., Lin P., Chang K.A. & Sakakiyama T. *'Numerical Modelling of Wave Interaction with Porous Structures'*. Journal of Waterway, Port, Coastal & Ocean Engineering, 2002

[25] Locke M., Indraratna B. & Adikari G. *Time-Dependent Particle Transportation through Granular Filters'*. Journal of Geotechnical and Geoenvironemental Engineering, June 2001

[26] Lone M.A., Hussain B. & Asawa G.L. *'Filter Design Criteria for Graded Cohesionless Bases'*. Journal of Geotechnical and Geoenvironmental Engineering ASCE, February, 2005

[27] Martín F., Martínez C., Lomónaco P. & Vidal C. '*A new Procedure for the Scaling of Core Material in Rubble Mound Breakwater Model Tests*'. International Conference on Coastal Engineering, Cardif, 2002

[28] Os P,. '*Hydraulic loading on a geometrically open filter structure*', MSc thesis, Delft University of Technology, 1998

[29] Oumeraci H. & Partenscky H.W. *'Wave-Induced Pore Pressure in Rubble Mound Breakwaters'*. Coastal Engineering, Ch 100, 1990

[30] Oumeraci H. *'Role of Large-Scale Model Testing in Coastal Engineering -Selected Examples Studies performed in GWK Hannover'*. Towards a Balanced Methodology in European Hydraulic research, Budapest, May 2003

[31] Schiereck G.J., Fontijn H.L., d'Angrmont K. & Steijn B. *'Filter Erosion in Coastal Structures'*. International Conference on Coastal Engineering, Sydney,2000

[32] Tirindello M. & Lamberti A. *'Wave Action on Rubble Mound Breakwaters: the Problem of Scale Effects'*. DELOS EVK3-CT-2000-00041

[33] Troch P. 'VOFbreak, *'A Numerical Model for Simulation of Wave Interaction with Rubble Mound Breakwaters'*. Environmental and Coastal Hydraulics, 1996

[34] Troch P., De Rouck J. & Burcharth H.F. *'Experimental Study and Numerical Modeling of Wave induced Pore Pressure Attenuation inside a Rubble Mound Breakwater'*. International Conference on Coastal Engineering, Cardif, 2002

[35] Troch P., De Rouck J. *'Development of Two-Dimensional Numerical Wave Flume for Wave Interaction with Rubble Mound Breakwaters'*. International Conference on Coastal Engineering, Copenhagen,1998

[36] Troch P., de Somer M., de Rouck J., van Damme L., Vermeir D., Martens J.P. & van Hove C. *'Full Scale Measurements of Wave Attenuation inside a rubble Mound Breakwater'*. International Conference on Coastal Engineering, Orlando, Florida, 1996

[37] van Gent M.R.A. *'Porous flow through rubble mound material'*. Journal of Waterway, Port, Coastal & Ocean Engineering, May/June 1995

[38] van Gent M.R.A. *'The Modeling of Wave Action on and in Coastal Structures'*. Elsevier, Coastal Engineering 22 311-339, 1994

[39] van Gent M.R.A., Tönjes P., Petit H.A.H. & van den Bosch P. *'Wave Action on and in Permeable Structures'*. Coastal Engineering 125, 1994

[40] Watanabe A, *'A Sheet-Flow Transport Rate Formula for Asymmetric, Forward-Leaning Waves And Currents'*, International Conference on Coastal Engineering, Lisbon, 2004

[41] Wörman A. *'Riprap Protection without Filter Layers'*. Journal of Hydraulic engineering Vol 115, no. 12, 1989

[42] Zhao Q., Armfield S. & Tanimoto K. *'Numerical Simulation of Breaking Waves by Multi-Scale Turbulence Model'*. Elsevier, Coastal Engineering 51 53-80, 2004

[43] de Vries M. *'Waterloopkundig onderzoek college handleiding b 80'*. Delft, 2004

[44] van der Hoeven M.A. '*behavior of a falling apron*'. Msc thesis TuDelft, 2002

8 Appendix

Appendix 1; Sieve-curves of the 3 Utilised Filter Materials

The sieve curves have been obtained by taking samples from each grading of approximately 400 stones. Each stone was weighted on a scale with an accuracy of 0.1 gram. To go from weight to stone diameter the weight was divided by its density then raised to the power 1/3 and then divided by 0.84.

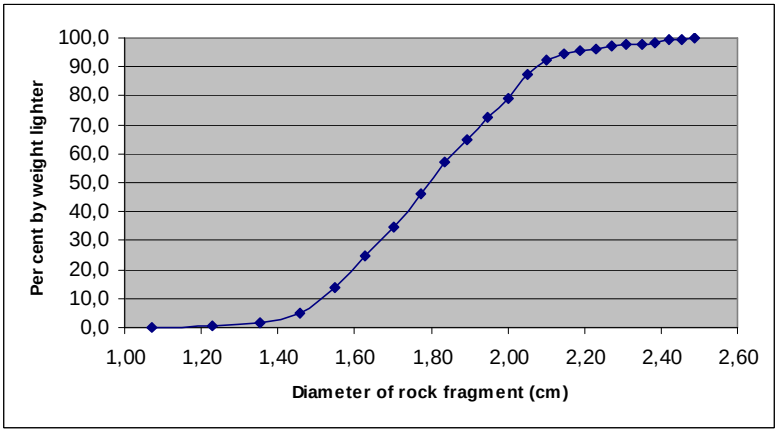

Figure 1 Sieve-curve, diameter of rock fragment, with D_{f50} 18,0 mm

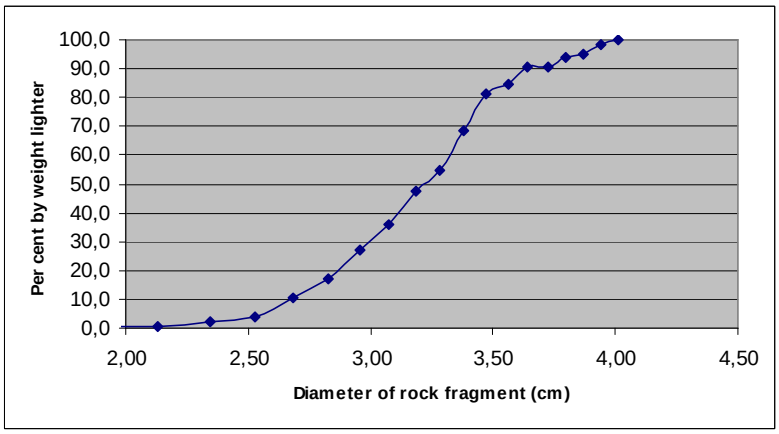

Figure 2 Sieve-curve, diameter of rock fragment, with D_{f50} 32,5 mm

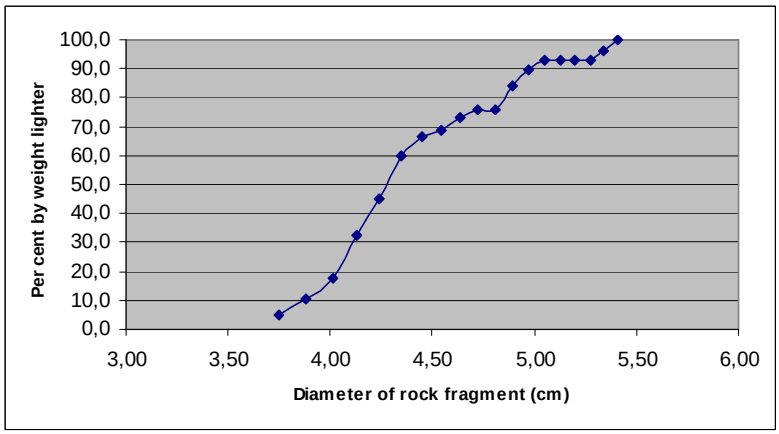

Figure 3 Sieve-curve, diameter of rock fragment, with D_{f50} 44,0 mm

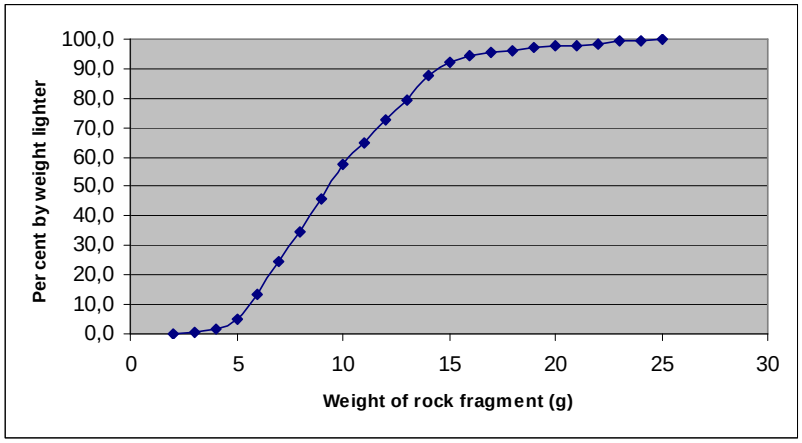

Figure 4 Sieve-curve, weight of rock fragment, with D_{f50} 18,0 mm

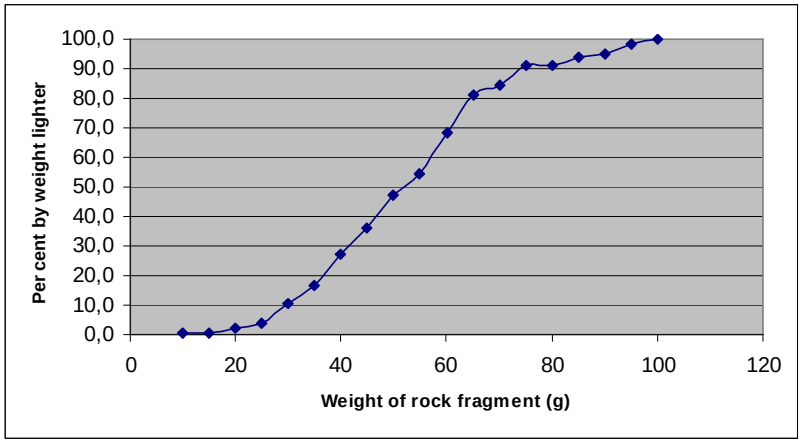

Figure 5 Sieve-curve, weight of rock fragment, with D_{f50} 32,5 mm

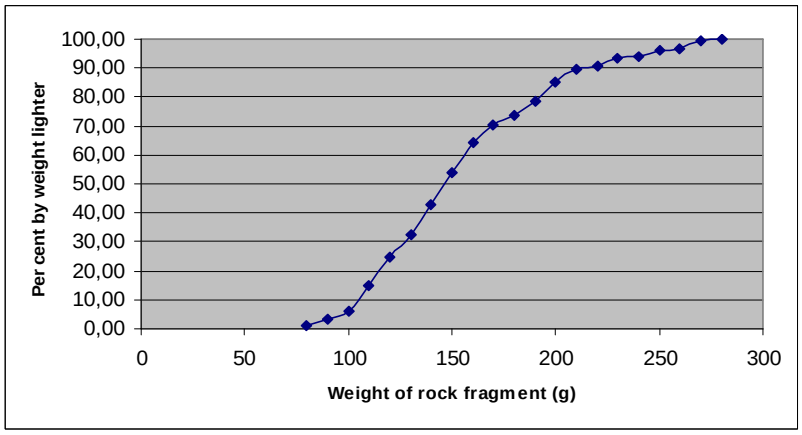

Figure 6 Sieve-curve, weight of rock fragment, with D_{f50} 44,0 mm

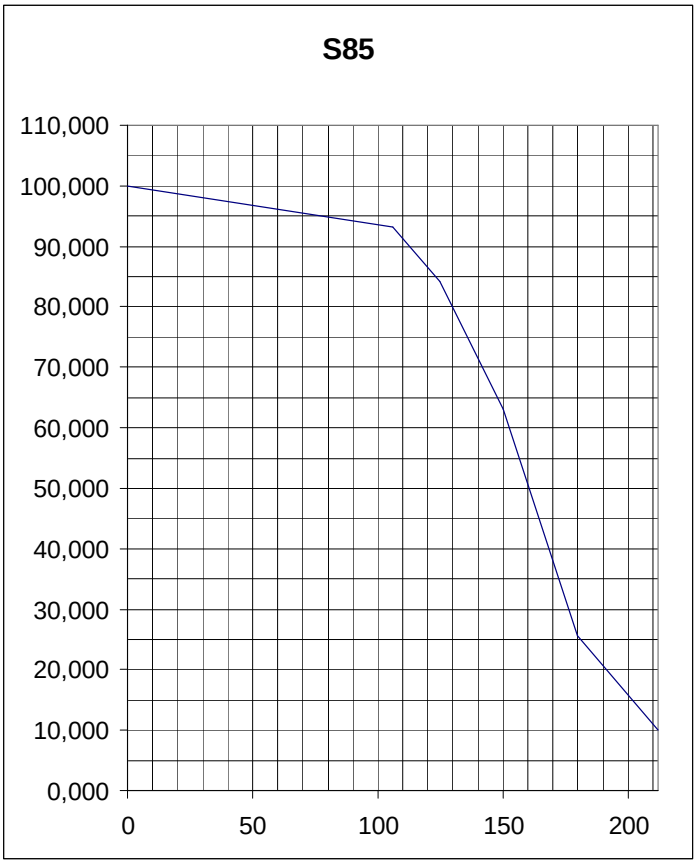

Figure 7 Sieve-curve (′% - μ)

Appendix 2; Photographs Experiments, at 0, 600 & 2400 Waves

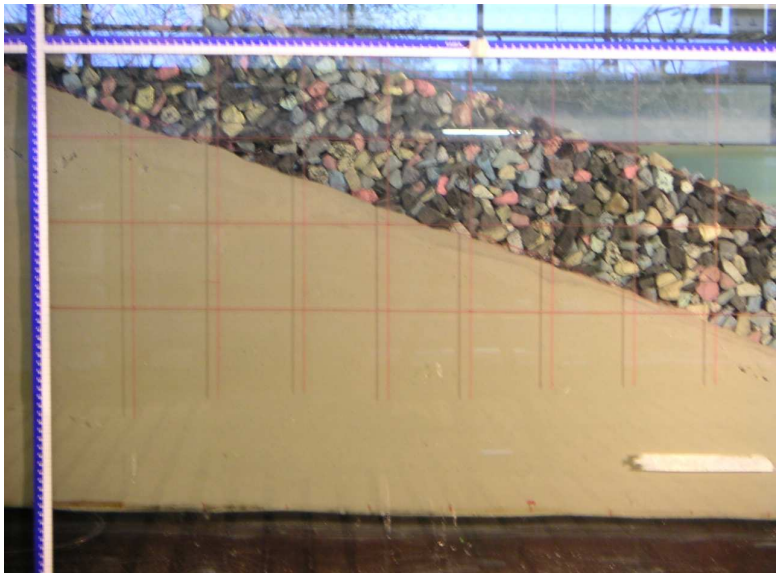

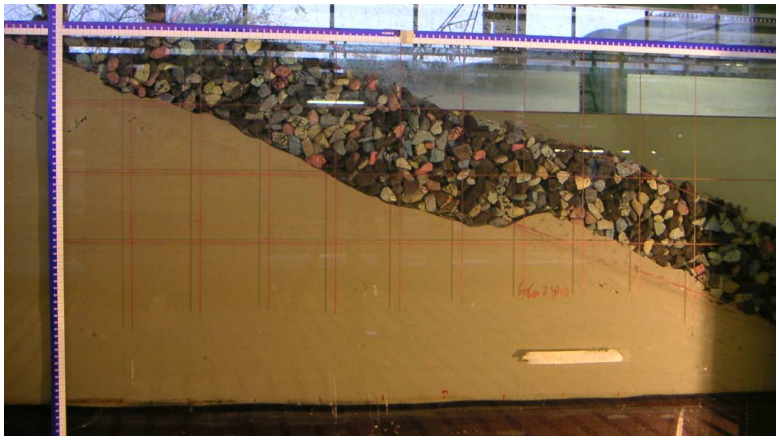

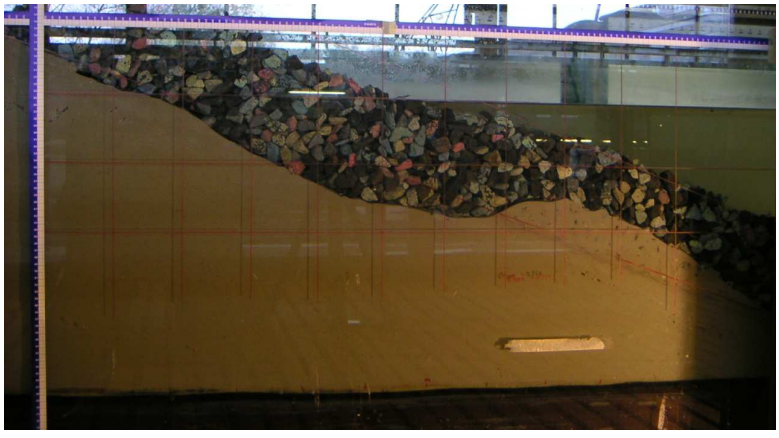

Figure 8 Photograph experiment 3 at start (a), 600 (b) & 2400 (c) waves

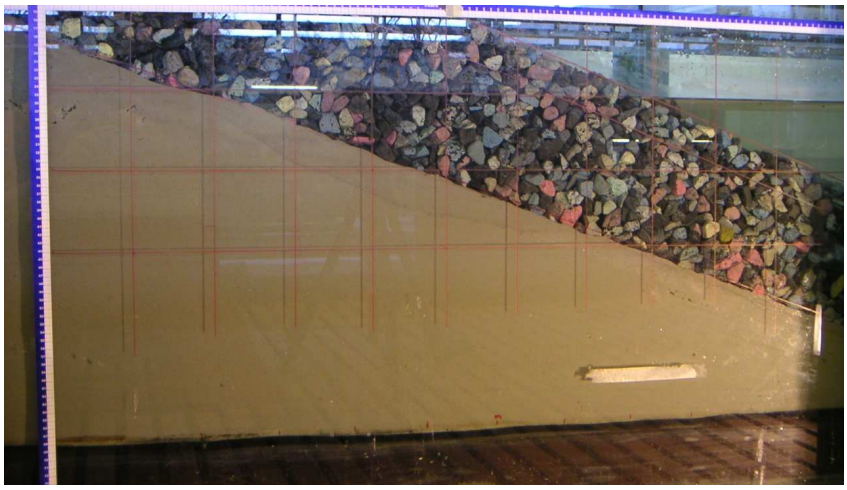

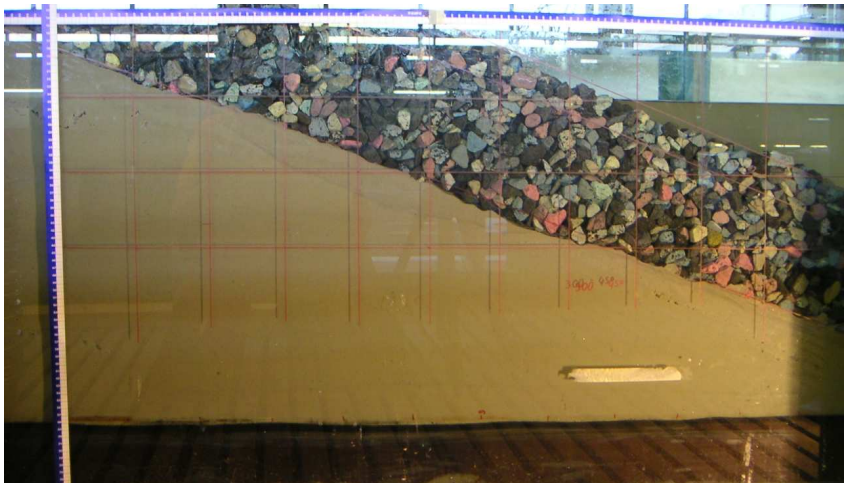

Figure 9 Photograph experiment 4 at start (a), 600 (b) & 2400 (c) waves

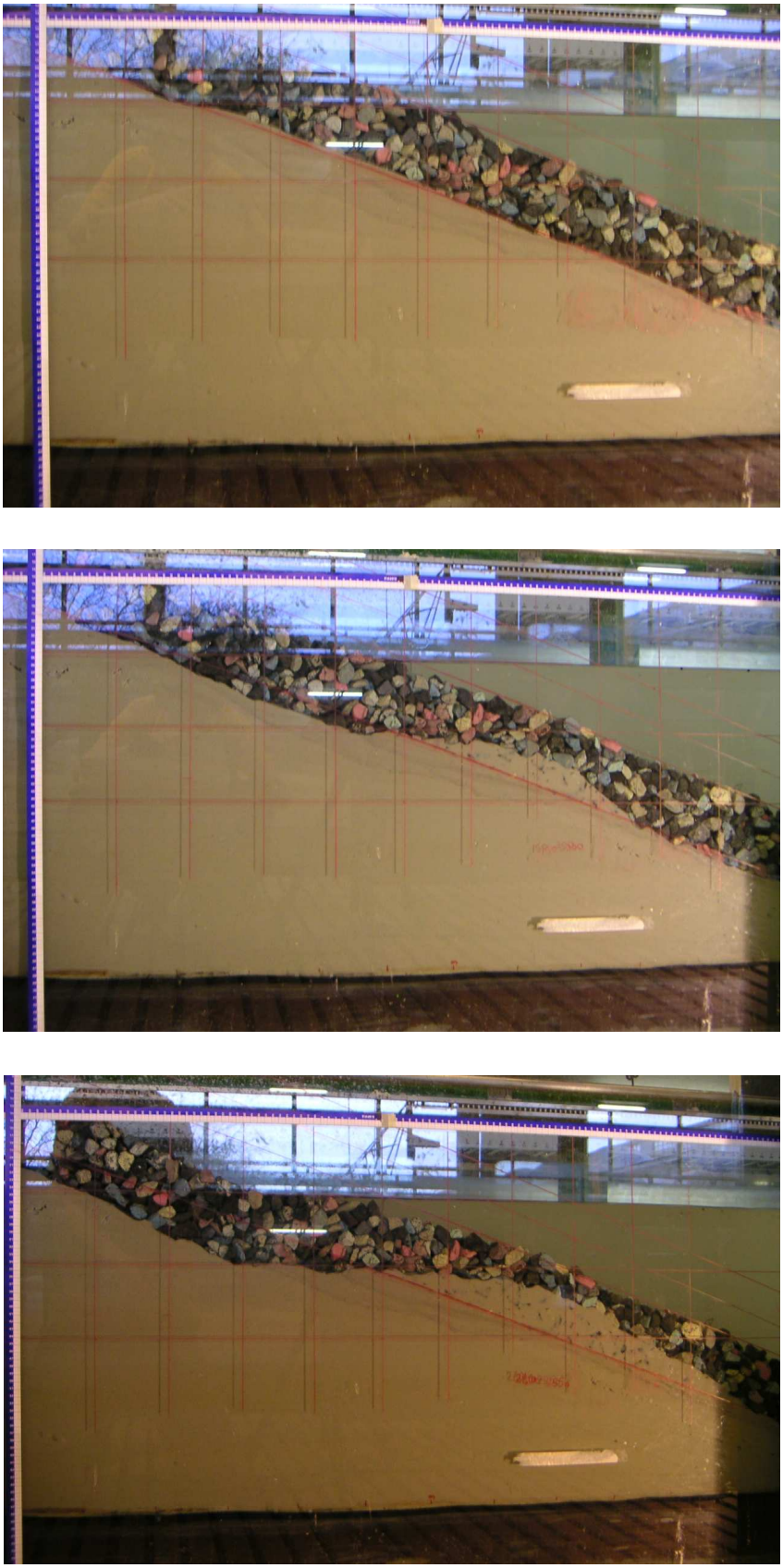

Figure 10 Photograph experiment 5 at start (a), 600 (b) & 2400 (c) waves

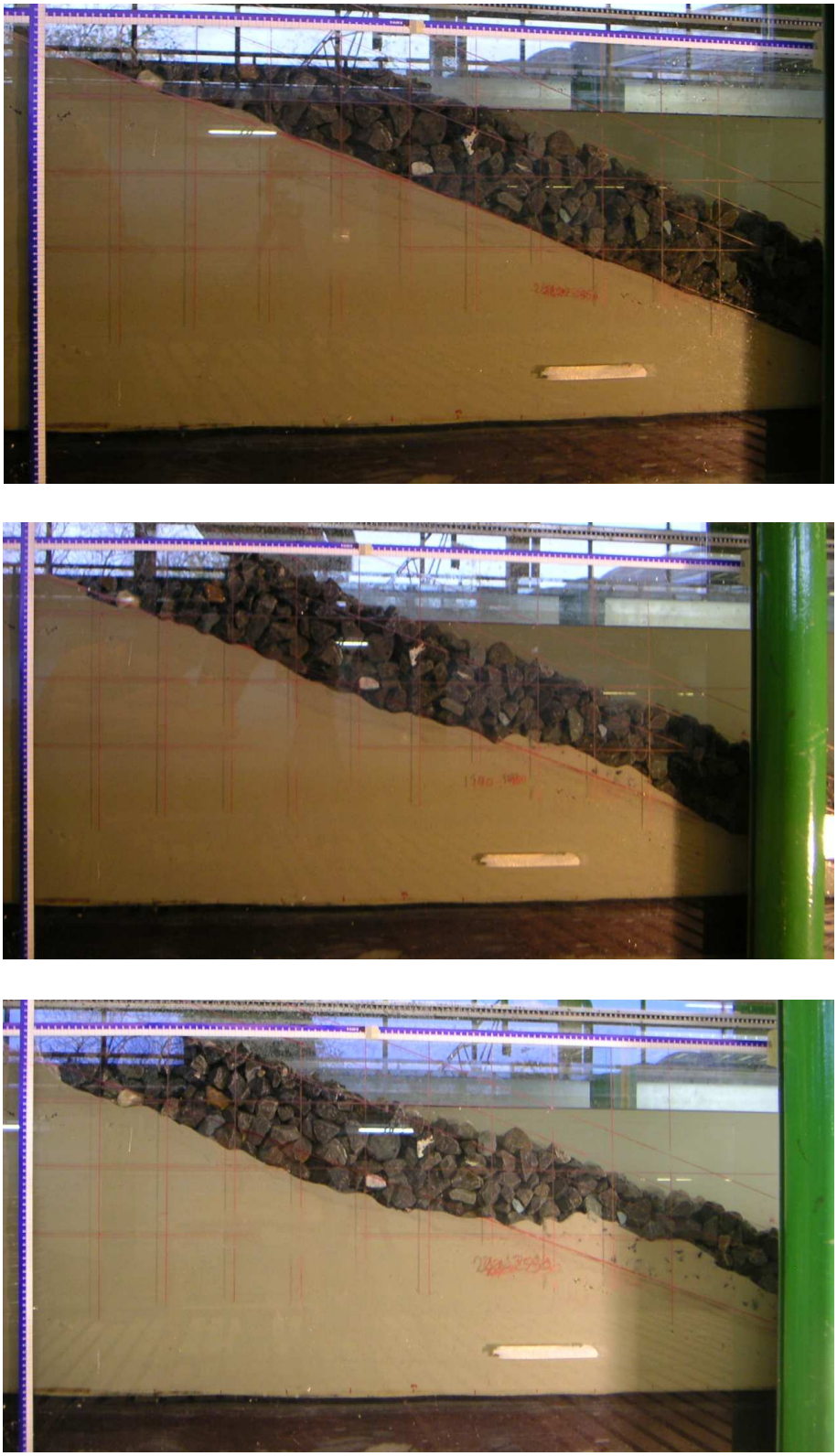

Figure 12 Photograph experiment 6 at start (a), 600 (b) & 2400 (c) waves

Figure 13 Photograph experiment 7 at start (a), 600 (b) & 2400 (c) waves

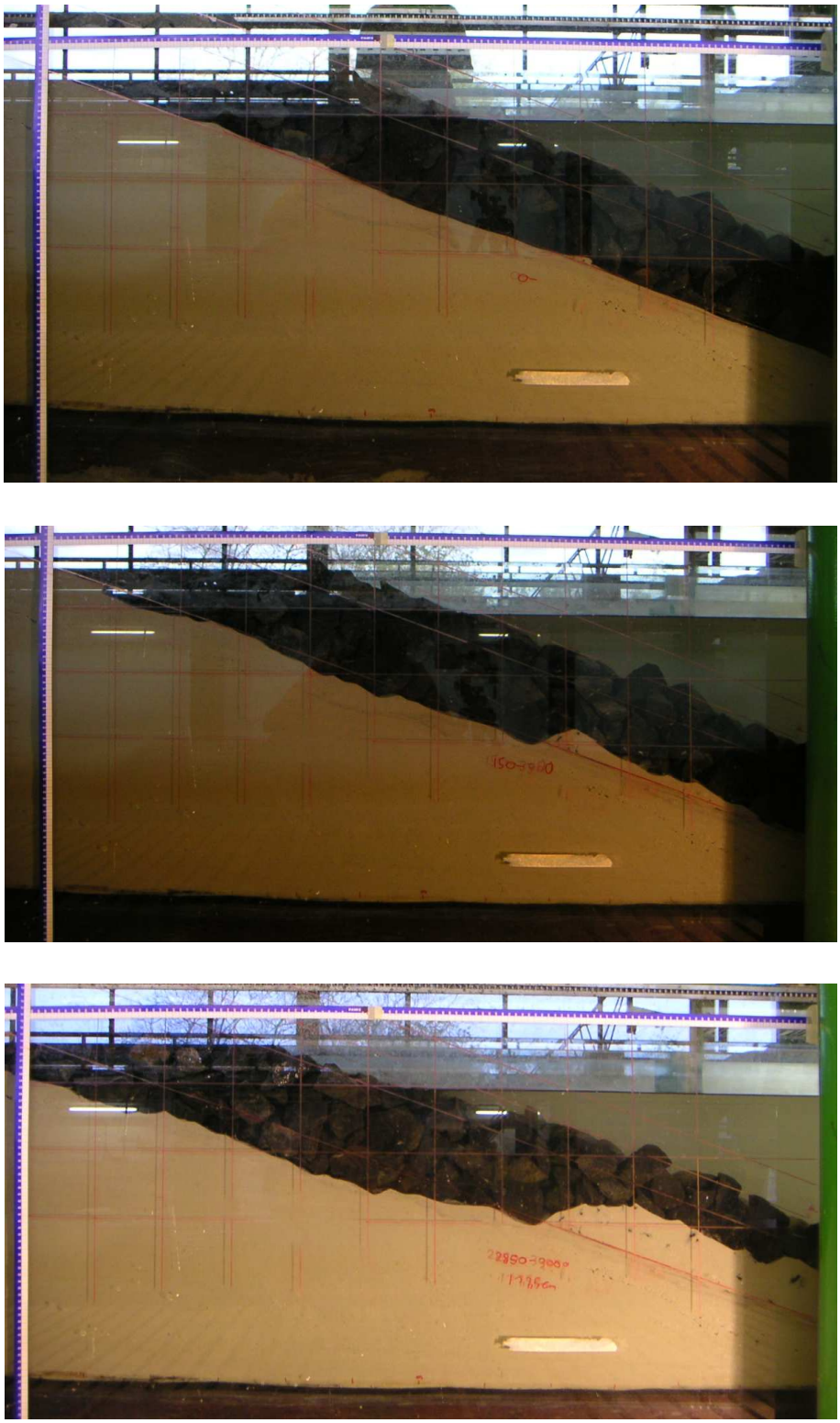

Figure 14 Photograph experiment 8 at start (a), 600 (b) & 2400 (c) waves

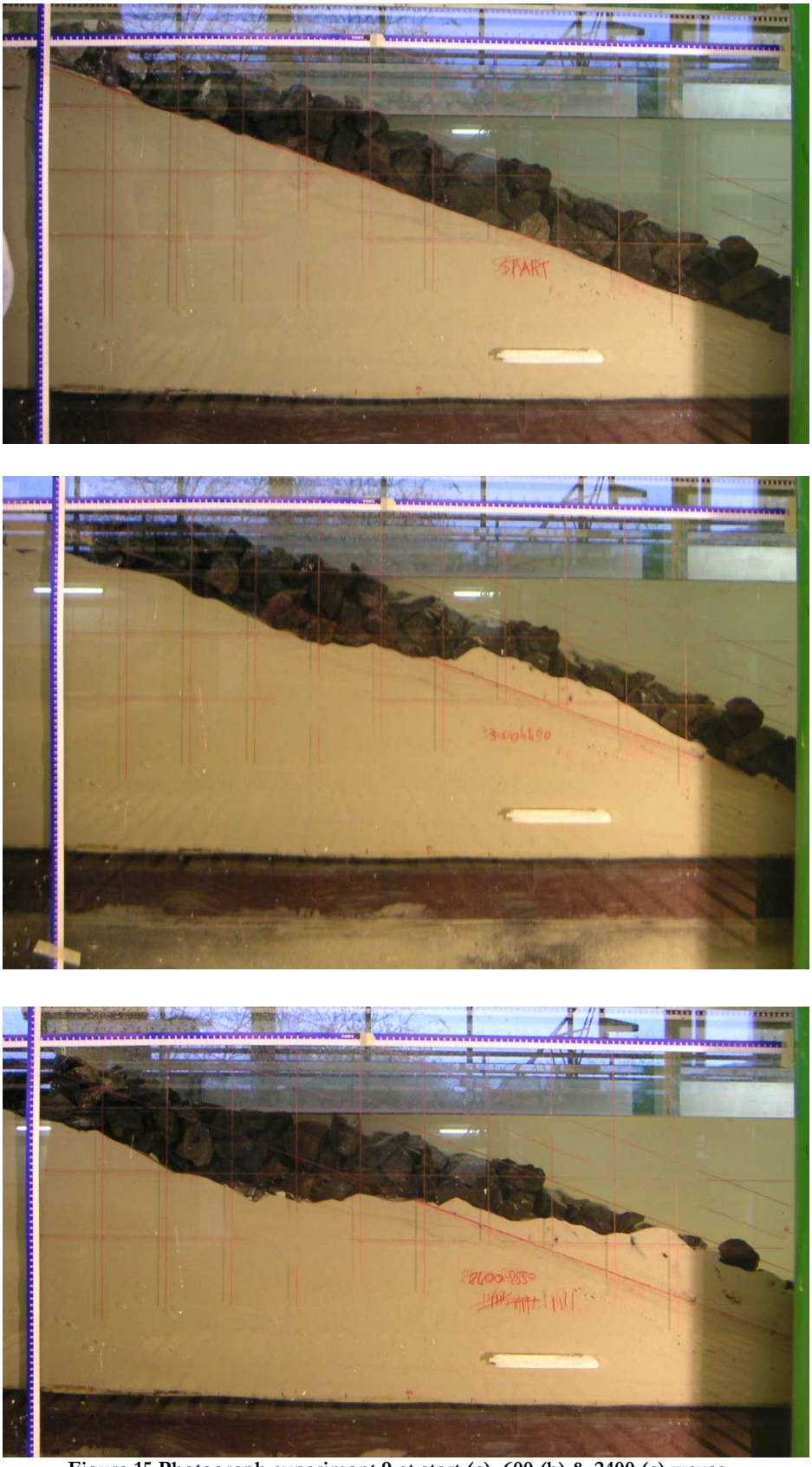

Figure 15 Photograph experiment 9 at start (a), 600 (b) & 2400 (c) waves

Appendix 3; Relations (d_y toe – d_x toe) for the Experiments

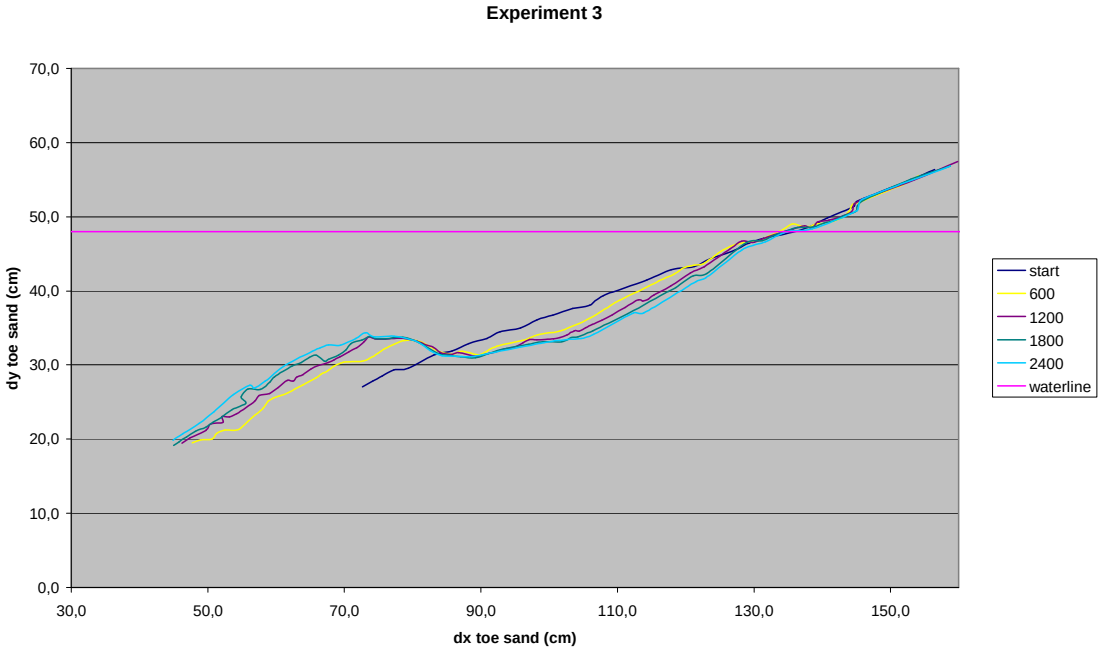

Figure 16 Experiment 3

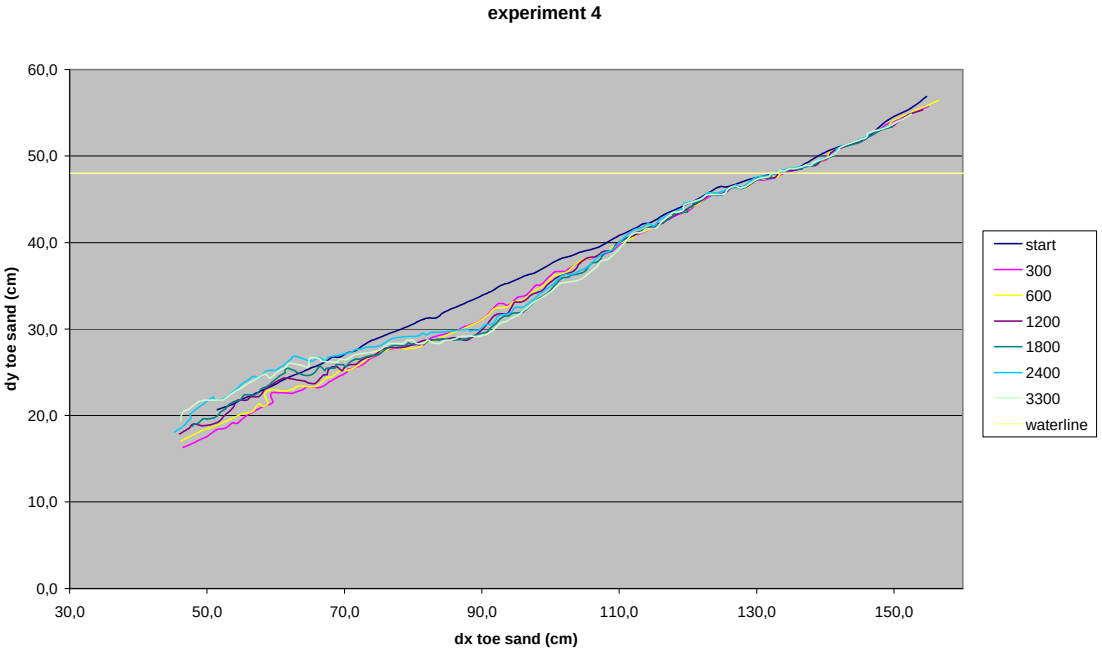

Figure 17 Experiment 4

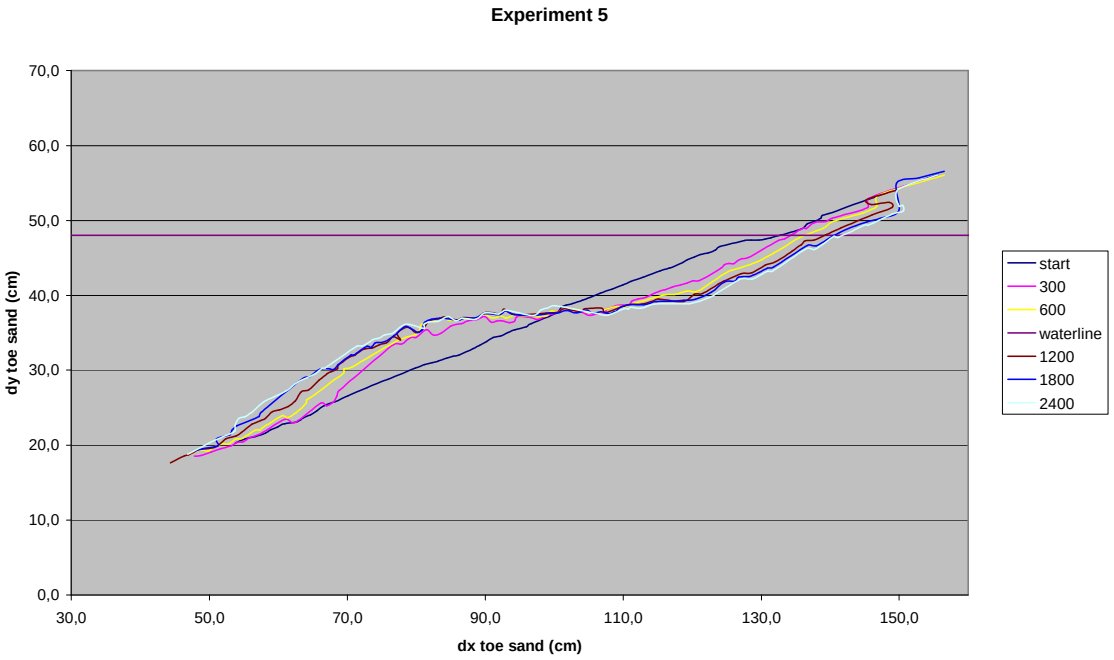

Figure 18 Experiment 5

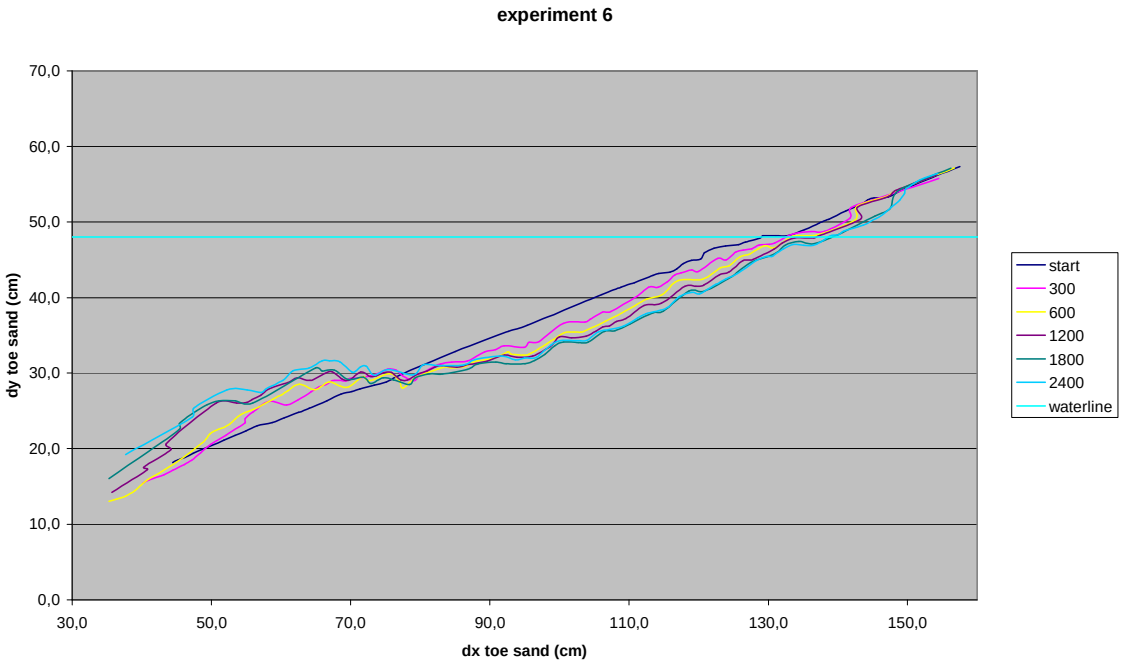

Figure 19 Experiment 6

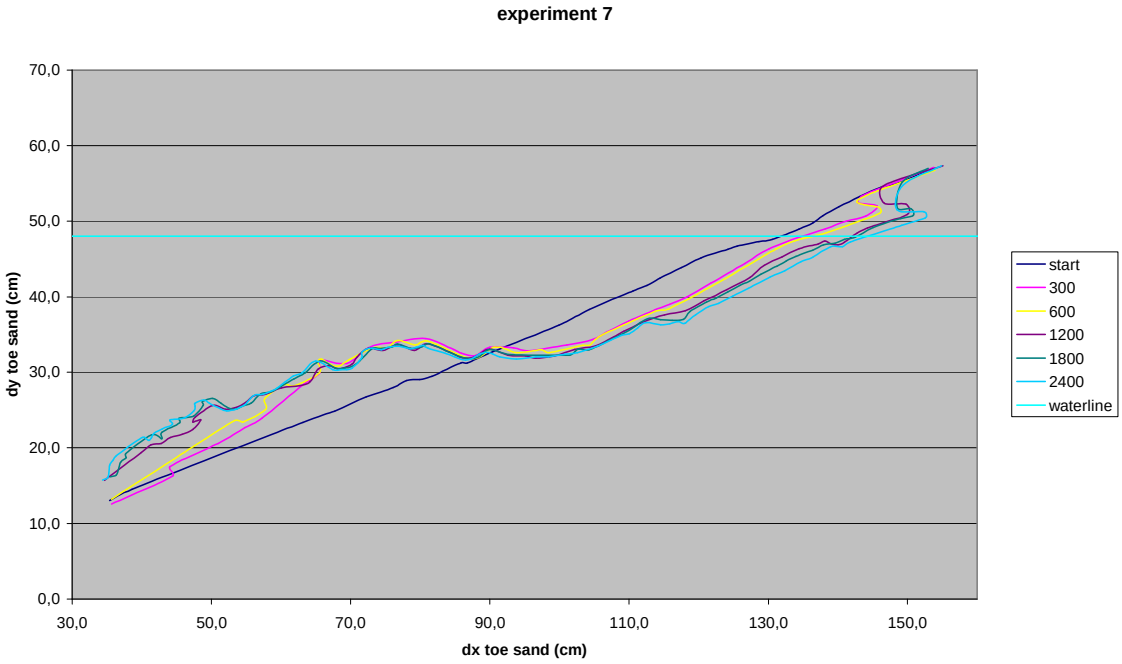

Figure 20 Experiment 7

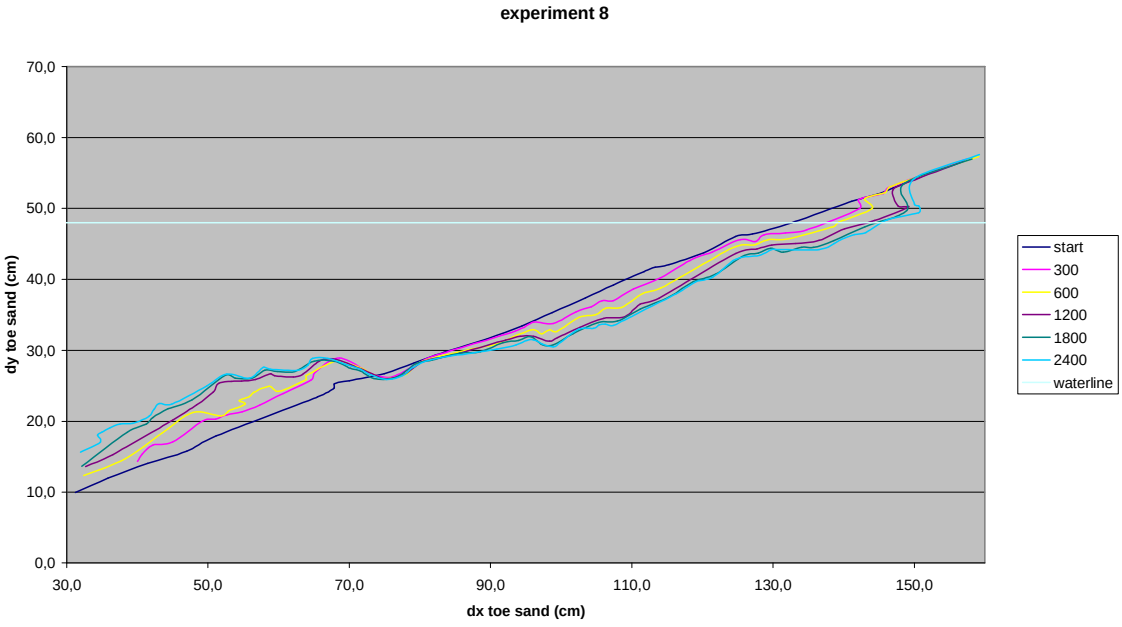

Figure 21 Experiment 8

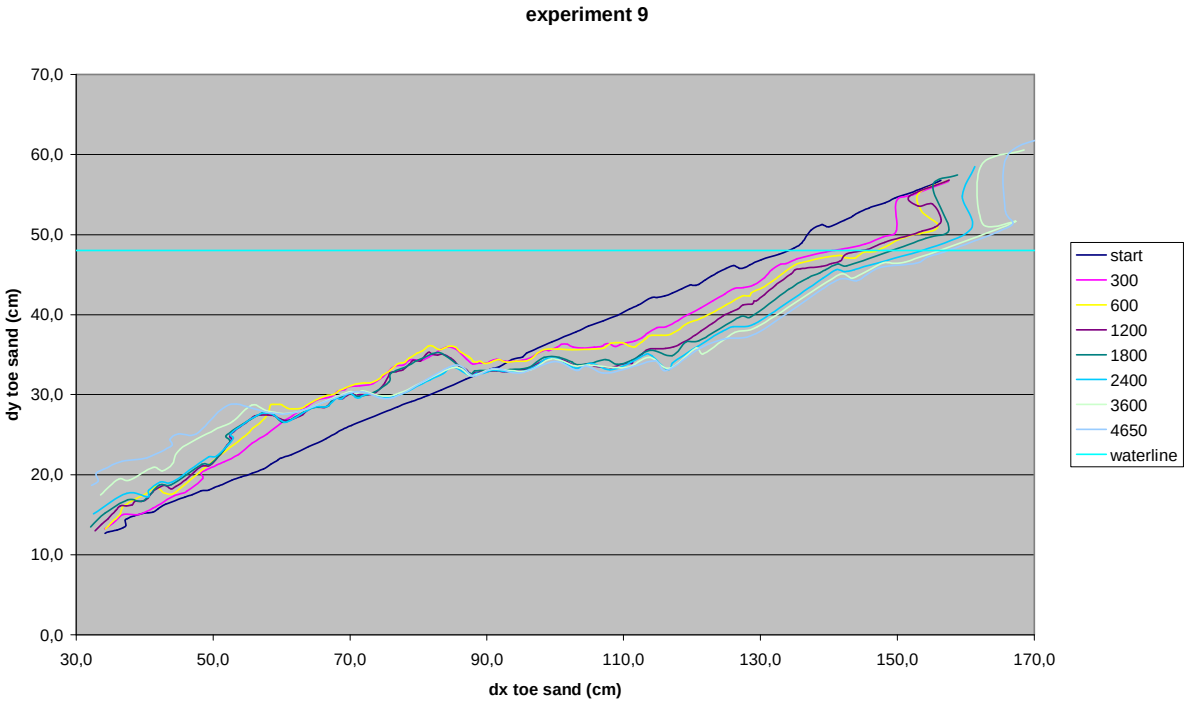

Figure 22 Experiment 9

Appendix 4; Relation (d_y toe – d_x toe) for D_{f50}, after 2400 waves

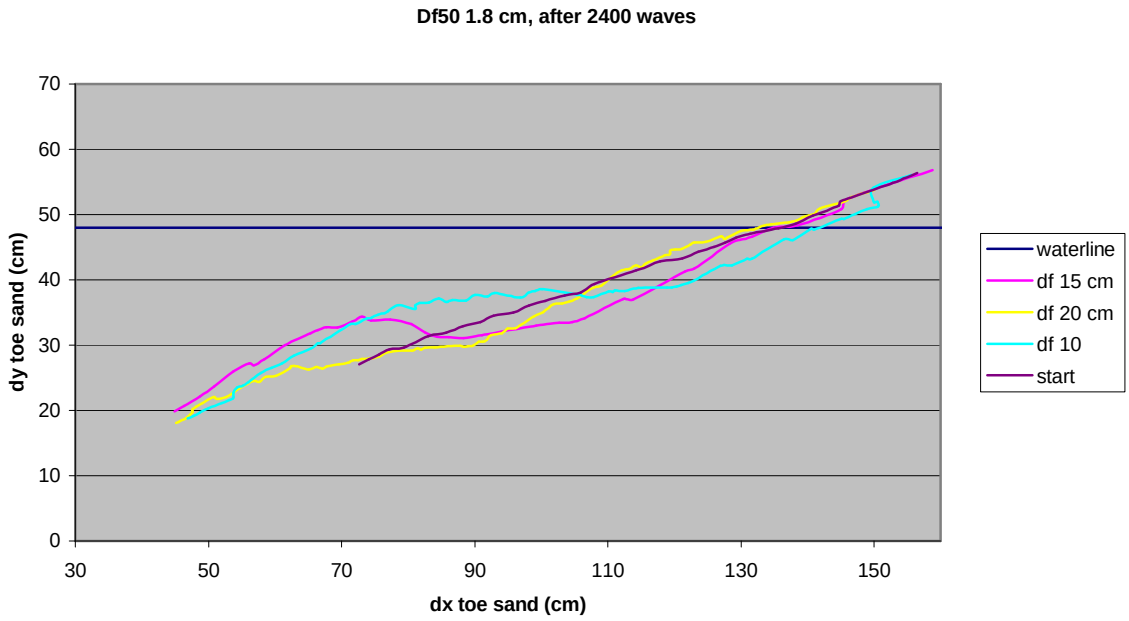

Figure 23 Relation for D_{f50} 1.8 cm, after 2400 waves

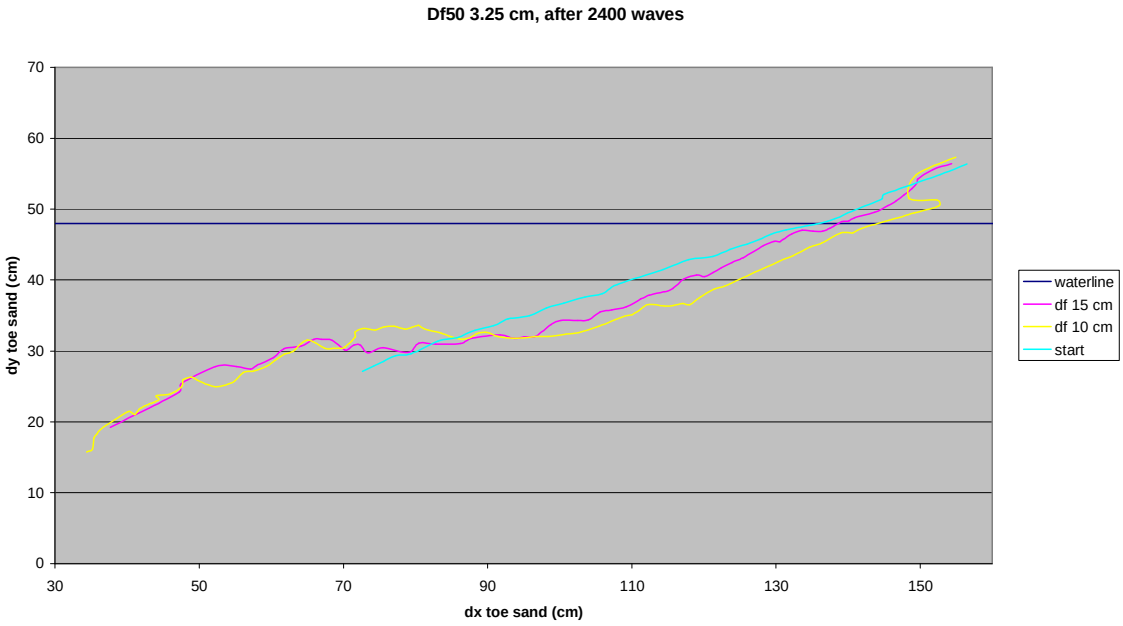

Figure 24 Relation for D_{f50} 3,25 cm, after 2400 waves

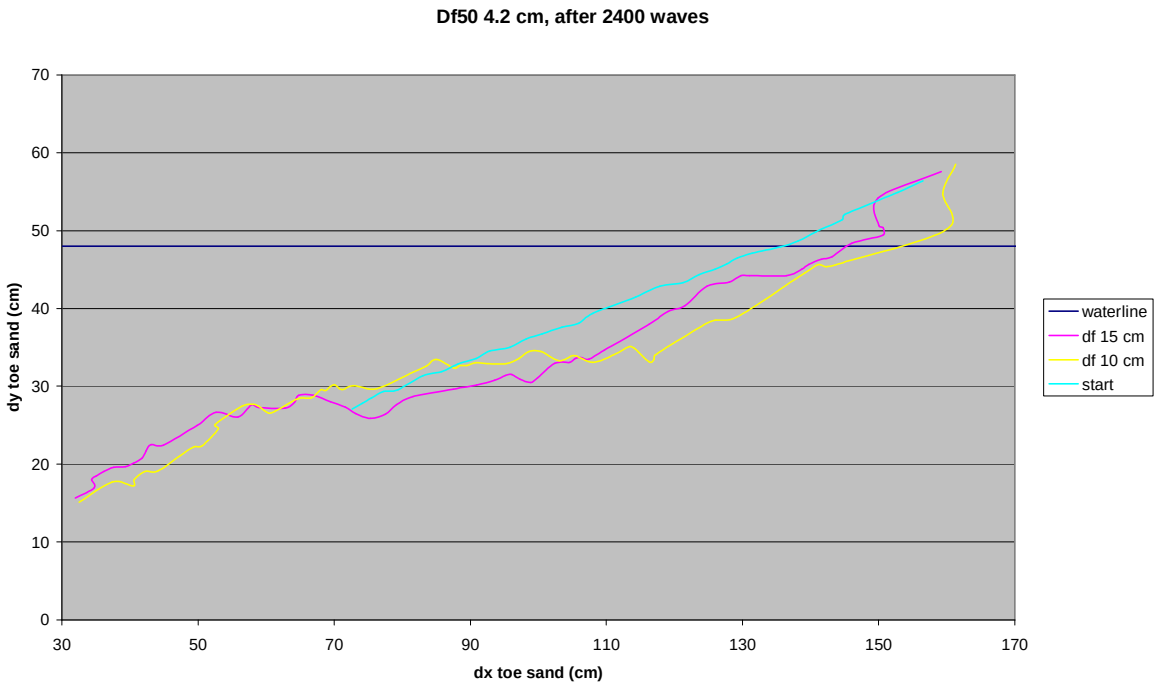

Figure 25 Relation for D_{f50} 4,2 cm, after 2400 waves

Appendix 5; Experiments after 2400 Waves

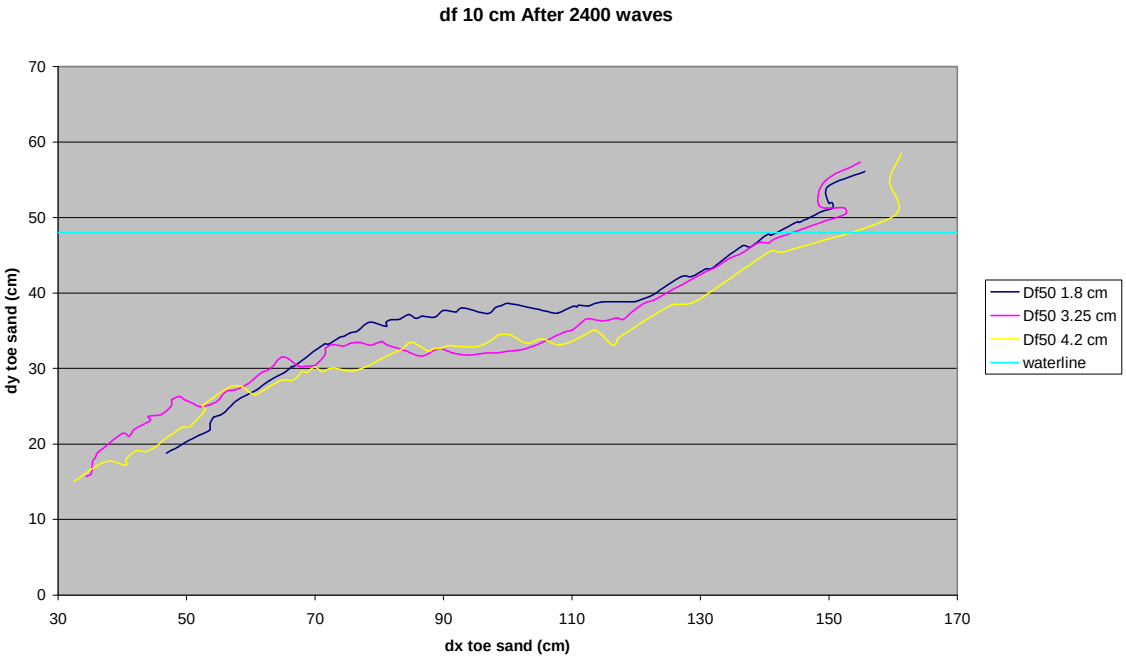

Figure 26 Experiments after 2400 waves with a filter thickness d_f of 100mm

Figure 27 Experiments after 2400 waves with a filter thickness d_f of 150mm

Appendix 6; wave records

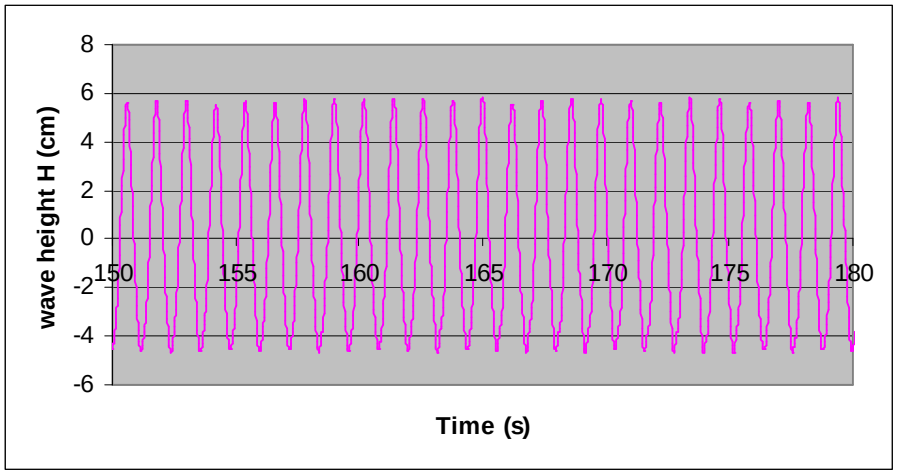

Figure 28 wave record experiment 3

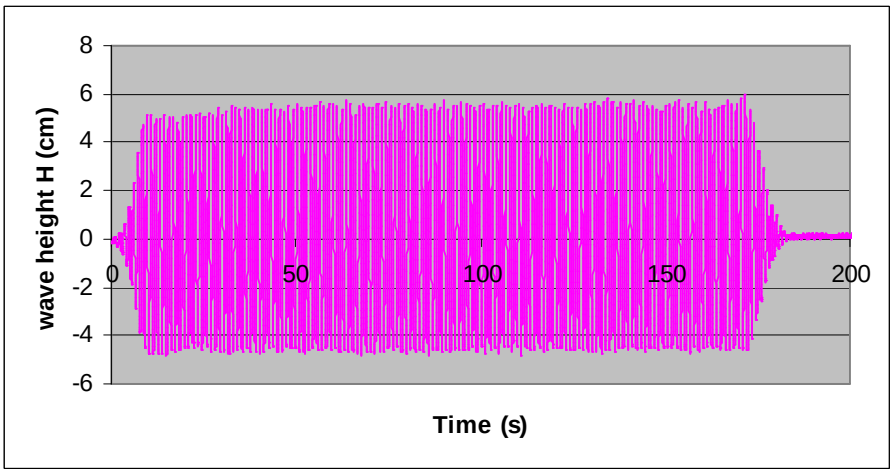

Figure 29 wave record experiment 3

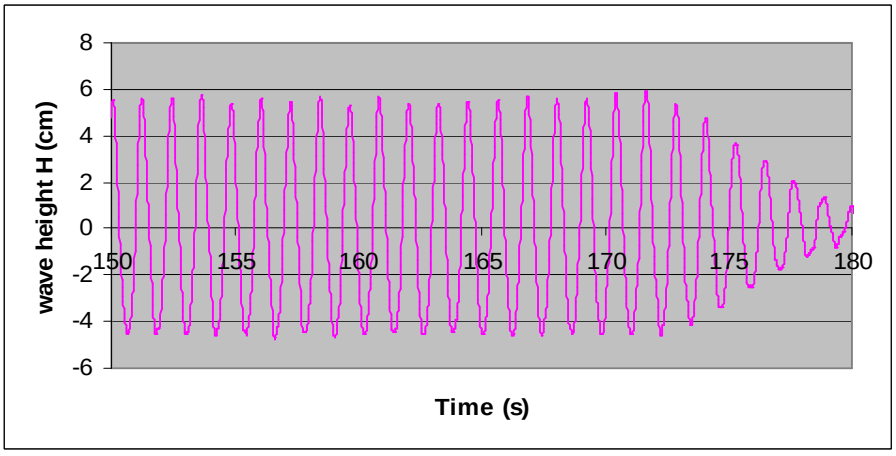

Figure 29 wave record experiment 5